Simulation of Energy Storage Tanks with Surface Heat Exchangers

by

Jörg Michael Baur

A thesis submitted in partial fulfillment of
the requirements for the degree of

Master of Science
(Mechanical Engineering)

at the

University of Wisconsin Madison
1992

Abstract

Cold climate protection for solar domestic hot water systems is usually implemented using an antifreeze solution in the collectors with heat exchange to water in the storage tank. The heat exchanger can be external or internal to the tank. The different types of internal heat exchangers can be classified as internal coil, wrap-around heat exchange wall or mantle heat exchanger. This paper investigates the performance of a mantle heat exchanger. A mantle heated water storage tank is a cylindrical storage tank surrounded by an annulus. The hot liquid from the collector flows through the annulus (mantle) and transfers energy to the contents of the tank. The separating wall is the heat exchange surface. An advantage of this design is the reduced system complexity achieved by combining the heat exchanger and the storage unit into one element. In addition flow in the tank occurs only when water is delivered to the load, resulting in better temperature stratification compared to tanks using external heat exchangers. Regarding temperature stratification tanks with mantle heat exchangers are also better than coil in tank systems as the heat input to the tank is spread over a much wider vertical range. A high degree of stratification is desirable because it increases the useful output of the collector by supplying it with colder water.

Mantle heat exchangers are limited to small scale solar hot water systems because the mantle heat transfer area to volume ratio decreases with increasing storage capacity.

A numerical model of the heat exchanger was written as a subroutine (type) for TRNSYS, the transient system simulation program. The tank is split into a user-specified number of horizontal layers each with a uniform temperature. The energy transferred to or from a node includes mass flow due to the load, heat exchange with the environment, heat transfer from the fluid in the mantle, and conduction between the layers. Classic correlations are used to determine heat transfer coefficients. The energy balances lead to a set of differential equations which are solved iteratively.

The program is tested by comparing simulation results with experimental data. In order for the model and experiments to agree it is necessary to modify the heat transfer coefficients on the inside of the tank and in the mantle with a correction factor. The results of a parametric study to find the impact of different factors on the solar fraction of a complete solar domestic hot water system is presented.

Acknowledgments

Not only to my own surprise the œuvre really is completed. Even though anthropomorphic computers turned the letters of the newly written last chapter irreversibly into little pictures and Arabic letters, crashed just in time before the imminent autosave and in two out of three cases refused to read the valuable contents of my diskettes - I reached the goal.

I want to thank Sandy for giving me valuable hints for my research and for taking time to help me when I got stuck, even during times when he was extremely busy. I also want to thank Bill, my second adviser during the last semester, who helped me finding some inconsistencies in my work. Special thanks go to Osama and Prof. Dave Otis who helped me to bring some light into the jungle of free convection in hot water tanks.

This thesis would have been completely impossible without the exchange program of the Institut für Werkzeugmaschinen and the German Academic Exchange Service (DAAD). I thank them for organizing the program and for funding me during the first nine month. During summer and fall 1992 I was funded by the Department of Energy as a research assistant. Thank you for that opportunity.

My research would have been meaningless without the experimental data I got from Thermal Insulation Laboratory in Denmark and from the Solar Calorimeter Laboratory in Denmark. Thanks to Simon Furbo for immediately answering my requests and thanks to Prof. Steve Harrison and Brian Weir for taking the experimental tank apart and providing me with the information needed.

Many thanks to my office mates Jürgen, Øystein, Bernd, Dick, Doug, Jeff, Todd, Emily and Tim who helped me with infinite patience and expertise in the sometimes desperate battle against the computers. I also want to thank all the nice people who were in the Solar Lab with me for the enjoyable time.

I had a wonderful time in Madison and I want to thank all my friends and my roommates for making my stay a great experience. I will miss Madison and its friendly inhabitants very much.

Table of Contents

Nomenclature

A_{env}	common surface area of tank node and environment
A_m	common surface area of tank node and mantle
A_c	cross sectional area of the mantle
A_t	cross sectional area of the tank
C_1	heat transfer correction factor on mantle side of heat exchanger surface
c_p	specific heat of water in tank
$c_{p,af}$	specific heat of anti freeze in collector loop
D_{man}	diameter of mantle
D_{tank}	diameter of inner tank
D_h	hydraulic diameter of mantle (twice spacing)
e_{man}	distance to bottom of mantle from bottom of tank
h_{man}	distance to top of mantle from bottom of tank
k	constant
k_{af}	conductivity of anti freeze fluid in mantle
k_{st}	conductivity of steel walls
L_i	height of tank node i
m	number of nodes in the mantle

m_i	mass of water in tank node i
$\dot{m}_H$	mass flow rate to and from heat source
$\dot{m}_L$	mass flow rate to load
n	number of nodes in the storage tank
Nui	Nusselt number in node i
$\overline{Nu}(x)$	average Nusselt number from start of flow to x
p	propylene glycol percentage anti freeze liquid in %
Pr	Prandtle number
$\dot{Q}_{cond}$	heat transfer by conduction
$\dot{Q}_{load}$	heat transfer caused by load flow
$\dot{Q}_{loss}$	heat transfer from tank or mantle to environment
$\dot{Q}_{man}$	heat transfer from mantle to tank
$\dot{Q}_{tank}$	heat transfer from mantle to tank
Re	Reynolds number in mantle
R_i	conduction resistance between node i and node i+1
t	time
Δt	length of time step
t_w	thickness of heat transfer surface
T_{env}	temperature of environment
$T_{m,avg}$	average temperature over height of mantle nodes
$T_{m,in}$	inlet temperature of mantle node
$T_{t,i}$	average temperature in tank node i
$T_{t,\ initial}$	temperature in tank node at beginning of time step
$T_{t,\ final}$	temperature in tank node at end of time step
$T_{t,\ avg}$	average temperature in tank node during time step

T_w	weighted average temperature of environment and tank node
$U_{t\text{-}env}$	loss coefficient from tank to environment
$U_{t\text{-}m}$	heat transfer coefficient from tank to mantle
$U_{m\text{-}env}$	loss coefficient from mantle to environment
V	tank volume
x_i	length from mantle inlet to end of ith node
Δx_i	distance between center of node i and node i+1

Greek letters

m	viscosity of anti-freeze liquid in mantle
ρ	density of fluid in tank

1. Introduction

A major concern of current research in solar thermal processes is to improve the efficiency and consequently the feasibility of existing systems. Simulations are a tool for investigations in these areas because they allow the user to obtain rapid system performance estimates without running expensive experiments.

The two most important components of thermal solar systems for domestic applications are the solar collector and the heat storage unit. The object of this thesis is to describe a modeling approach for a sensible hot water storage tank with a built in heat exchanger. The investigated tank is cylindrical with an annulus (or mantle) around it. The hot liquid coming from the collector flows through the mantle and transfers energy to the contents of the tank. The separating wall is used as the heat exchanger surface.

This concept is an interesting alternative to conventional tanks with a separate heat exchanger unit. One advantage of the surface heat exchanger storage tanks is that it reduces the complexity of the system by combining the heat exchanger and the storage unit in one element. The main difference compared to the conventional tank is that the flow from the heat source does not go through the tank so that the load flows through the tank in a less

disturbed manner. The effect is reduced turbulence and, as a result, better temperature stratification. High stratification is desirable because it increases the efficiency of the solar system. The efficiency increases because the water returned to the collector is colder than in tanks with a more homogeneous temperature distribution which reduces the thermal losses of the collector.

In Chapter 2 three different designs of hot water storage tanks with built in surface heat exchangers are introduced. They are compared to conventional systems with external heat exchangers. The procedure and design goals of simulation software is discussed. This particular code is written as a subroutine for the TRaNsient SYstem Simulation program (TRNSYS). Consequently a summary of TRNSYS is included. Two different modeling approaches for this kind of sensible heat storage exist already and are investigated at the end of this chapter.

Different collector flow rates make different modeling assumptions necessary. The two different models used are described in Chapter 3. For high collector flow rates (i. e. mantle flow rates) the flow through the mantle is assumed to be in a quasi-steady state during the whole time step. For low flow systems, the energy stored in the mantle has to be included as it can be a significant part of the total energy stored.

To validate the model, simulations of real test situations have been performed. The procedure of the experiments is described in chapter 4. The results are compared to the real experiments, and deviations are discussed.

The surface heat exchanger tank model is used in chapter 5 to compare this kind of storage component to the conventional system. The impact the stratification has on the performance of the system is also investigated.

2. Background

2. 1 Differences between Conventional Systems and Surface Heat Exchanger Tanks

2. 1. 1 Description

In most climates in the United States and in Europe, freezing conditions occur regularly. To avoid damage to exposed system components like piping and the solar collector, an anti-freeze liquid is run through the collector. The anti-freeze liquid has to be separated from the water used in the house by a heat exchanger. The heat exchanger can be located either on the collector side (i. e. water is stored in the tank) or on the load side (i. e. anti-freeze liquid is stored) of the sensible heat store. In most designs the first option is chosen because it reduces the necessary amount of anti-freeze liquid. Furthermore, the draw rate is less restricted because the load flow doesn't have to run through a heat exchanger with a limited heat transfer capacity.

The main difference between the conventional system and the surface heat exchanger tank is the mode in which heat is transferred from the anti-

freeze liquid to the water stored in the tank. As displayed in figure 2.1 the conventional system requires an additional intermediate loop between the collector and the tank. In the conventional system water is drawn out from the bottom of the tank (using an extra pump), heats it up in a separate heat exchanger and fills the heated water back in the top of the tank. The locations of the inlets and outlets are chosen according to the temperature profile, which is hotter at the top and colder at the bottom of the tank. This method creates an additional flow through the tank which is unnecessary when a surface heat exchanger is used. This design allows the hot anti-freeze to run directly over the side wall of the tank in a containment surrounding the tank. The contents of the tank are directly heated from the top to the bottom. As the load flow is upwards, the tank acts as a counterflow heat exchanger. The mantle typically covers the lower three quarters of the tank height (except in the tank-in-tank design, compare chapter 2. 2). The mantle has to start at the bottom otherwise the volume below the mantle could not be used for heat storage.

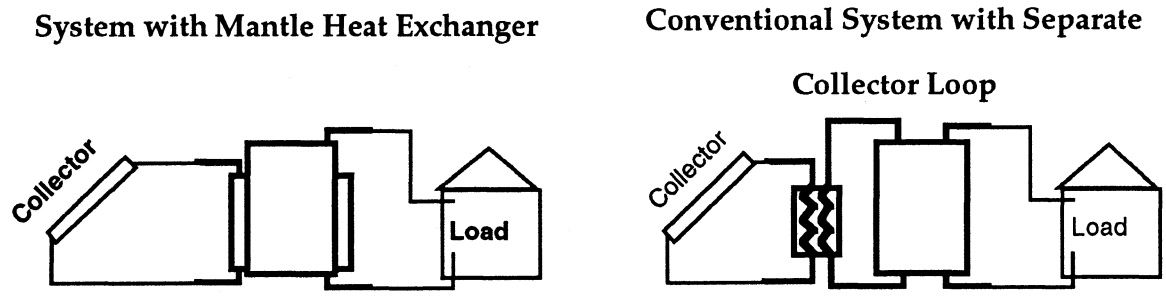

Figure 2.1: Comparison of Systems

A big advantage of the tank with a surface heat exchanger is, that it significantly reduces the complexity of the system. The system consists of one less separate heat exchanger, which not only saves space but it also saves the four attachments at the heat exchanger, two pipes a pump and depending on the design a controller. Even though the tank with the surface heat exchanger is more expensive than a regular tank, the overall system may be substantially cheaper. Also the pumping costs are slightly reduced as the pressure drop is not as high as in a conventional heat exchanger.

The most important advantage, however, is improved thermal stratification in the surface heat exchanger tank. This effect was seen by Fanney and Klein [2] who performed yearly experiments comparing different solar systems. The improved stratification is due to a reduction in mixing since only the load flow goes through the tank instead of two flows in the opposite direction as it is the case in conventional systems. The advantages of a good thermal stratification are described in the next section.

The application of surface heat exchanger tanks is generally limited to domestic hot water systems as the effectiveness of this kind of heat exchangers declines with growing volumes. This behavior occurs as the mantle area to volume ratio decreases with increasing storage capacity.

2. 1. 2 Advantages of Thermal Stratification

Thermal stratification is a temperature distribution where the top of the tank is at the highest temperature and decreases gradually down the tank. The reason for this effect is that the density of hotter water is lower than of cooler water.

All solar thermal storage tanks exhibit some degree of stratification but to illustrate the effect of high stratification in a tank, it is compared to a fully mixed tank. In a stratified tank the bottom of the tank is colder than in a fully mixed tank therefore the water fed into the collector is colder. The colder the liquid going into the collector, the higher is the efficiency of the collector. The reason for that is that the losses are reduced. The losses are proportional to the difference between the average liquid temperature in the collector and the ambient temperature. Therefore low insulated collectors like collectors with single or no glazing have the biggest benefits from the low stratification.

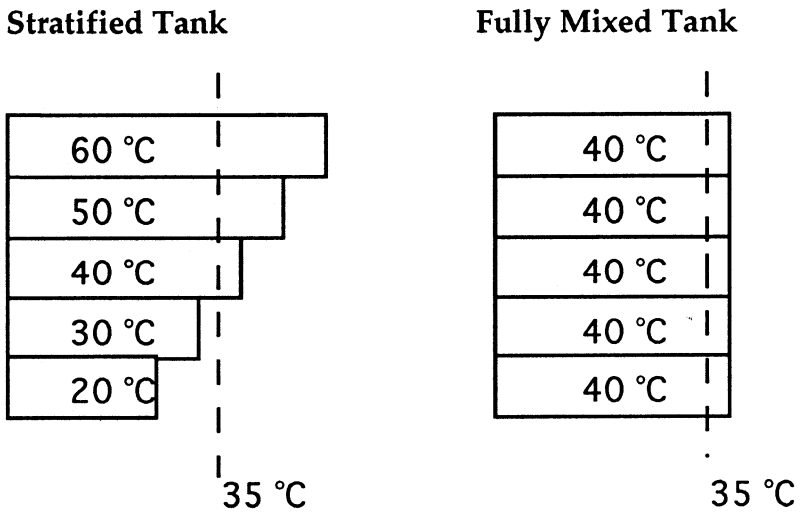

Figure 2.2: Increased Useful Energy due to Stratification

Stratification not only increases the collector efficiency, it also increases the storage effectiveness under certain conditions. For example consider the situation in figure 2.2: A highly stratified and a fully mixed tank contain the same energy. If the critical temperature is, for example, 35 °C the useful energy is proportional to the area to the right of the critical temperature line.

This useful energy or utilizability [5] is 1. 8 times higher in the stratified tank compared to the fully mixed tank.

2. 2. Different Tank Designs

The model must consider the various designs for tanks with built in heat exchangers which perform slightly different. One design is an immersed coil inside of the tank. It is not examined here, because it does not maintain stratification very good. The three most common types of tanks with surface heat exchanger are displayed in Figure 3.

A mantle heat exchanger is an annulus shaped cylinder around the wall of the tank. The mantle starts slightly above the bottom and goes up to approximately three quarters of the height of the tank. The tank-in-tank system is a containment which is completely immersed in a bigger tank through which the collector flow runs. In the third design a coil is wrapped around the side wall and welded to it.

As all three of these designs are not very common it is hard to say which one is the most economical. It is very likely that the tank-in-tank system can be produced pretty inexpensively using, for example, plastic as material for the outer tank. The most expensive design seems to be the tank with the coil welded to it as it is the most labor intensive design. Although there is a method called roll bonding where two sheets of metal are bonded together in some areas. The not bonded area is in the form of a spiral like the coil in the classic method. The not bonded area is then filled with water or air and pressurized to form a coil like shape.

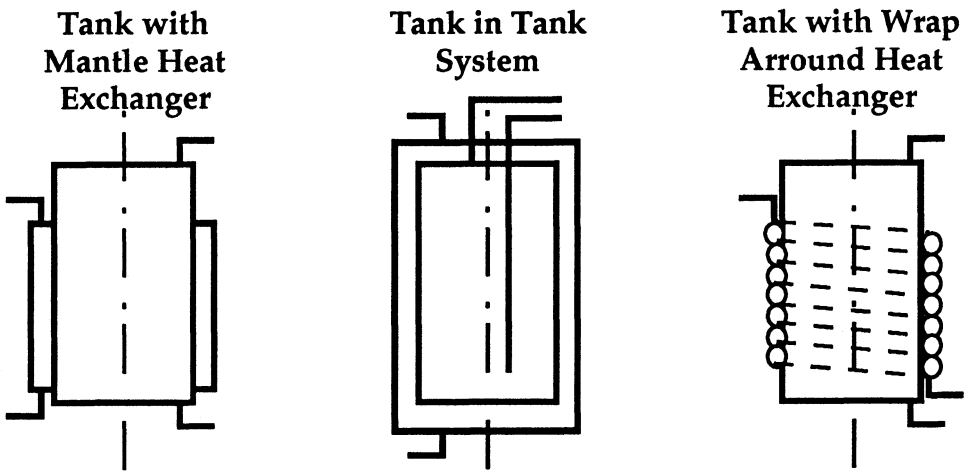

Figure 3: Different Tank Designs

From a heat transfer point of view the designs are very similar. The tank-in-tank design can be viewed as a mantle heat exchanger with the mantle going up all the way from the bottom to the top. The tank-in-tank has the disadvantage that if the collector outlet is colder than the top node of the tank the collector flow actually cools down the top part. The wrap around heat exchanger tank has the advantage of higher flow speed and therefore a higher heat transfer coefficient. The disadvantage is that the necessary pumping power increases also.

2. 3. Aspects of Modeling

2. 3. 1. Design of a model

Before a computer program can be written, the thermal behavior in the tank has to be approximated by a model. The model can never take into account all the phenomena that actually occur. Therefore the required exactness of the model depends very much on the application. If the flow pattern in the tank is of importance or an equation to calculate the Nusselt number is to be developed a finite element approach with a fine mesh would be appropriate. In that case the computation would take many times longer than an experiment. If only a fast and very rough estimate is required maybe a simple energy balance at a fully mixed tank would be sufficient. This kind of approach lacks the ability to distinguish between different designs. In essence the problem is to find the right tradeoff between numerical exactness and computation speed. In this case the requirement for the exactness is that the model should show the distinctive behavior of the particular design and the error should be in the same margins like in other designs. The required computation time should be in the same order of magnitude like for other components in TRNSYS. The implied subroutine leaves a big part of this decision to the user as it allows him or her to choose the number of nodes in which the tank is split up between one and fifteen.

2. 3. 2. TRNSYS

The simulation code for the surface heat exchanger tank was written as a subroutine for the TRaNsient SYstem Simulation program (TRNSYS [4]). TRNSYS is capable of predicting the performances of several kinds of energy

systems like active and passive solar thermal energy systems, photovoltaic systems, solar cooling systems, air conditioning systems, and refrigeration systems. The diversity of the program is achieved by allowing the user to simulate a certain system by combining different TRNSYS components. The user specifies the system setup in a TRNSYS-deck. The main TRNSYS routine then calls the different components in form of subroutines. The program then calculates the temperatures and other transient values for every time step by iterating until the changes are within the specified tolerances.

2. 4. Previous Approaches

Today, there exist two simulation programs for surface heat exchanger tanks. The concepts behind these two models are quite different. The model by Furbo [1] of the Thermal Insulation Laboratory at the Technical University of Denmark uses a finite difference method. The model used in WATSUN [6], which is a solar energy simulation program by the WATSUN Simulation Laboratory at the University of Waterloo in Ontario, Canada uses heat exchanger equations.

In the Danish program the water in the tank, the water in the mantle, and the steel walls of the tank are divided into elements. The temperatures in these nodes are evaluated by an implicit finite difference formulation. The energy balances used include only thermal conduction. Flow streams are accounted for by exchanging entire control volumes. If a temperature inversion occurs, the affected nodes are mixed. Heat (or liquid) transfer by free convection is considered to be negligible. The heat transfer coefficient from

the mantle liquid to the heat exchanger surface and the heat transfer coefficient from that surface to the liquid in the tank are equal. These coefficients were obtained by a linear curve fit to experimental data. This method leads to a relatively high computational effort and is therefore not appropriate for the use in TRNSYS. The heat transfer coefficients used during charging periods (ranging from 550 to 200 W/m^2K from mantle inlet to outlet) were found to be roughly three times greater than the values obtained when equations for laminar flow between parallel plates with one side insulated [5] were used.

A second approach, which is very different from the Danish approach, has been found in Canada. This model assumes the storage tank to be fully mixed and the temperature in the mantle (or the coil) to change continuously over the height of the mantle. This assumption makes it possible to derive an analytical solution for the mantle outlet temperature. The heat exchanger wall is considered to be at the same temperature as the liquid in the mantle (or coil) at every height. The heat transfer coefficient from the wall to the storage medium is calculated by a correlation for turbulent free convection. For every time step, where this calculation is performed, a heat exchanger effectiveness is found.

3. Description of Models

3. 1. Modeling Assumptions

To account for the fact that different users have different needs related to the tradeoff between exactness and computational effort (compare chapter 2.3.1), the user is offered multiple options. The user has the choice of splitting the tank up into any number of nodes between one and fifteen. More important though, one has the choice between two models. The first model treats the liquid in the mantle as a volume of liquid, where the temperature of the liquid changes gradually over the height of the mantle, but is constant over the time step. This means that during a time step, the flow through the mantle can be assumed to be at steady state. In the second approach, the mantle is divided into fully mixed control volumes to which energy balances are applied to account for the energy change in the mantle during that particular time step. Model I is also referred to as quasi steady state model while model II is referred to as a model including mantle energy storage.

3. 1. 1. Discretization of Time

When simulating any kind of transient behavior there are two ways to take care of the time influence. Occasionally it is possible to derive an analytical solution, where the equations depend directly on the time. However, in most cases, especially with variable input values, the only possibility is to solve the differential equations numerically using discrete time steps. In the latter case the derivative of a variable is approximated by using the difference of their present value and their value from the time step before, divided by the length of a time step. The referenced models use a combination of the two methods. Time is discretized in time steps so that the changing input values can be taken care of. The temperature at the end of a time step in a tank node is evaluated using an analytical equation. The calculation starts with the respective initial temperature. For the heat transfer calculations an average temperature is determined. This average temperature results in the same amount of heat transfer that the changing temperature would have caused.

3. 1. 2. Storage Tank

The size and shape of the control volumes, which both have to be good approximations of the real three-dimensional temperature distribution in the tank, affect the performance of the simulation the most. In both models the liquid in the main tank is split up into horizontal layers. Temperature changes over the radius are thus neglected. This configuration reflects the physical occurring thermal temperature layers whereas it neglects the influence of the fluid being hotter at the heat transfer surface than in the middle of the nodes The convective flow of the load and the heat transferred from the mantle and to the environment change the temperature in the

entire control volume permanently, as the liquid in the control volume is fully mixed at every point in time. In Figure 3. 1. it is shown how a tank could be designed to behave exactly like the model. Between the tank nodes divisions are located and the liquid in each section is always fully mixed by a fan.

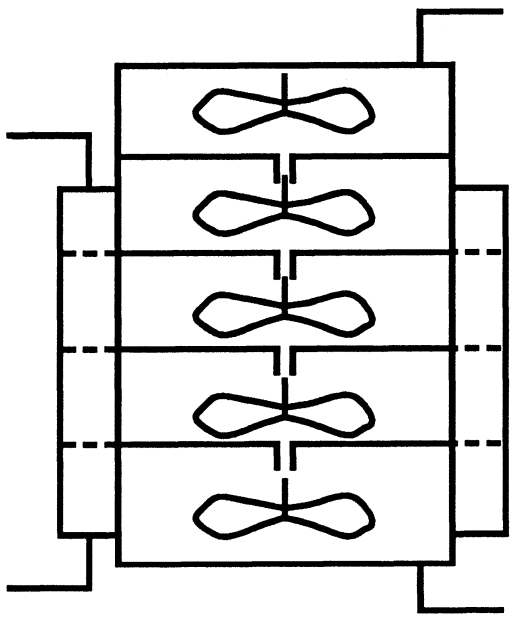

Figure 3. 1.: Illustration of Tank Model

3. 1. 3. Mantle

The mantle is split up into horizontal layers, matching the nodes in the tank so that the average tank node temperature can be used to calculate the heat transfer from the mantle. The determination of the temperature distribution depends on the mass flow rate through the collector. For high flow rates, model I is used, and the flow in the mantle is considered to be at steady state during the time step. The temperature in the mantle nodes are assumed to

change gradually, usually to cool down as it flows down. In every mantle node an equivalent temperature is determined, which results in the same heat transfer as the existing temperature distribution in the mantle node would cause. This equivalent temperature is calculated using the inlet temperature in the node and by assuming that both the temperature of the environment and the temperature of the tank node do not vary over the height of the tank node. The inlet temperature of the top node is the inlet temperature to the mantle and the inlet temperatures of the lower nodes are calculated like the average temperature from the inlet temperature of the node above. Therefore the mantle node temperatures are calculated sequentially from the top to the bottom.

In model II, the energy change in the mantle is taken into account by applying the same kind of energy balance on the mantle nodes as it was used for the tank nodes (compare to section 3.1.2.). The mantle nodes are considered to be fully mixed and a temperature averaged over time is determined. This average temperature is used for the heat transfer calculations.

3. 1. 4. Heat Transfer Coefficient

For the model to perform well, it is important to use good estimates for the heat transfer coefficient between the mantle and the tank. The previous approaches (section 2. 4.) use completely different approaches. The WATSUN model for wrap-around heat exchangers neglects the resistance from the mantle to the wall and uses heat transfer coefficients from a turbulent free convection equation on the inside of the wall. In the TIL-model the heat transfer coefficients are obtained by fitting them to experimental data.

The heat transfer from one fluid to the other through a wall splits up into the heat transfer from the hotter fluid to the wall, the conduction through the wall and the heat transfer from the wall to the colder fluid. The heat transfer coefficient is the reciprocal value of the sum of the three resistances. Comparing the orders of magnitude it turns out that the resistance for the conduction through the wall can be neglected compared to the resistance from the mantle to the wall. The resistance on the tank side of the wall can be defined by setting the corresponding heat transfer coefficient to a constant value in the TRNSYS deck. This resistance can be assumed to have only a small influence on the overall heat transfer coefficient. Therefore it is suggested to set this heat transfer coefficient to a high value in the TRNSYS deck. The heat transfer from the mantle fluid to the wall is calculated with an empirical equation for laminar flow between flat plates with one side insulated and constant heat flux on the other side.

The heat loss coefficient to the environment is an input parameter to the TRNSYS-deck. It is usually obtained by a cool down test.

3. 1. 5. Temperature Inversions

Liquids naturally stratify in a way so that the temperature of the fluid is high at the top and gradually decreases towards the bottom as the density of hot water is lower compared to cold water. Sometimes situations occur where a control volume in the middle of the tank is hotter than a node at the top. This situation occurs because in most cases the mantle does not extend to the top of the tank, therefore middle nodes are heated, while the top nodes have comparably high losses to the environment. A situation like this is unstable. Therefore it is assumed that the hot water rises and mixes with the colder

water above. If the mixing temperature continues to be higher than the temperature of the next node above, then this node is mixed in also.

3. 1. 6. Conduction between Nodes

Heat transfer by conduction between the nodes can be taken into account. The heat is conducted two different ways. Heat is conducted directly from one control volume of water to the next. The distance for the heat transfer is chosen to be the distance between the centers of the two control volumes in question. Apart from the direct heat transfer, energy is transferred from the node to the tank wall, into the wall, and finally back to the next node.

3. 2. Mathematical Description

3. 2. 1. Tank Nodes

The equations used to determine the temperature in the tank and mantle nodes are based on the first law of thermodynamics and the most basic heat transfer equation. The first law of thermodynamics requires that the change in enthalpy, which is proportional to the change in temperature in a fixed mass of matter, is proportional to the rate of the net energy input in this mass of matter. The heat transfer law says that the rate of energy transferred from one medium to the other is proportional to the temperature difference between the two media.

Equation (3.1) is the energy balance at a representative tank node including the energy transferred by the load flow, by heat transfer to the

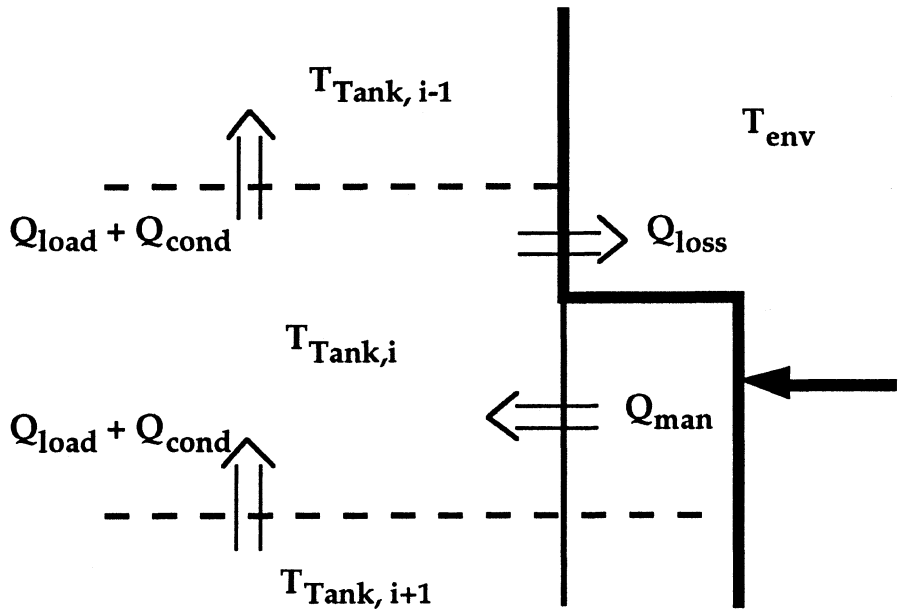

Figure 3. 2.: Schematic of Energy Balance on Tank Node

mantle or environment, and by conduction to the neighbor nodes. The energy flows are schematically displayed in figure 3. 2. .

$$m_i c_p \frac{dT_{t,i}}{dt} = \dot{Q}_{load,i} + \dot{Q}_{cond,i} + \dot{Q}_{man,i} + \dot{Q}_{loss,i} \qquad (3.1)$$

with the energy flow by the load

$$\dot{Q}_{load,i} = \dot{m}_L c_p (T_{t,i+1} - T_{t,i}) \qquad (3.1a)$$

and the heat conducted through water and wall

$$\dot{Q}_{cond,i} = \frac{1}{Re_{i-1}} (T_{t,i-1} - T_{t,i}) + \frac{1}{Re_i} (T_{t,i+1} - T_{t,i}) . \qquad (3.1b)$$

The values for the resistances can be obtained from equation (3.18) in section 3.2.6. The heat transferred from the mantle can be determined as

$$\dot{Q}_{man,i} = U_{t\text{-}m,i} A_{m,i} (T_{m,avg\,i} - T_{t,i}) . \qquad (3.1c)$$

The heat transfer coefficient is calculated as described in section 3. 2. 4 in equation (3.12). The heat transferred from the environment (which is usually negative as the environment is colder than the contents of the tank) can be obtained by

$$\dot{Q}_{loss,i} = U_{t\text{-}env} A_{env,i} (T_{env} - T_{t,i}) \qquad (3.1d)$$

A maximum of two nodes have a common surface with both, the environment and the mantle. For all other nodes the heat transfer term that doesn't apply is set to zero by setting the according heat transfer area to zero.

Equation (3.1) can be written in the form

$$\frac{dT_{t,i}}{dt} = A\, T_{t,i} + B \qquad (3.2)$$

with A and B being constants independent of the temperature in the regarded node

$$A = -\left(\dot{m}_L c_p + \frac{1}{Re_{i-1}} + \frac{1}{Re_i} + U_{t\text{-}m,i} A_{m,i} + U_{t\text{-}env} A_{env,i}\right) \qquad (3.2a)$$

$$B = -(\dot{m}_L c_p T_{t,avg\ i+1} + \frac{1}{Re_{i-1}} T_{t,avg\ i-1} + \frac{1}{Re_i} T_{t,avg\ i+1} + U_{t\text{-}m,i} A_{m,i} T_{m,avg\ i} + U_{t\text{-}env} A_{env,i} T_{env}) \quad (3.2b)$$

The differential equation can be solved analytically to obtain the temperature at the end of the time step

$$T_{t,\ final\ i} = (T_{t,\ initial\ i} + \frac{B}{A})\, e^{(A*\Delta t)} - \frac{B}{A} \qquad i = 1, n \quad (3.3)$$

and the average node temperature of the time step

$$T_{t,\ avg\ i} = \frac{(T_{t,\ initial\ i} + \frac{B}{A})}{(A*\Delta t)} (e^{(A*\Delta t)} - 1) - \frac{B}{A} \qquad i = 1, n \quad (3.4)$$

If the storage tank is split up into n nodes and the mantle in m nodes (with m being smaller or equal to n), equation (3.3) and equation (3.4) really are sets of n equations each as there is one of each per tank node. Unknowns are the final temperatures and the average temperatures of each node at each time step. The initial temperatures in a time step are set to the final temperatures of the previous time step. The value of B depends on the average temperatures of the nodes above and below as well as the average temperature in the mantle, if the node has contact to the mantle. Summarized there are 2n equations with 2n+m unknowns. The m missing equations are provided by equation (3.7) if model I is used and by equation (3.11) for model II.

The 2n+m equations are all linear dependent on the 2n+m variable therefore there are two options how they can be solved. One possibility is to set the equations up in a matrix and solve them with the Gauss-algorithm. This method is very fast when the parameters do not change, as the same converted matrix could be used in every time step. Because some of the parameters change with time and the heat transfer coefficient depends on the mantle temperature an alternative solution method has been used in which the temperatures are calculated based on average temperatures of the previous time step and then evaluated iteratively.

3. 2. 2. Mantle Nodes with Quasi Steady State Model

In this model the flow through the mantle is considered to be at steady state during the time step. The temperatures in the storage tank nodes are assumed to be at a constant temperature throughout the time step in order to calculate the mantle node temperatures. To find the temperature variation with height in the mantle an energy balance is applied to a differential element in the control volume as displayed in Figure 3.3.

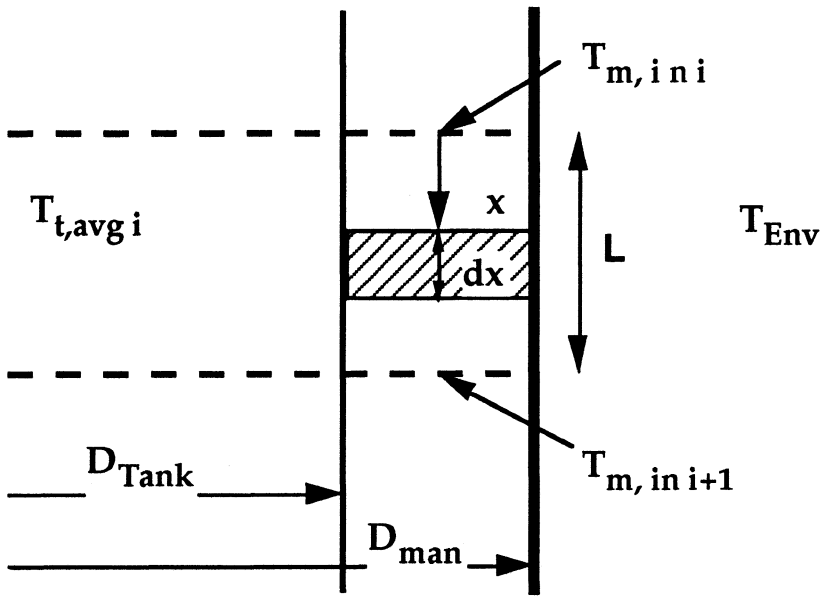

Figure 3.3.: Energy Balance on Differential Element

Equation (3.5) shows that the change in temperature of the liquid in the mantle with height is proportional to the heat transfer rate to the environment and into the tank.

$$\dot{m}_H c_{p,af} \frac{dT}{dx} = \dot{Q}_{loss,i} + \dot{Q}_{tank,i} \tag{3.5}$$

with the heat lost to the environment being

$$\dot{Q}_{loss,i} = U_{m\text{-}env} D_{man} \pi (T_m(x) - T_{env}) \tag{3.5a}$$

and the heat transferred to the tank

$$\dot{Q}_{tank,i} = U_{t\text{-}m,i} D_{tank} \pi (T_m(x) - T_{t,\,avg\,i}) \tag{3.5b}$$

When the mass flow rate in the mantle is zero equation (3.5b) is adapted to take into account the heat losses through the mantle. To account for the heat losses from the tank through the mantle $U_{t\text{-}m,i}$ is replaced with $U_{m\text{-}env,i}$ and $T_{t,avg\ i}$ is replaced with T_{env}. The linear differential equation (3.5) can be solved analytically for the temperature at any vertical distance from the top of the node. An equation for the outlet temperature (equation 3.6) can be obtained by setting x to the node height.

$$T_{m,out} = T_w + (T_{m,in} - T_w)\ e^{-kL} \tag{3.6}$$

The inlet temperature is set to the mantle inlet temperature for the first mantle node from the top. For the following nodes the inlet temperature is set to the outlet temperature from the node above. T_W is the weighted average of environment and tank temperature and can be obtained from equation (3.6a)

$$T_w = \frac{U_{m\text{-}env} D_{man} T_{env} - U_{t\text{-}m,i}\, D_{tank} T_{t,\ avg\ i}}{U_{m\text{-}env} D_{man} - U_{t\text{-}m,i}\, D_{tank}} \tag{3.6a}$$

The exponential constant k is calculated as shown in equation (3.6b).

$$k = \frac{\pi\ (U_{m\text{-}env} D_{man} - U_{t\text{-}m,i}\, D_{tank})}{\dot{m} c_{p,\ af}} \tag{3.6b}$$

The equations (3.3) and (3.4) contain in the constant B (equation 3.2b) the average mantle node temperature. This temperature is determined in a way so that the heat transfer from the mantle to the tank and to the environment equals the amount obtained by integrating the local temperature differences times the heat transfer coefficient over the height of the node. The relationship to obtain that average (or better) equivalent mantle node temperature is shown in equation(3.7).

$$T_{m,avg\,i} = T_W + \frac{T_{m,in} - T_W}{k\,L}(1 - e^{-kL}) \qquad (3.7)$$

The weighted temperature T_W and the exponential constant k are the same as used to determine the node outlet temperature (equation 3.6) and are obtained by equations (3.6a) and (3.6b).

3. 2. 3. Mantle Nodes with Transient Model

In contrast to model I, the temperature in a mantle node in model II is allowed to change over the time step, but it is set to be constant over the height of the node. The differential equation (3.8) describing this model is very similar to the one for the tank nodes, equation (3.1).

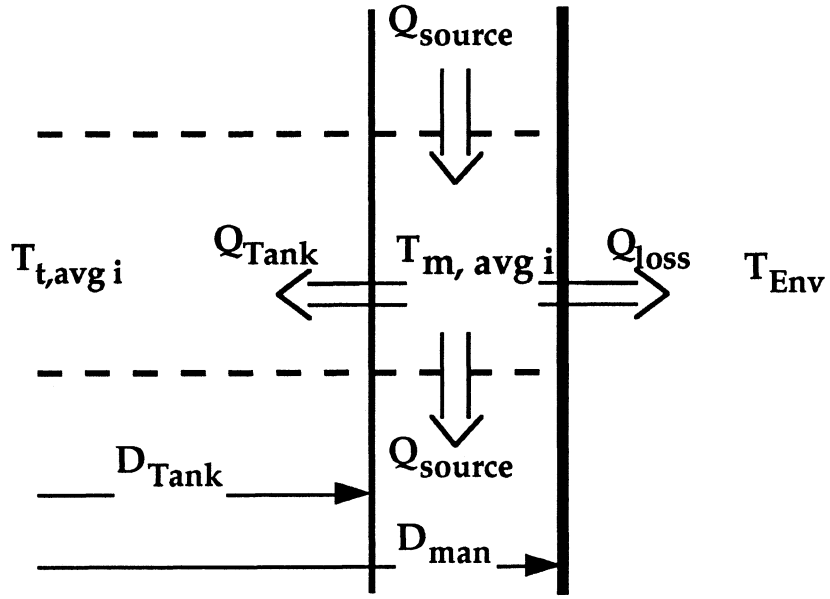

Figure 3.4.: Energy Balance on Mantle Node

In figure 3.4 the relevant energy flows into and out off the fully mixed controlled volume are displayed. An energy balance applied on the fully mixed control volume yields the differential equation (3.8) for the average mantle node temperature.

$$m_{m,\,i} c_{p\,af} \frac{dT_{m,i}}{dt} = \dot{Q}_{source,\,i} + \dot{Q}_{tank\,i} + \dot{Q}_{loss,\,i} \qquad (3.8)$$

with the rate of enthalpy provided by the flow from the heat source

$$\dot{Q}_{source,\,i} = \dot{m}_S c_{p\,af} (T_{m,avg\,i-1} - T_{m,\,i}) \qquad (3.8a)$$

The heat transferred from the mantle to the tank can be determined as

$$\dot{Q}_{tank,\,i} = U_{t\text{-}m,\,i} A_{m,\,i} \left(T_{t,\,avg\,i} - T_{m,\,i}\right) \tag{3.8b}$$

and the heat transferred from the environment (which is usually negative as the environment is colder than the contents of the tank) can be obtained by

$$\dot{Q}_{loss,\,i} = U_{m\text{-}env} A_{env,\,i} \left(T_{env} - T_{m,\,i}\right) \tag{3.8c}$$

Equation (3.8) can be brought into the form

$$\frac{dT_{m,\,i}}{dt} = C\,T_{m,\,i} + D \tag{3.9}$$

with C and D being constants independent of the temperature of node i

$$C = -\left(\dot{m}_S c_{p\,af} + U_{t\text{-}m,\,i} A_{m,\,i} + U_{m\text{-}env} A_{env,\,i}\right) \tag{3.9a}$$

$$D = -\left(\dot{m}_S c_{p\,af} T_{m,\,i\text{-}1} + U_{t\text{-}m,\,i} A_{m,\,i} T_{t,\,avg\,i} + U_{m\text{-}env} A_{env,i} T_{env}\right) \tag{3.9b}$$

The differential equation can be solved analytically to obtain the temperature at the end of the time step in the mantle node at every point in time. Equation (3.10) shows how the final temperature of a time step is computed starting with the initial temperature at the time step.

$$T_{m,\,final\,i} = (T_{m,\,initial\,i} + \frac{D}{C})\, e^{(C^*\Delta t)} - \frac{D}{C} \qquad (3.10)$$

To calculate the heat transferred to the tank and the environment an equivalent temperature is found that has a value which results in the same heat transferred as if the momentary heat transfer rate had been integrated over the time step. This average mantle node temperature is obtained from equation 3.11).

$$T_{m,\,avg\,i} = \frac{(T_{m,\,initial\,i} + \frac{D}{C})}{(C^*\Delta t)} (e^{(C^*\Delta t)} - 1) - \frac{D}{C} \; . \qquad (3.11)$$

Like the equations for the tank nodes (equation (3.3) and (3.4)) equations (3.10) and (3.11) are a set of coupled differential equations.

3. 2. 4. Heat Transfer Coefficient

As discussed in section 3.1.4. the heat transfer coefficient from the anti-freeze liquid in the mantle to the water stored in the tank can be approximated with only the heat transfer coefficient from the mantle liquid to the wall, since the heat transfer mechanism is the major heat transfer resistance. This heat transfer coefficient can be obtained from equation (3.12). It depends on the conductivity of the anti-freeze liquid, on the hydraulic diameter of the mantle which is twice the spacing between the outer and the inner mantle wall, the local Nusselt number, and the correction factor C_1. This correction factor accounts for the fact that the empirical equation (3.14) is only an

approximation for the application in a mantle heat exchanger. The correction factor C_1 is fitted with experimental data.

$$U_{t\text{-}m,\,i} = C_1 \frac{k_{af}\, Nu_i}{D_h} \tag{3.12}$$

Equation (3.14) provides an average value of the Nusselt number from the starting point of the laminar flow to the point looked at. With equation (3.13) the average Nusselt number for the ith node can be obtained. x_i is the distance from the top of the mantle to the end of the ith node.

$$Nu_i = \frac{\overline{Nu}(x_i)*x_i - \overline{Nu}(x_{i-1})*x_{i-1}}{x_i - x_{i-1}} \tag{3.13}$$

The average Nusselt number in equation (3.14) was developed by Mercer et al. (1976) [7]. It is intended for laminar flow between two flat plates with constant heat flux on one side and insulated on the other.

$$\overline{Nu}(x) = 4.9 + \frac{0.0606(Re\ Pr\ D_h/x)^{1.2}}{1 + 0.0909(Re\ Pr\ D_h/x)^{0.7}\ Pr^{0.17}} \tag{3.14}$$

Equation (3.14) depends on the flow length, the hydraulic diameter, the Reynolds number of the flow and the Prandtl number of the anti-freeze liquid in the mantle. The Reynolds number is a dimensionless value characterizing the flow. As displayed in equation (3.15) it can be determined from the hydraulic diameter, the mass flow rate in the mantle, the viscosity of the anti-freeze liquid and the cross sectional area of the mantle.

$$Re = \frac{D_h \dot{m}_h}{\mu A_{cr}} \tag{3.15}$$

The Prandtl number and the viscosity both depend on the temperature of the liquid and they change for different liquids. They can be obtained from temperature dependent curvefits using third order polynomials.

3. 2. 5. Temperature Inversions

The purpose of the temperature inversion algorithm is to convert an unstable temperature distribution in the tank into a stable one, i. e. with no node being hotter than the node above. The algorithm starts at the bottom of the tank with its search for temperature inversions. If one is detected the mixing temperature of the two nodes is determined. This mixing temperature then is compared to the next node above. Should this node still be colder than the mixed temperature it is also mixed in. This procedure is continued until a node with a higher temperature than the temperature mix is reached. Then all nodes from which the mixed temperature was determined are actually assigned the mixed temperature. After that the algorithm continues its search for temperature inversions, and treats them the same way. After the whole tank has been investigated and the temperatures corrected if necessary the whole tank is checked again. This final check is necessary, because the mixing algorithm can create inversions as the mixing usually reduces the temperature of the lowest node mixed in. Should there still be inversions the whole process is repeated.

3. 2. 6. Conduction between Nodes

The conductive resistances as they are used in the term for the heat transferred between the nodes, consist of two parallel resistances. One resistance is for the heat transferred directly through the water from one node to the other, and the other is a series of three resistances. The three resistances are the resistance by the boundary between the fluid at a node and the wall of the tank, the resistance of tank wall itself and the resistance of the boundary between the tank wall and the liquid in the next node. The direct resistance can be obtained from equation (3.16). To get this equation the fully mixed model cannot be used, as for a realistic estimate of the conductive heat transfer a constant temperature gradient over the regarded distance has to be assumed. As distance the length between the centers of the two nodes is used.

$$R_{d,i} = \frac{\Delta x_i}{k_{H_2O} A_t} \tag{3.16}$$

The cumulative effect of a series of resistances is obtained by summing them. In the case of the heat transfer through the wall the resistance to the wall, through the wall, and from the wall have to be summed. The total resistances put up by the wall is calculated with equation (3.17).

$$R_{w,i} = \frac{1}{h_i \pi d_{tank} L_i} + \frac{\Delta x_i}{k_{St} \pi d_{tank} t_w} + \frac{1}{h_{i+1} \pi d_{tank} L_{i+1}} \tag{3.17}$$

The total value for the resistance between the two nodes can be obtained from the two parallel resistances with the same equation (equation (3.18)) which is used for parallel electrical resistances.

$$\frac{1}{R_i} = \frac{1}{R_{d,i}} + \frac{1}{R_{w,i}} \tag{3.18}$$

3. 3. Discussion of Chosen Assumptions

3. 3. 1. Mantle Nodes

The disadvantage of model I is, that it does not take into account the transport time it takes for the fluid to flow through the mantle. Every change of the mantle inlet temperature instantly effects all the nodes within the same time step, even though it should take, for example, several time steps. The second disadvantage is that in heating up the tank the temperature comes out a little to high from the mantle, as the energy to heat up the tank doesn't have to be provided. The advantage is that there is no numerical limit to the mantle flow rate or the time step which is imposed by the mantle.

Model II takes into account the change in energy in the mantle, and it also respects the "temperature history" of the mantle. This big advantages have to be paid for by strict limitations to the time step or the mantle flow rate. To obtain correct results at a given time step the flow rate can be at a maximum so high, that it just exchanges one entire control volume in the mantle per time step.

3. 3. 2. Conduction

During the normal charging and decharging cycle the influence of conduction is hardly important for the temperature distribution in the tank. The energy transfer through the mantle and the load flow through the tank is completely overwhelmed compared to the conductive heat transfer. During the night though when the flow from the source is shut off, and no water is drawn from the tank, conduction is the only mode of heat transfer. Over the whole night conduction has quite a significant effect. A hot temperature in a strongly stratified tank loses in many cases more heat to colder nodes than to the environment.

3. 3. 3. Free Convection

Heat transfer by free convection was considered as a mode of heat transfer between the nodes. The cooling down and simultaneous destratification of a hot water tank is simulated, assuming free convection due to the cold outside wall would occur. The mass of water flowing from one node to the next lower is calculated using an equation derived from a relationship for a vertical isothermal plate in a medium of constant temperature. Every node is split up into a center part and a boundary layer part as shown in figure 3.5.. Energy and mass balances are applied on both.

The development of the temperature distribution is calculated using a finite difference method. The results from the simulation are then compared to real experimental data displayed in figure 3.6.. The simulation results are shown in figure 3.7. The cool down and destratification characteristic in the two graphs is fairly similar, but the time scale is almost two orders of magnitude different. This difference shows that the free convection equation

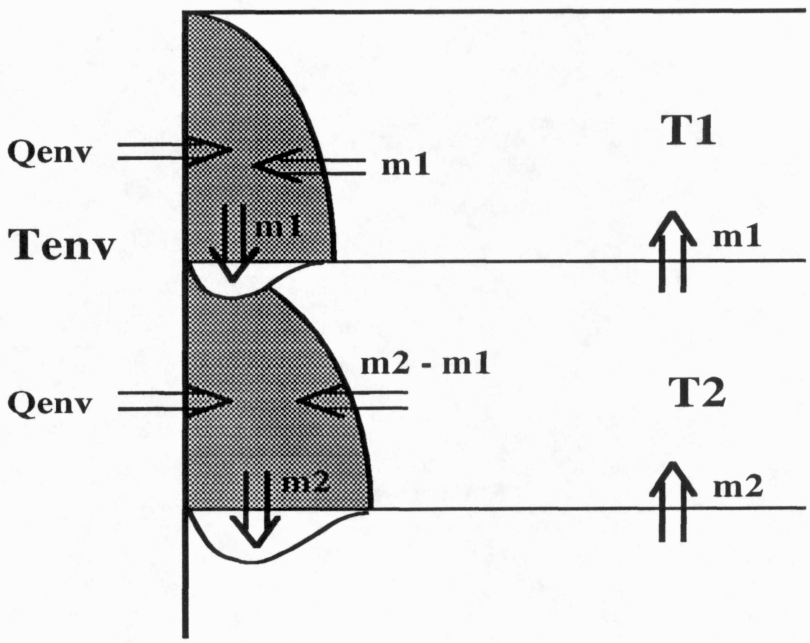

Figure 3.5.: Mass flow Induced by Free Convection

for a plate at uniform temperature in a infinite medium at constant temperature is far from being appropriate in this case. Neither analytical nor empirical equations for free convective mass flow in enclosures could be found, but it can be assumed that hardly any free convective mass flow occurs. The effects of free convection are therefore neglected in the simulation model.

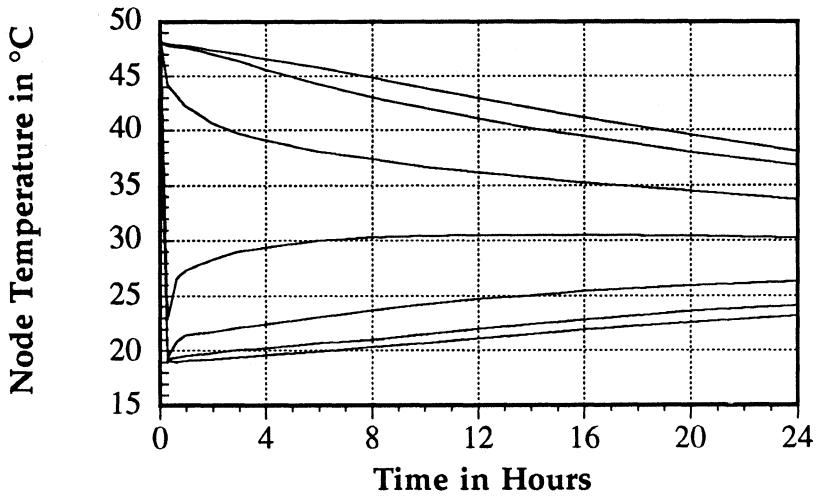

Figure 3.6.: Experimental Data for Cool Down Test

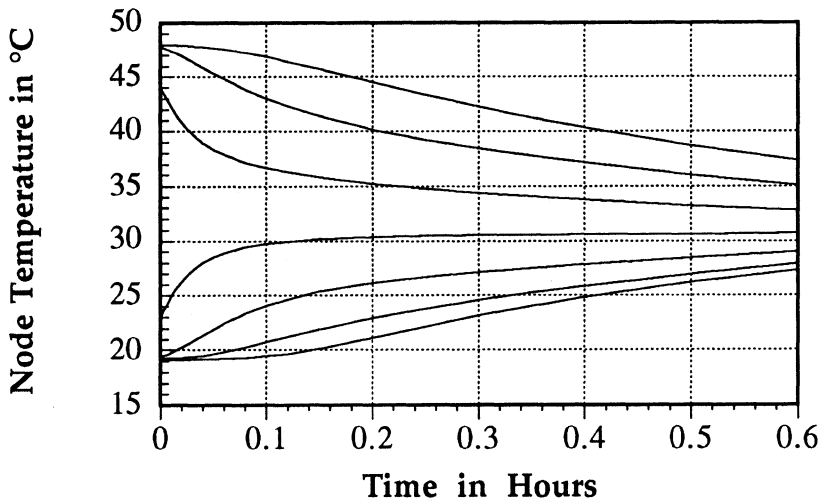

Figure 3.7.: Simulation Results

3. 4. Algorithm

In this section the calculation procedure used in the mantle heat exchanger subroutine is outlined. The TRNSYS-main routine calls the subroutines that are specified in the TRNSYS-deck. The specified connections are executed by giving the current output values of a subroutine to one or more other subroutines as input values. During one time step the main program compares all output values with the ones from the iteration step before. If the maximum difference is larger than the tolerance specified the iteration process is continued.

In its first call the mantle heat exchanger subroutine reads in the specified parameters and initial conditions. In the beginning of every call the subroutine reads in the required input values. At the first iteration of a time step the temperature profile in the tank is checked for temperature inversions. If any are detected they are eliminated according to the algorithm described in section 3.2.5.. Also at the first iteration of a time step the initial temperature is set to the final temperature of the time step before. In every iteration the temperatures in the tank are calculated from the top to the bottom. In model I (section 3.2.2.) the average temperature in the mantle is calculated first, using the average tank temperature from the iteration before. With the new mantle node average temperature the tank node average temperature is evaluated.

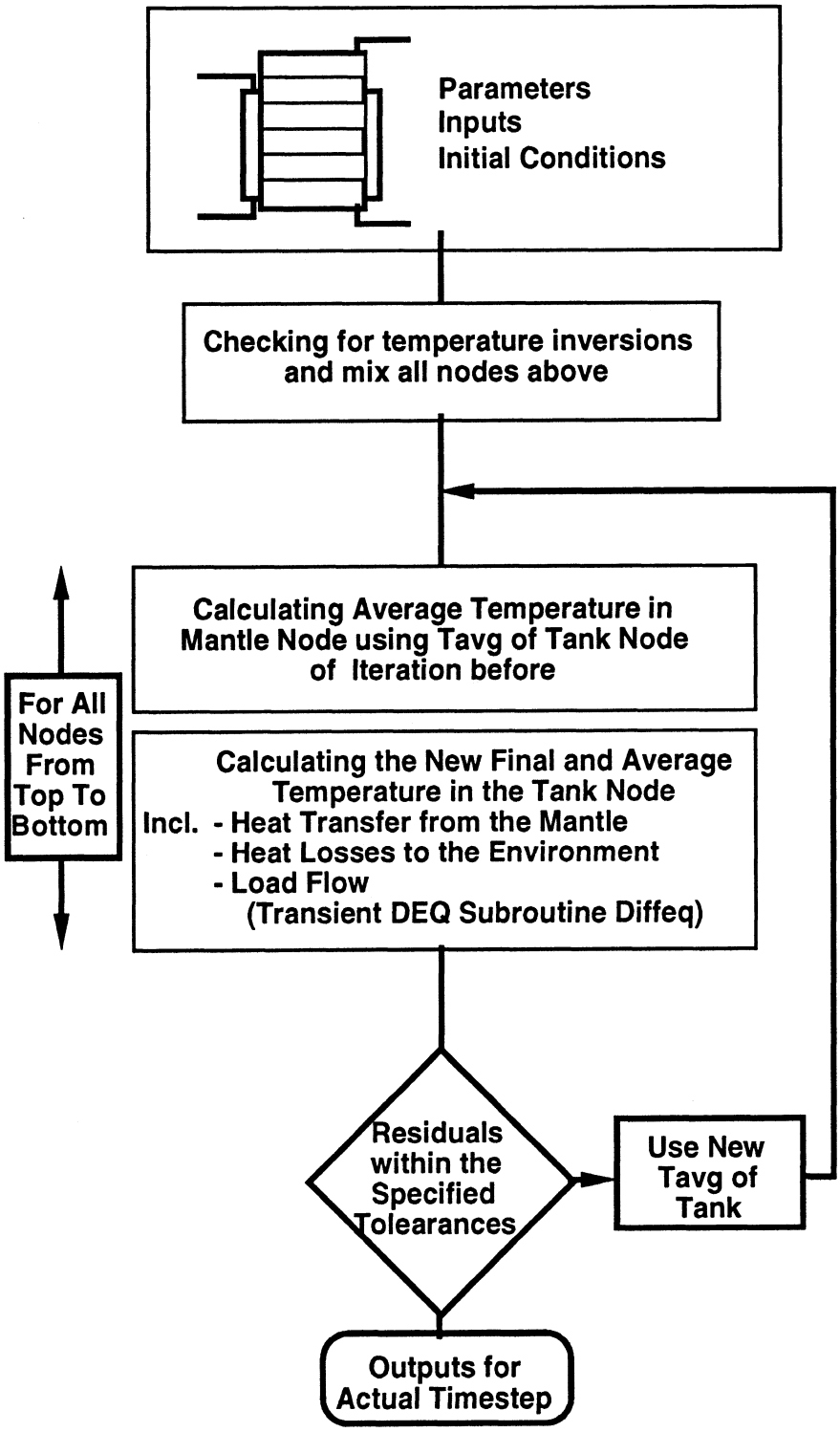

Figure 3.8.: Flow Chart of Algorithm for One Time Step

In model II (section 3.2.3) the average temperature of nodes touching the mantle is calculated using the mantle average temperature from the iteration before (or in the first iteration of the times step, of the time step before). To evaluate the temperature in the tank the newly calculated average tank node temperature is used.

4. Verification of Model

4. 1. Testing of a Model

Real situations include a much broader variety of possibilities than a computer program ever can take into account. Therefore it is impossible to come up with reasonable assumptions without comparing the simulation results with data from real experiments. Some additional features might have to be included to make the model work better, others might only add to the computation time without improving the exactness of the results significantly.

To come up with a meaningful error value that represents the accuracy of the simulation as the mantle heat exchanger subroutine calculates multiple temperatures at different locations and at different points in time. Apart from that, only temperatures at some particular spots are recorded in real experiments. The values for the change of energy stored in the tank, the energy extracted from the tank, and the losses to the environment can be calculated from the temperatures in the tank node at different time steps. The energy going into the mantle can be determined from the difference of the

inlet and outlet temperatures of the mantle. Therefore the state of the tank can be completely described with the values of the temperatures in the tank nodes, and the outlet temperature of the mantle assuming the inlet temperatures from the solar collector and from the mains are known. Therefore it is sufficient to take into consideration only the values of these temperatures for error calculations. For short tests (over a time period of less than one or two days) there are two possibilities to determine a useful error value for the simulation exactness. One is to calculate the average of the squared residuals of the temperatures for the nodes at certain times. This method is very similar to the least squares method. The alternative to that is to calculate relative errors either for certain nodes at certain times or the maximum relative error. The relative error is the error at a point in time divided by the temperature change in the real data since the beginning of the experiment as shown in equation (4.1).

$$\text{error} = \frac{\left| T_{exp,\,t} - T_{sim,\,t} \right|}{\left| T_{exp,\,0} - T_{exp,\,t} \right|} \tag{4.1}$$

This approach only makes sense for monotonic temperature changes. As soon as the temperature goes up and down this approach has to be modified. because these changes in temperature are likely to introduce a bigger simulation error. The absolute error is now divided by the difference between the highest and the lowest temperature which were measured in a certain node.

$$\text{error} = \frac{\left| T_{exp,\,t} - T_{sim,\,t} \right|}{\left| T_{exp,\,max} - T_{exp,\,min} \right|} \tag{4.2}$$

When judging an error which was obtained with equation (4.1) or (4.2) it has to be kept in mind that the error accumulates during the simulation. For that reason the error is expected to be larger toward the end of the simulation.

4. 2. Experiments with Low Collector Flow Rates

Experiments with mantle heat exchangers have been performed by S. Furbo and P. Berg in the Thermal Insulation Laboratory in Denmark [1]. In their tests they use low flow rates through the solar collector of, for example, 25 liters per hour in the experiment described in section 4.2.1.

The experiments used in this chapter are idealized in a sense that the influence of the permanently changing solar intensity is eliminated by supplying the mantle with water of a constant temperature. The three experiments represent results from different operation situations. In the first experiment a tank at a uniform low temperature is heated. The second experiment imitates a day cycle with a hot mantle inlet temperature during a part of the experiment, and two hot water draws out off the tank. In the third experiment, the decay of stratification during a 24 hour period is investigated. The tank is not exposed to draws nor a flow through the mantle. All three experiments have been performed with a 200 liter (53 gallon) tank as displayed in Figure 4.1. The cylindrical tank is 1.2 m (3.45 ft) high and 0.46 m (18.1 in) in diameter. An annulus shaped mantle as described in section 2.2. is welded around it. The mantle covers the tank over a height of 0.91 m (35.8 in) positioned 0.1 m (3.94 in) from the bottom and 0.19 m (7.48 in) from the top.

The outer diameter of the mantle is 0.50 m (19.8 in). The thickness of the tank wall is 5 mm (0.20 in); the thickness of the mantle wall is 3 mm (0.12 in). The inlet to the mantle, where the hot anti-freeze liquid from the collector enters, is right at the top of the mantle. The outlet from the mantle is at the bottom of the mantle on the opposite side of the tank to reduce short circuiting of the hot water in the mantle. The inlet to the storage tank, where the cold water from the mains enters is in the middle of the bottom surface of the tank. The outlet from the tank, where the hot water for the load is extracted, is in the middle of the top surface. The tank is isolated. The heat loss coefficient of the insulation material at the sides of the tank is 0.89 W/m^2K. At the top it is 1.79 W/m^2K and at the bottom 2.79 W/m^2K. The material of the wall is

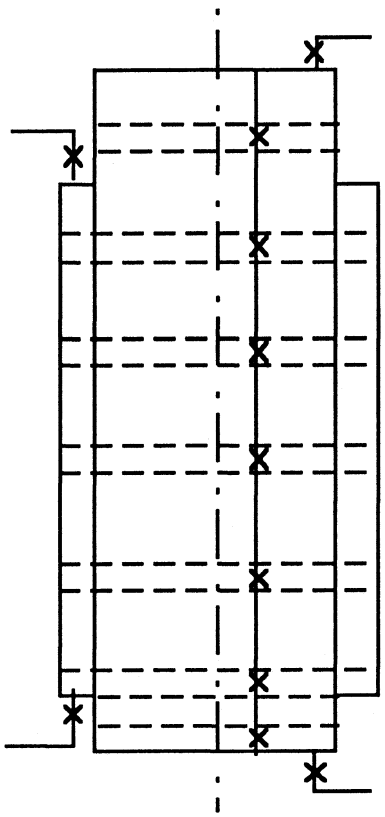

Figure 4.1.: Hot Water Storage Tank with Thermocouples

assumed to be plain carbon steel with a conductivity of 60 W/mK. The heat transfer coefficient from the heat exchanger surface to the liquid in the tank is set to be 2000 W/m^2K, which is equivalent to setting the resistance at that place to zero.

The mantle tank in the Thermal Insulation Laboratory has been equipped with thermocouples (the positions of the thermocouples are represented by crosses in Figure 4.1.). Water is used for both mantle flow and hot water storage in the tank in this experiment.

The temperatures obtained experimentally are measured at a position close to the middle of the tank. The model predicts the average temperature in a node, which is not necessarily equal to the temperature at the middle of the node. With the current model it is not possible to account for temperature changes in radial direction. To limit the influence of the temperature change in vertical direction, relatively small control volumes are laid symmetrically around the thermocouples reaching 2.5 cm (1 in) up and down from the location of the thermocouples. This control volume thickness of 5 cm (2 in) was chosen to obtain a node temperature which is close to a temperature that would be measured in the center of the node. On the other side there is a limit to how small the control volumes can be chosen, as numerical problems occur for too small control volumes. The control volumes between the ones with thermocouples are not split up and their size is therefore fixed.

4. 2. 1. Heating Experiment

4. 2. 1. 1. Description of Experiment

In the heating experiment, the temperatures in the tank are initially between 27 °C and 30 °C. Apart from a transient effect during the first hour, the mantle inlet temperature is fixed at 49.3 °C. The flow rate in the tank is at roughly 30 liters/hour. During this test there are no draws from the tank. The temperatures measured by the thermocouples in the tank are displayed in Figure 4.2. The top temperature curve represents the output from the thermocouple at the top of the tank, the second curve represents the output from the second thermocouple and so on. This thermal stratification follows nicely what would be expected from the physical laws described in section 2.1.2.

The hot liquid flowing through the mantle heats the tank from the top to the bottom because the liquid in the mantle cools as it heats the upper nodes. When the temperatures of the upper nodes get closer to the temperature in the mantle the lower nodes are heated. The temperature at the outlet of the mantle which is displayed in Figure 4.3, never cools to the temperature of the second thermocouple from the bottom which is at the height where the mantle ends. The outlet temperature of the tank is always between the temperature of the second and third thermocouple from the bottom. At the end of the experiment the temperature in the tank and the mantle almost reach a steady state, in which all the energy that is transferred from the mantle to the tank is lost to the environment.

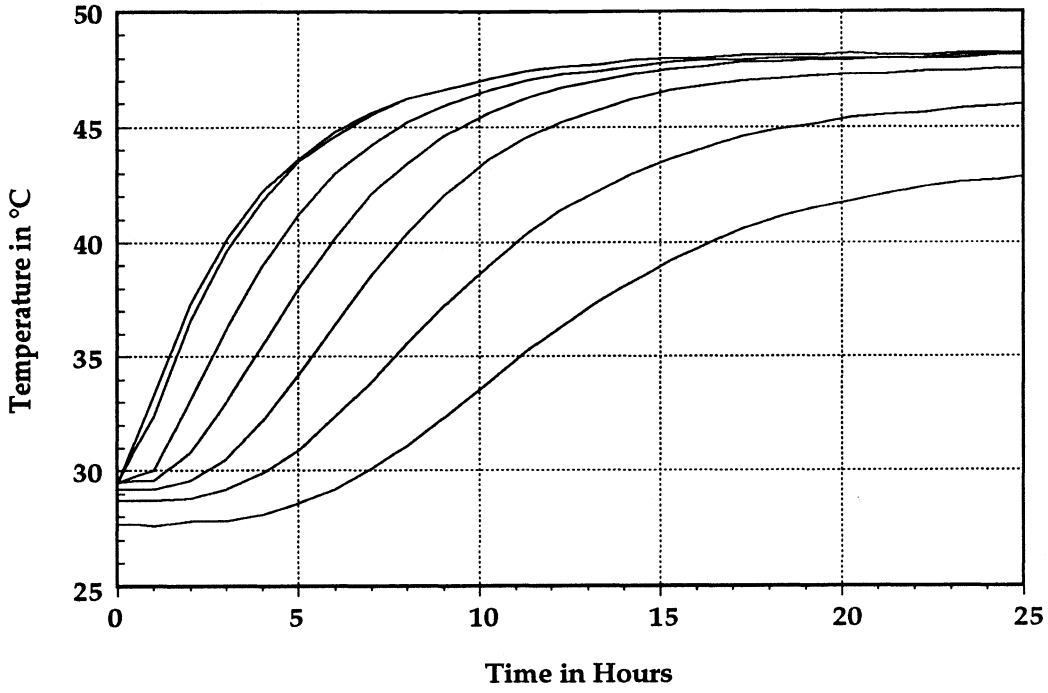

Figure 4.2.: Temperature of the Tank Nodes

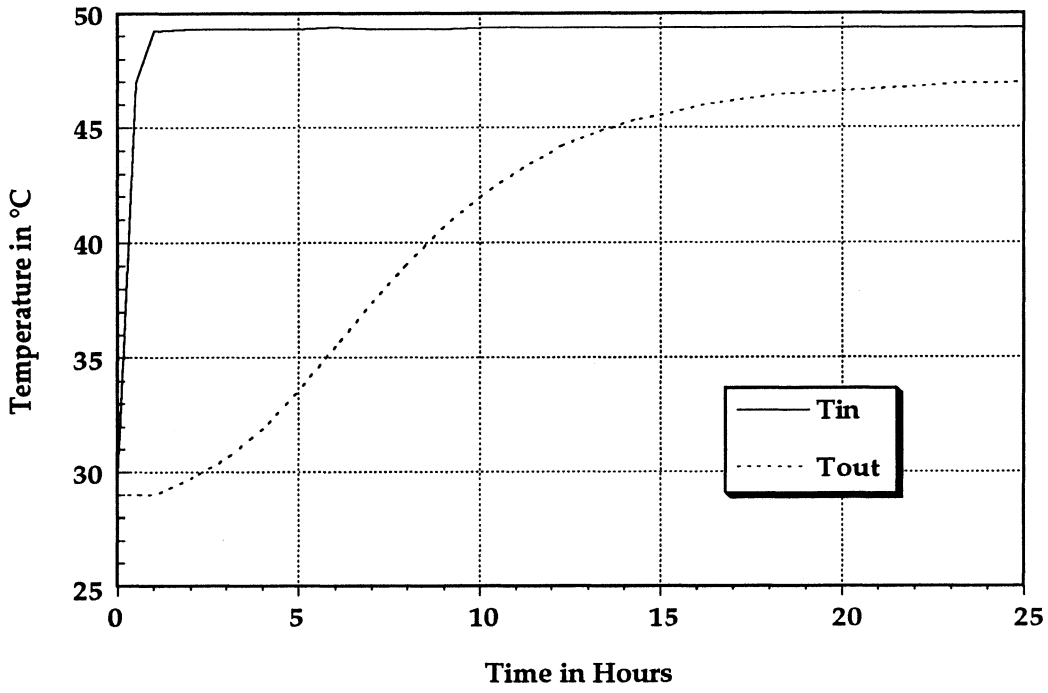

Figure 4.3.: In- and Outlet Temperature of the Mantle

The set up of experiment 1, as described in this and the preceding section, is specified in the according TRNSYS-deck in Appendix B. The only modifications were to halve the number of derivatives for model I, and to change the heat transfer correction factor C_1.

4. 2. 1. 2. Simulation Results for Model I

The temperatures in the tank nodes during the experiment are plotted in Figure 4.4 together with the simulation results for the same experiment. The simulation used a heat transfer correction factor of $C_1 = 1.0$. For this value of C_1, the shape of the simulated curves and their matching with experimentally obtained curves is optimized. The optimization was done by plotting the simulation results for different correction factors together with the experimental data and picking the set of curves with the smallest deviation from the experimental data. With the exception of the temperature at the tank bottom, the simulated temperatures are always higher than the respective experimental results. The error defined in equation (4.1) is large in the beginning for the nodes in the middle of the tank. The maximum error then decreases to roughly 6 % at the end of the simulation. Temperatures in the mantle nodes and the inlet temperature to the tank are shown in Figure 4.5. No temperature measurements were taken in the mantle, therefore only the simulated values of the temperatures in the mantle are shown. The simulated temperature at the mantle outlet is compared to the measured temperature. The simulated temperature is substantially higher throughout the run. It is surprising that the simulated temperature is higher because an energy balance would show, that for similar losses, and a faster rise

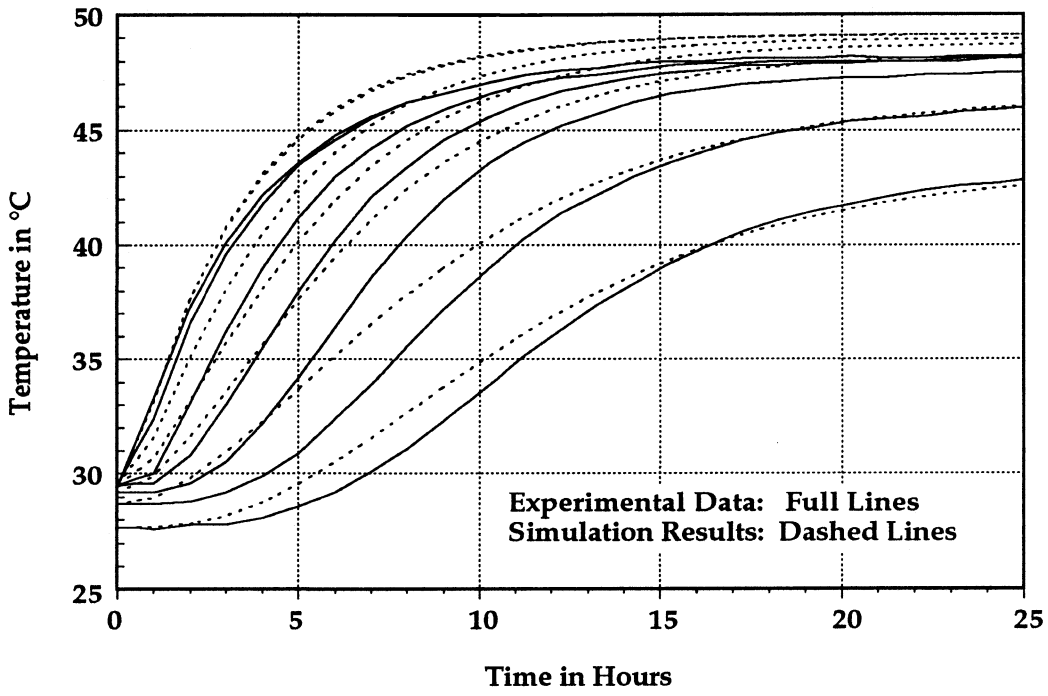

Figure 4.4.: Tank Node Temperatures with Model 1 and C_1=1.0

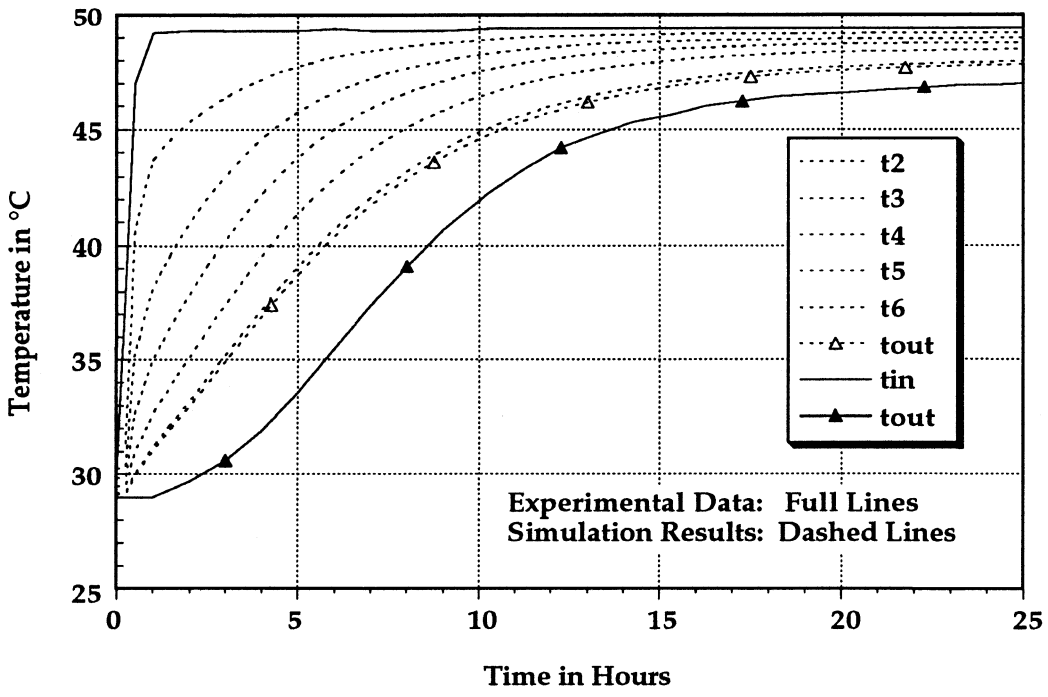

Figure 4.5.: Mantle Node Temperatures with Model 1 and C_1=1.0

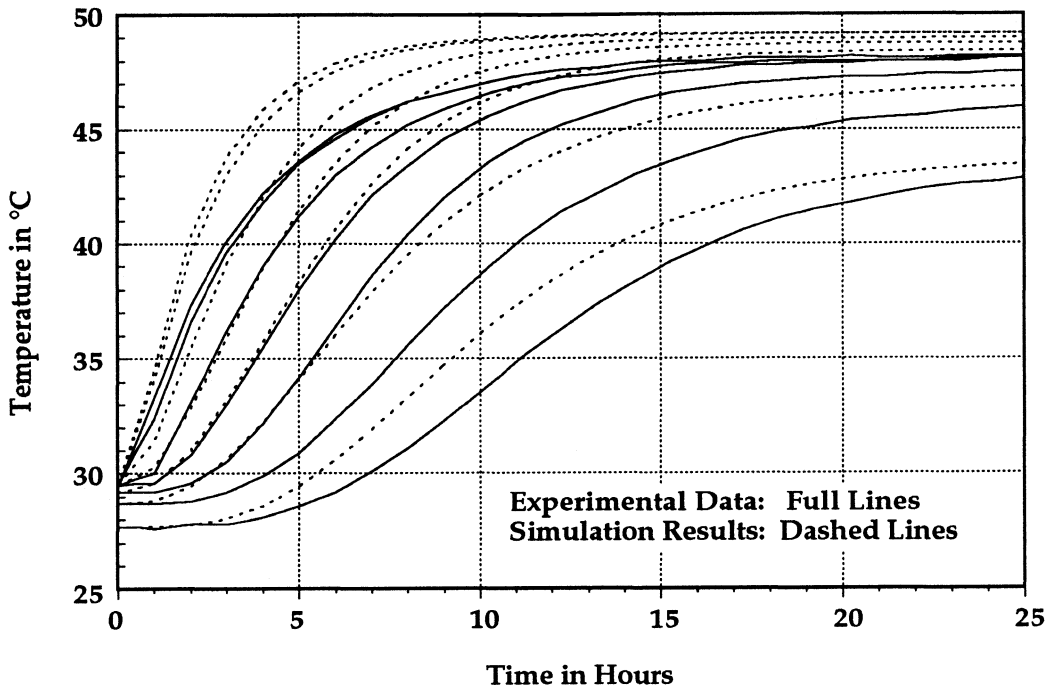

Figure 4.6.: Tank Node Temperatures with Model 1 and C_1=1.8

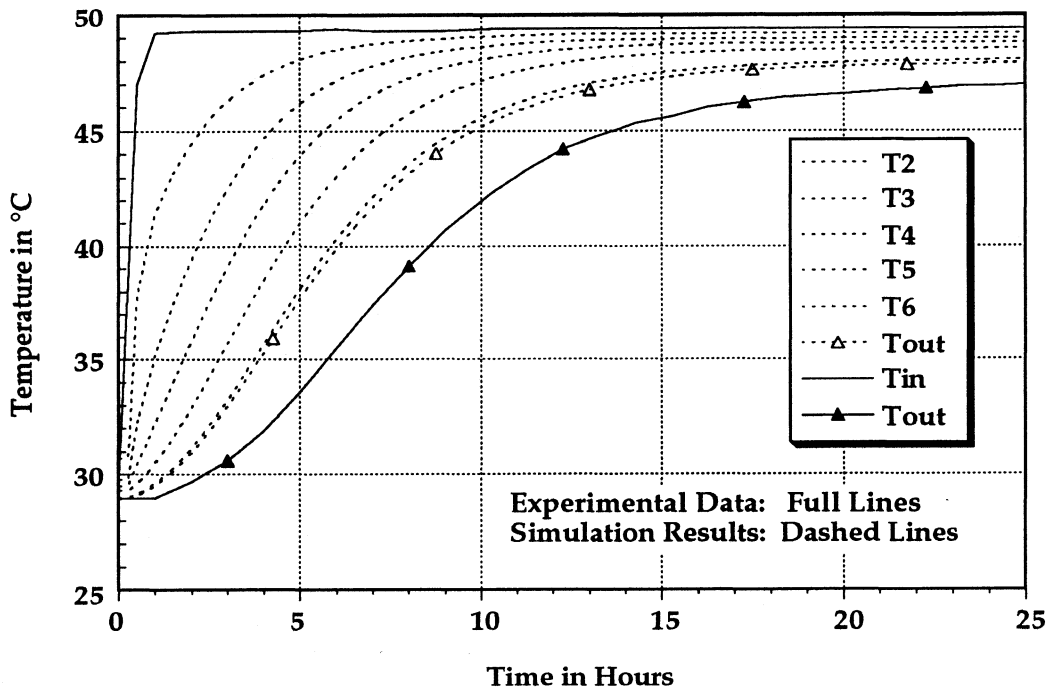

Figure 4.7.: Mantle Node Temperatures with Model 1 and C_1=1.8

in internal energy in the simulation (which is equivalent to a rise in temperature of the tank nodes) the calculated energy input in the mantle would be higher than in the experiment. However the mantle outlet temperature in the simulation which would be expected to be lower is actually higher than in the experiment. If the mantle outlet temperature is higher, the temperature difference between in- and outlet decreases and with it the energy put into the tank. The energy that seems to disappear in the experiment is needed to heat the mantle. The problem lays in the assumption that the flow through the mantle is at steady state during every time step. Therefore the temperature of the liquid in a particular control volume in the mantle is constant during a time step. Consequently the internal energy in the mantle cannot change within the time step either. This effect is only a problem in simulations for short time periods. As soon as the system goes through more than a couple of energy cycles, meaning that after being heated up the tank is cooled again, the effect becomes less important. The storage in the mantle in this case can be regarded as an increase in the total storage capacity.

Another problem with model I can be seen in Figure 4.5. In this steady state model the temperatures in all mantle nodes react immediately when the mantle flow starts even though in the experiment it takes approximately an hour for the water to travel from the top of the mantle to the bottom at the experimental flow rates.

To obtain Figure 4.6 and 4.7 the heat transfer coefficient between mantle and tank was increased by changing the correction coefficient C1 from 1.0 to 1.8. The results of this simulation are shown here even though they are a lot worse than with the correction factor 1.0, because $C_1 = 1.8$ is used in model II. The temperatures in the upper nodes of the tank rise much faster in the

beginning when the higher heat transfer coefficient is applied. The rise in temperature in the lower nodes and at the mantle outlet is delayed because the mantle fluid transfers more energy at the top of the mantle. Slightly higher final temperatures are reached.

4. 2. 1. 3. Simulation Results for Model II

The temperatures in tank and mantle obtained with model II are shown in Figure 4.8 and 4.9 together with the experimental results. Compared to model one the simulated curves follow the experimental results closely. The absolute value of the deviation between experiment and simulation never exceeds one degree. At the end of the simulation the maximum relative error from equation (4.1) is roughly 3 %. The predicted temperatures in most tank nodes and at the outlet of the mantle are slightly higher than the temperatures obtained in the experiment, but the simulated and experimental results are much closer together than in model I. Nevertheless these results indicate that the heat loss coefficient to the environment in the experiment was slightly higher than the one assumed for the simulations.

In Figure 4.8. the simulated temperature of mantle node 6 (T6) and the simulated mantle temperature (Tout) are identical, because model II assumes the mantle nodes to be fully mixed.

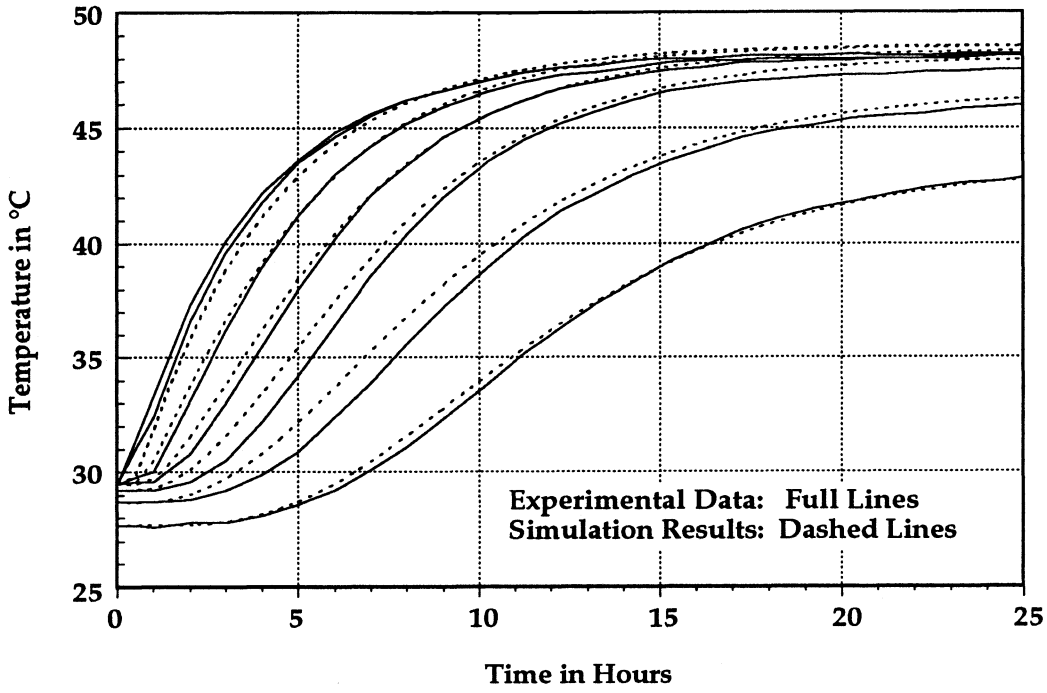

Figure 4.8.: Tank Node Temperatures with Model 2 and C_1=1.8

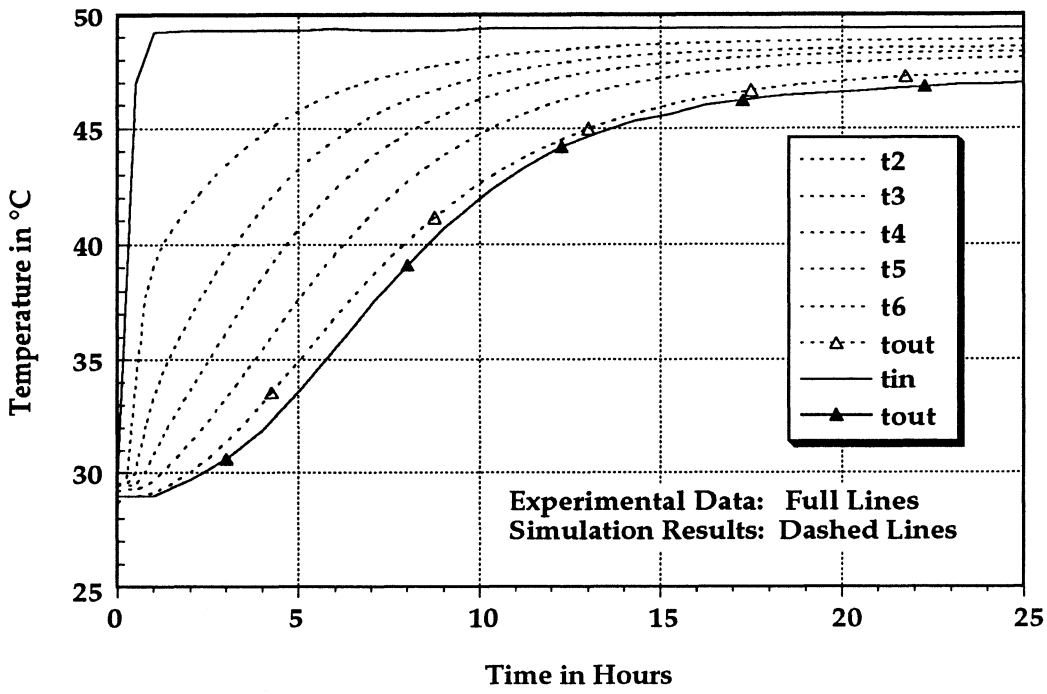

Figure 4.9.: Mantle Node Temperatures with Model 2 and C_1=1.8

4. 2. 1. 4. Comparing Simulation Results from Model I and Model II

To make it possible to compare model I and model II, model I was also simulated for C_1=1.8 as shown in Figure 4.6 and 4.7. Model I treats the flow through the mantle as being in steady state throughout the time step whereas model II accounts for the energy stored in the mantle nodes. This storage of energy in the mantle is the reason why the simulation using model II yields a much slower temperature rise in the tank as well as in the mantle nodes. Towards the end of the simulation however one would expect that the two models should converge because a steady state is almost reached. But the tank node temperatures and the temperature at the mantle outlet are calculated to be between half and one degree higher after 25 hours for model I compared to model II. The reason for that difference is that even in a steady state the average temperature in a mantle node are calculated differently. In model I, the temperature is calculated for every position and then the average temperature over the height of a node is determined. In model II the mantle nodes are considered to be fully mixed, and the time average is used to determine the heat transfer to the environment and into the tank. For that reason model I should provide improved results in cases like here at the end of this experiment where the steady state is approached.

The computational effort for the two models is very similar, provided the same time step is used. For a time step of 1/64 of an hour the tank subroutine is called 3330 times for the 26 hour simulation. 3330 calls mean exactly two calls per time step, which is the minimum for modules that have to be checked for convergence. The run, that uses model I takes 26.3 CPU seconds and a run with model II takes 28.2 CPU seconds.

4. 2. 2. Experiment with Draws

4. 2. 2. 1. Description of Experimental Set Up

This experiment approximates normal operation of a energy store in a solar domestic hot water system. The temperatures in the tank are initially between 16.5 °C at the bottom and 19.1 °C at the top. The mantle flow rate is, with small variations, 23.5 liters/hours. The temperature at the mantle inlet is 30 °C for the first hour and 45 minutes. It is then set to 70 °C for four hours, and finally set back to 30 °C for the rest of the experiment as it can be seen in Figure 4.11. The load flow is imitated by two 50 liter draws, the first after one hour and the second after 3.5 hours. The water which is drawn, is replaced with water from the mains at 14.2 °C. These draws cause the steep temperature drops in the tank in Figure 4.10. After 6.5 hours the mantle inlet temperature is smaller than the temperature in tank so that it actually cools the tank. It is surprising that the two bottom nodes in the tank, and the mantle outlet temperature are hardly effected either by the draws or by the big changes in mantle inlet temperature.

4. 2. 2. 2. Simulation Results from Model I

In Figure 4.12, the simulated temperatures obtained with model I and a heat transfer correction factor of one are plotted together with the experimental results. The simulated temperatures during most parts of the experiment are between two and three degrees higher than the corresponding measured temperatures. Most of the simulated temperature curves are closer to the

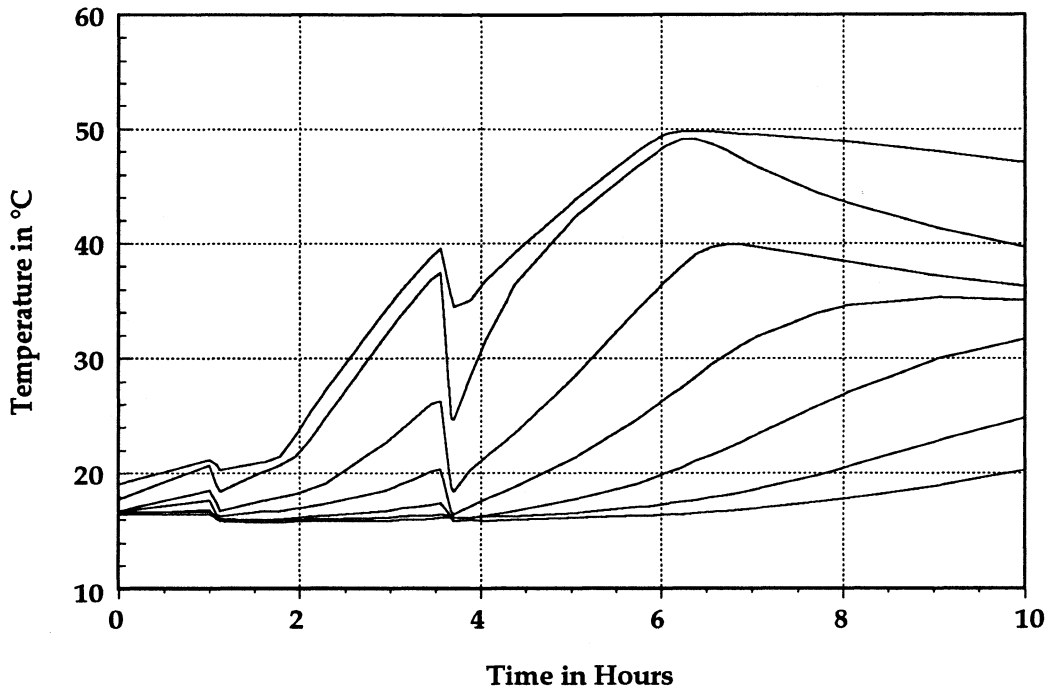

Figure 4.10.: Temperatures at Thermocouples in Tank

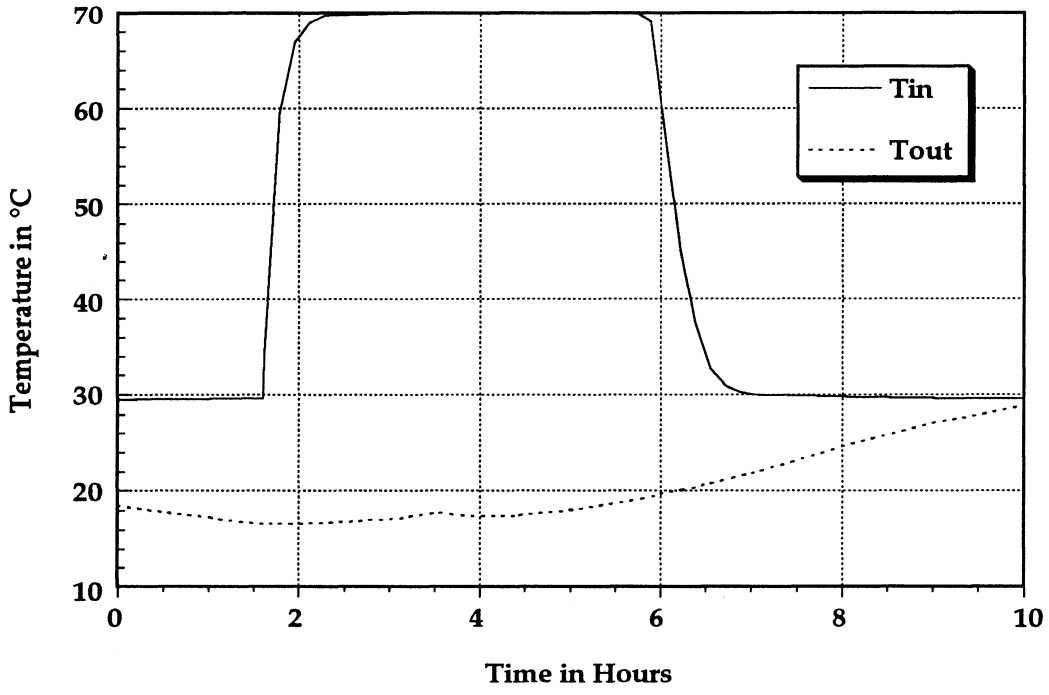

Figure 4.11.: Temperatures at Mantle Inlet and Outlet

temperature curve measured in the node above. In contrary to the experimental data, the simulated temperatures of the two bottom nodes and of the mantle node react strongly (with temperature drops) to the two draws. They also react stronger to the change in mantle inlet temperature than observed in the experiment. The simulated mantle node temperatures and mantle outlet temperature are plotted in Figure 4.13. The mantle outlet temperature is apart, form some periods during the first two hours always higher than the measured mantle outlet temperature. As in the heating experiment this effect is caused by the inability of model I to account for energy storage in the mantle. After 6.5 hours the mantle inlet temperature drops to 30 °C, and the temperature in the top two mantle nodes (T2 and T3) fall below the temperatures in the lower mantle nodes. This situation can occur as there is no algorithm that prevents temperature inversions in the mantle. It is assumed that under most flow conditions the flow velocity and liquid viscosity are high enough to sustain the inversions. In reality, some mixing occurs, but unfortunately the temperatures in the different mantle nodes were not recorded during the experiment.

In Figure 4.14. and 4.15 the results for the simulation with a correction factor C_1 = 1.8 are shown. As expected for a higher heat transfer coefficient the temperatures in the higher tank nodes are higher than for C_1 = 1.0. The lower tank nodes are heated slower because, due to the high heat transfer coefficient, more energy is transferred to the higher nodes and consequently the temperature in the mantle is lower once it reaches the lower nodes. For this reason the simulated temperatures in the mantle nodes are lower than for C_1 = 1.0 during periods with a high mantle inlet temperature and they are higher for the low mantle inlet temperature after 6.5 hours.

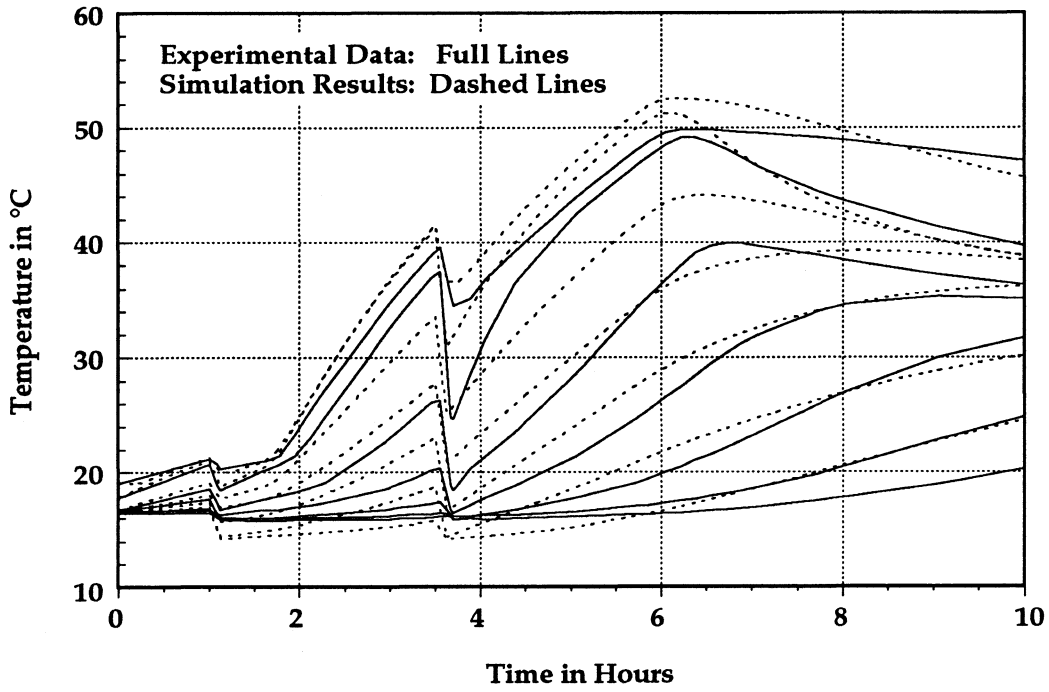

Figure 4.12.: Tank Node Temperatures with Model 1 and C_1=1.0

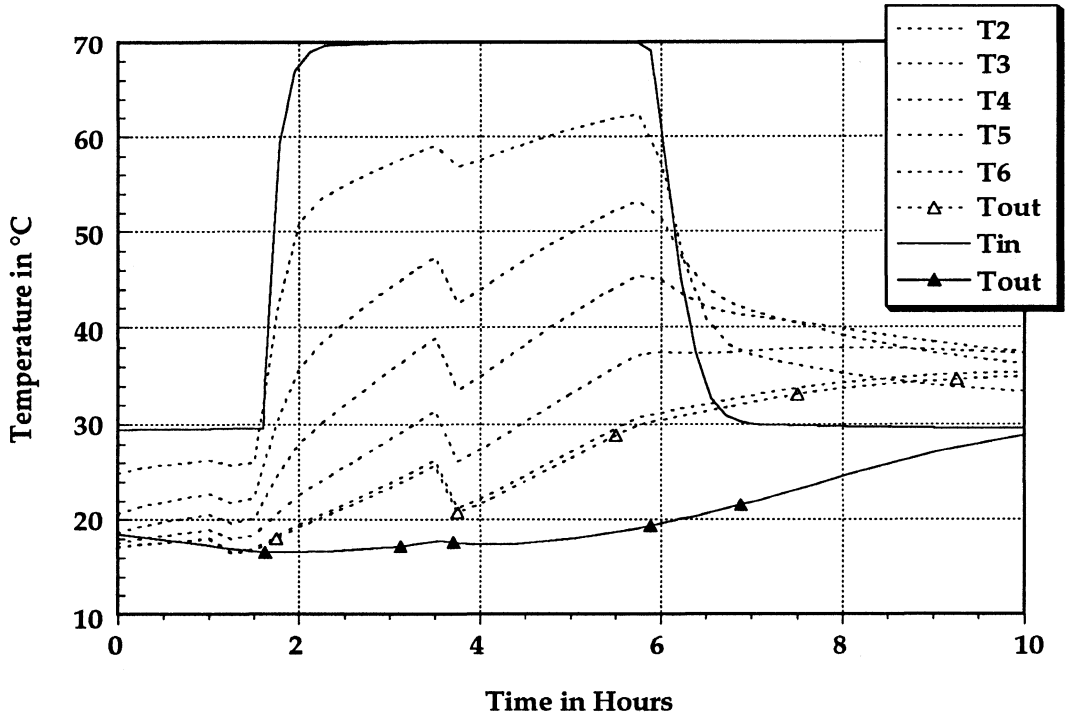

Figure 4.13.: Mantle Node Temperatures with Model 1 and C_1=1.0

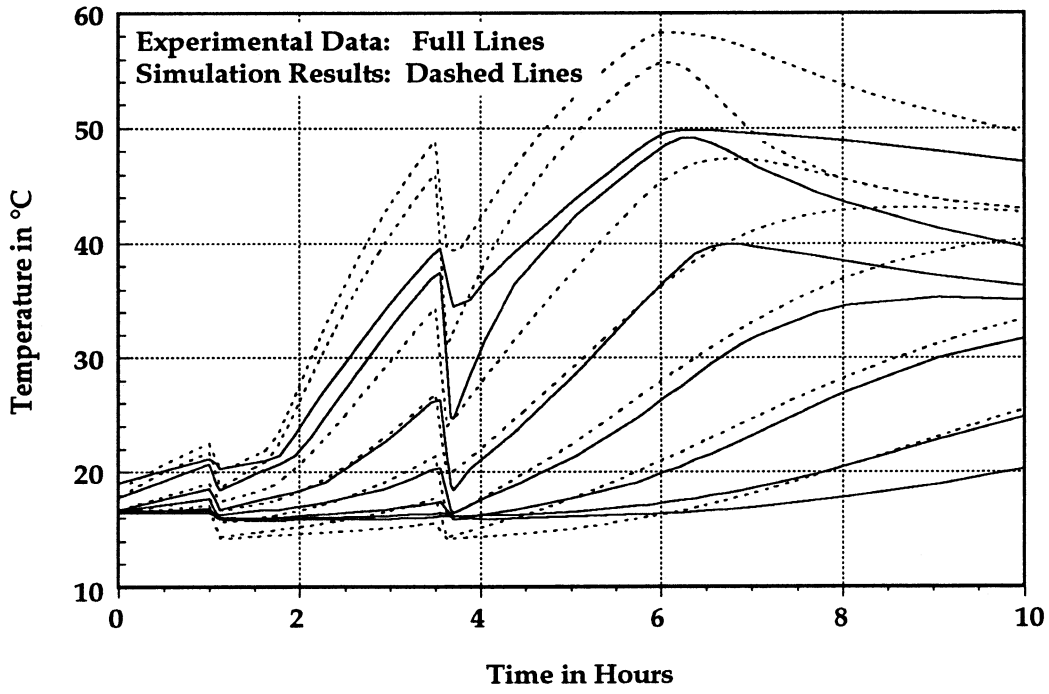

Figure 4.14.: Tank Node Temperatures with Model 1 and C_1=1.8

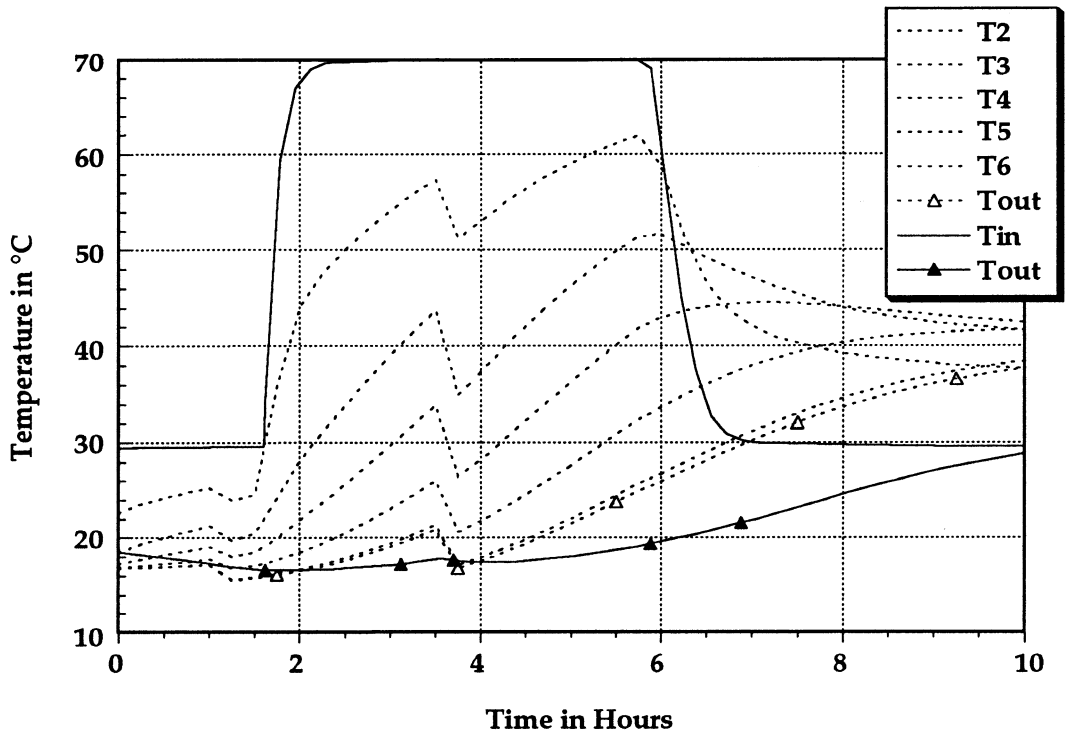

Figure 4.15.: Mantle Node Temperatures with Model 1 and C_1=1.8

4. 2. 2. 3. Simulation Results from Model II

The results of the simulation with model II and a heat transfer correction factor of C_1 = 1.8 are shown in Figure 4.16 and 4.17. The simulated temperature curves for the top two nodes stay under the measured value throughout the simulation. The simulation of the temperature in the third, fourth and fifth node yields temperatures that are between one and three degrees higher than the measured temperatures. The simulation for the two bottom nodes yield lower temperatures for roughly the first half of the simulation, and yield higher temperatures from there to the end of the simulation. The simulation using model II also reacts strong to the draws in the two bottom nodes. The temperatures in the mantle nodes are calculated to be a lot smaller than their values obtained with model I and C_1 = 1.8. The temperature at the mantle outlet is much closer to the experimental value than with model I. The difference between calculated and experimental temperatures is never greater than two degrees. The shape of the simulated mantle outlet temperature is also much closer to the experimental result as the effects of the draws are much smoother.

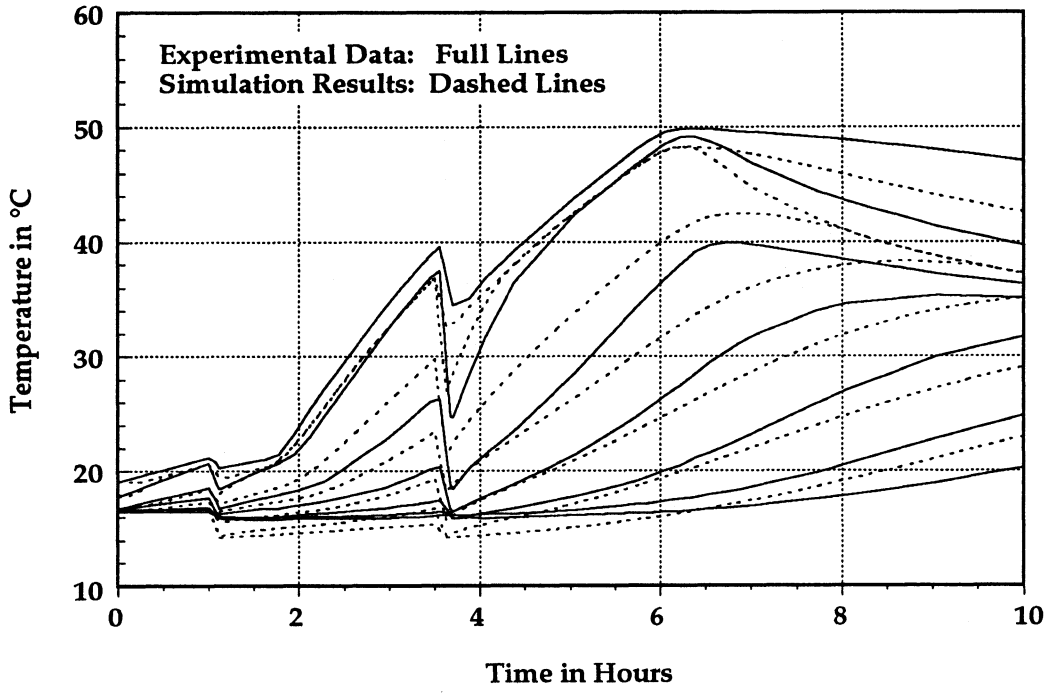

Figure 4.16.: Tank Node Temperatures with Model 2 and C_1=1.8

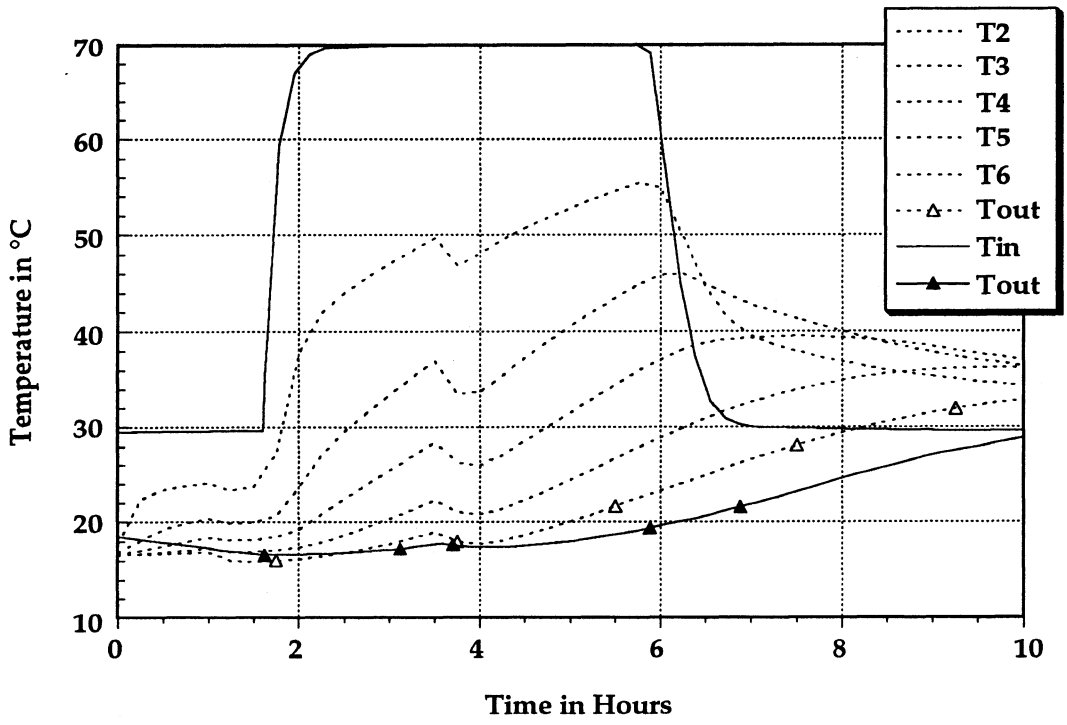

Figure 4.17.: Mantle Node Temperatures with Model 2 and C_1=1.8

4. 2. 3. Cooling Experiment

4. 2. 3. 1. Description of Experiment

In this test, not only the cooling of a tank filled with hot water is investigated, but also the decay of thermal stratification over time. The stratification of the tank that is originally at an almost uniform temperature of 48 °C, is obtained by tapping half of the volume of the water and replacing it with cold water from the mains at 16.8 °C. The initial situation obtained by this procedure is that the top half of the tank is at temperatures between 44 °C and 48°C and the bottom half is at temperatures between 19 °C and 22 °C. After the draw in the beginning no more water is drawn nor is any water run through the mantle. The top nodes of the tank cool down due to losses to the environment but they also loose energy to the lower nodes by conduction. The heat conduction from the top nodes heats the lower nodes.

4. 2. 3. 2. Simulation Results from Model I and Model II

The simulation results for model I with C_1 = 1.0 and for model II with C1=1.8 are plotted in Figure 4.18 and 4.19, respectively. Results from simulations with model I and C1=1.8 have not been plotted as they are not visibly different from simulations with C_1 = 1.0. The simulation results from the two models are fairly similar to each other and therefore discussed in one section. The similarity is not surprising as the difference between the two models is the way the mantle is treated when the flow rate in the mantle is non-zero. Both models equally underpredict the speed of the stratification decay. That means

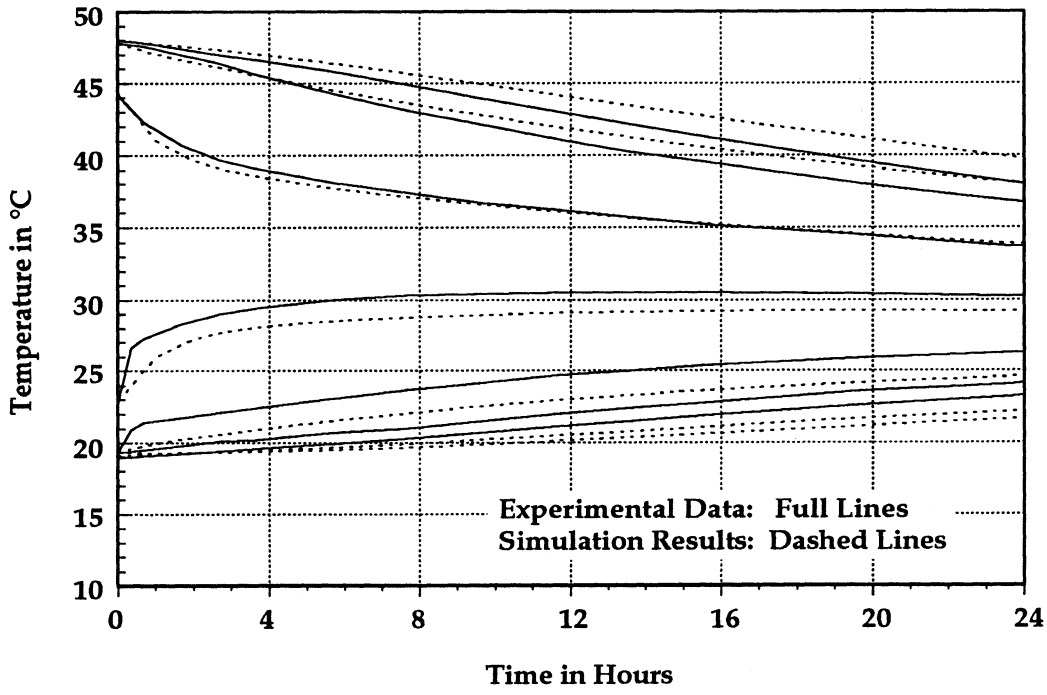

Figure 4.18.: Tank Node Temperatures with model 1 and C_1=1.0

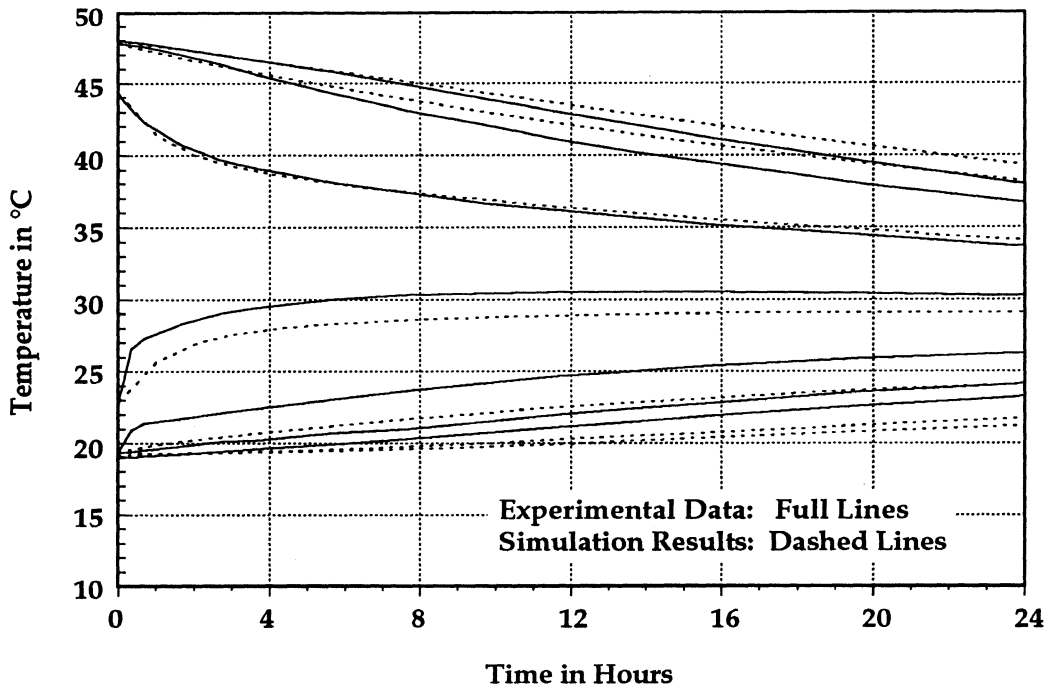

Figure 4.19.: Tank Node Temperatures with model 2 and C_1=1.8

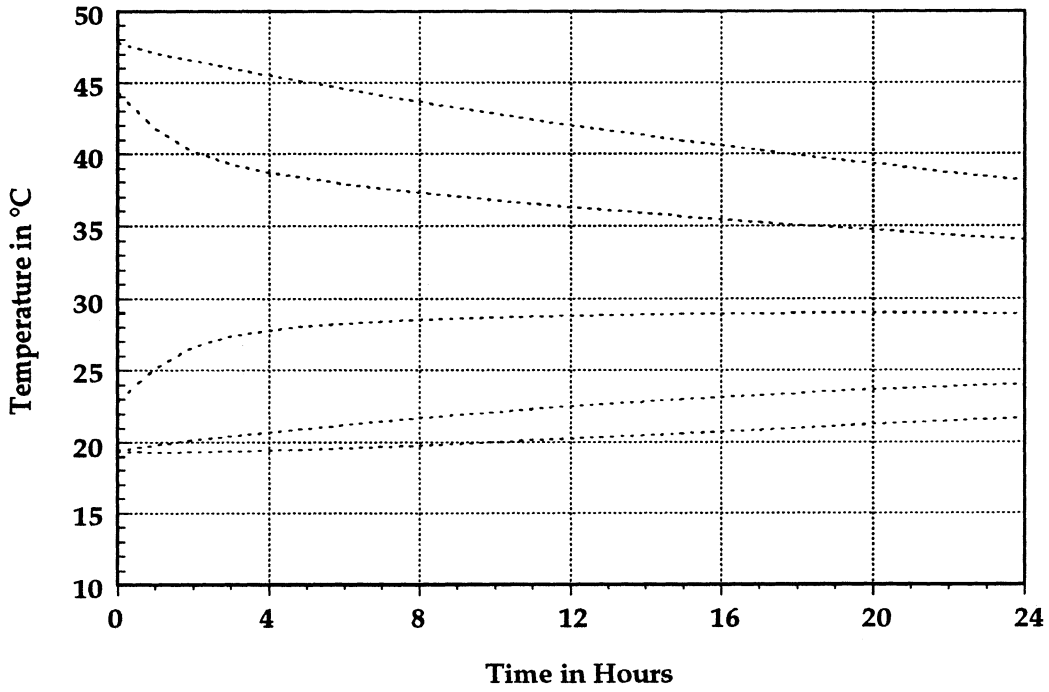

Figure 4.20.: Mantle Node Temperatures with model 2 and C_1=1.8

that the hot nodes are calculated to cool too slow, and the cool nodes are calculated to heat up too slow. The behavior of the third node from the top is predicted much better than the behavior of the other nodes. The stratification decays too slowly in the simulation because free convection has been excluded as a mode of heat transfer in both models. To improve the model free convection has to be taken into account, but as discussed in section 3. 3. 3. currently existing equations are not applicable in this circumstances.

The small difference between the two models are due to the fact that in model II, the mantle stores energy. The heat capacity of the mantle slows down the decay of stratification in the tank. The calculated temperatures in the mantle nodes 2, 3, 4, 5, and 6 from model II are displayed in Figure 4.20.

As the temperature changes are very slow the mantle temperatures are almost identical with the simulated temperatures in the tank.

4. 3. Experiment with Regular Flow Rates

4. 3. 1. Description of Experiment

A series of indoor experiments with solar systems have been performed in the Solar Calorimeter Laboratory. A solar simulation facility has been used for these experiment to have control over the environmental conditions. The experiment, which was simulated for this thesis was run during a period of 24 hours. The conditions during the experiment imitate the operation conditions of a typical day. The amount of incoming solar radiation in the experiment is equivalent to an average day in March in Madison, Wisconsin. Water is drawn to meet a standardized load at every hour between 7 am and 1 pm and between 4 pm and 9 pm. The draws are between 5 liters and 45 liters and total 225 liters for the whole day. The distribution of the draws is displayed in Figure 4.22. To exclude simulation errors from the solar collector, only the tank has been modeled in this simulation.

The storage system used is a tank-in-tank system similar to the one described in section 2.2. The tank-in-tank system is shown in Figure 4.21. The inner tank has a volume of 208 liters and the shell contains 19 liters. The height of the inner tank is 1.48 m, and the total height is 1.54 m. The diameter of the inner tank is 0.44 m. The boundary wall between shell and inner tank is 1.6 mm thick and undulated to increase the heat transfer coefficient and the heat exchanger surface. Due to the undulation, the smallest distance between

the inner and the outer tank wall is 9 mm and the largest distance is 25 mm. The undulations increase the heat transfer area by a factor of 1.2 compared to a flat wall. The outer tank is insulated with a 30 mm thick rubber foam layer. The rubber foam is coated with a PVC covering. The combined loss coefficient from the outer tank is estimated to be 1.2 W/m^2K.

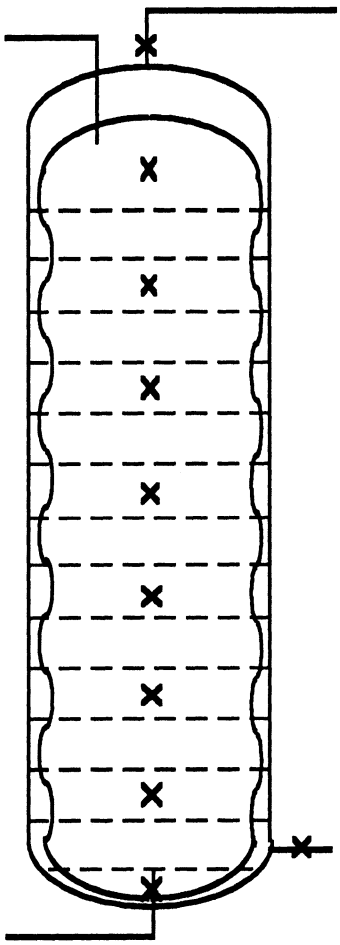

Figure 4.21.: Tank-in-tank System with Thermocouples

The mantle is fed with a 60-40 percent water-propylene glycol mixture from the solar collector. The measured inlet and outlet temperatures at the outer tank are displayed in Figure 4.23. The pump for the collector loop

operates between 8 am and 4 pm as shown in Figure 4.22. The storage tank is fed at the bottom with replacement water from the mains at a temperature of 18 °C. The eight thermocouples in the tank are positioned at the bottom of the tank and than at distances of 0.2 m above each other. The tank-in-tank system is approximated by using the mantle heat exchanger model for a mantle which extends from the shell outlet to the top of the tank . This procedure introduces an error in the determination of the temperature in the top node, as only the side walls of the heat transfer surface at the top node are used for the simulated heat transfer. For the numerical simulation the volume in the tank was split up into fifteen control volumes. All of the nodes except the top and the bottom node, have a thickness of 0.1 m and the thermocouples are positioned in the center of the node. The temperatures measured by the thermocouples in the tank during the experiment are displayed in Figure 4.24.

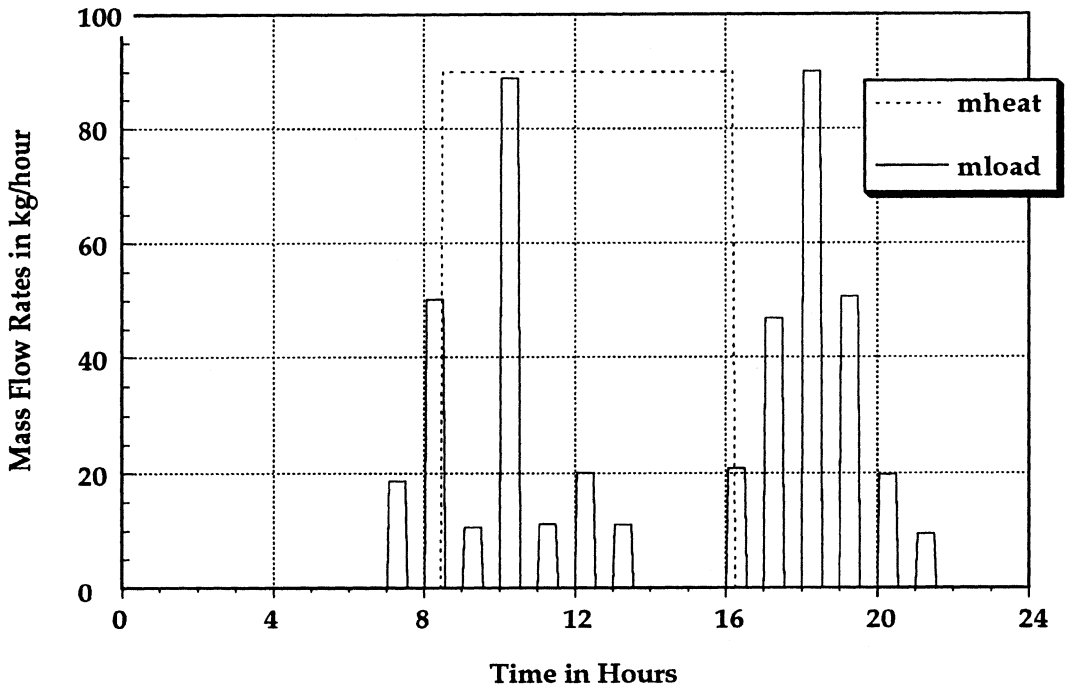

Figure 4.22.: Mass Flow Rate of Load and of Heat Source

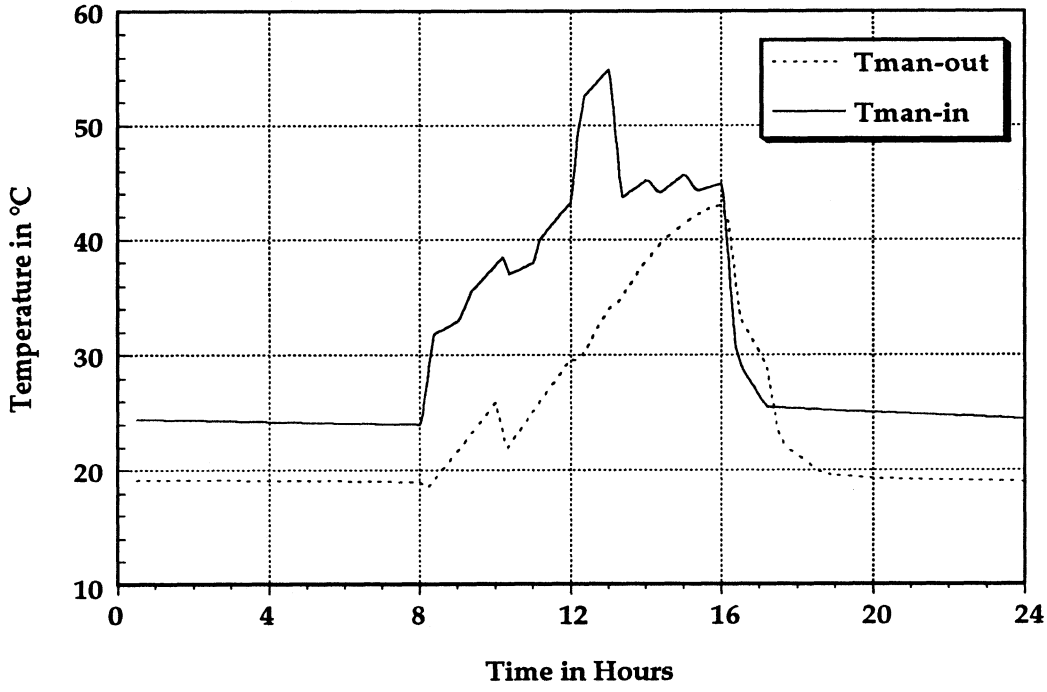

Figure 4.23.: Mantle Inlet and Outlet Temperature

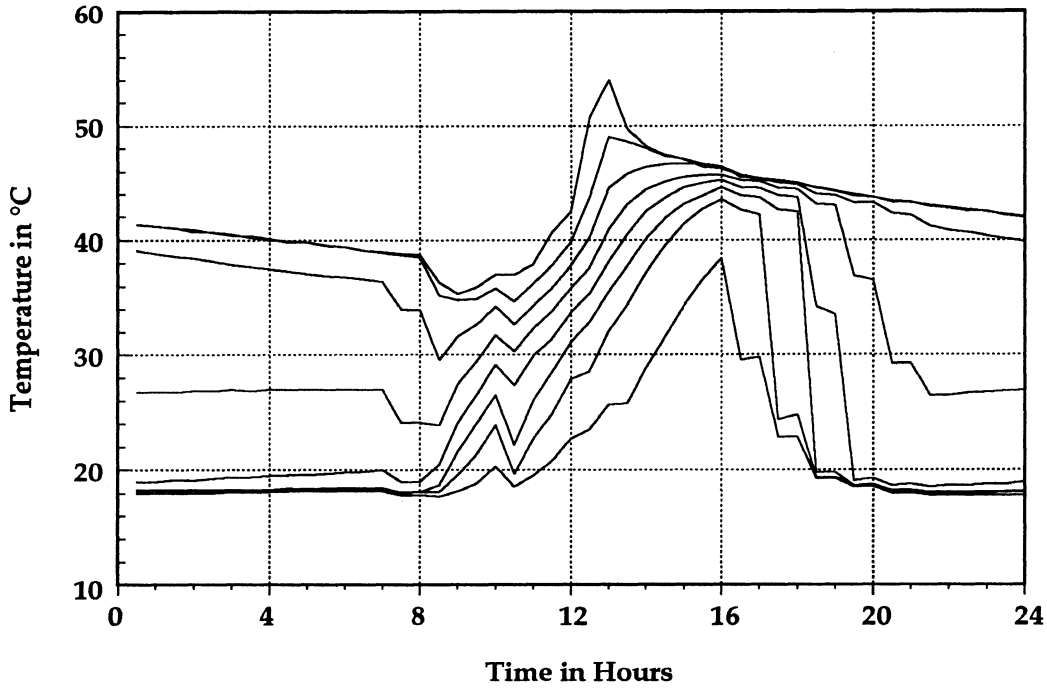

Figure 4.24: Temperatures Measured by Thermocouples in Tank

4. 3. 2. Simulation Results with Model I

In Figure 4.25a and 4.25b, the temperatures in the inner tank nodes obtained with model I and a heat transfer correction factor C_1=1.0 are plotted together with the experimental results. The temperature curves for nodes 1, 3, 5, and 7 are shown in Figure 4.25a and the curves for nodes 2,4,6, and 8 are shown in Figure 4.25b in order to make it easier to read the graphs. The first seven hours of the experiment are very similar to the cooling experiment discussed in chapter 4.2.3 as there is no draws and no flow through the shell. During the period with flow through the shell (from 8 am to 4 pm) the temperatures in the inner tank are underpredicted by one to four degrees. The calculated temperatures of the top and the bottom node differ from the measurements by as much as 16° C. The top node is underpredicted by a maximum of seven degrees and the bottom node is underpredicted by 16 degrees at the worst point. This strong deviation results from the fact that the mantle heat exchanger model does not account for the heat transferred through the top of the inner tank. As the mantle is specified to have its lowest point at the shell outlet, the bottom node is not surrounded by the shell. This specification was chosen to get a good estimate of the shell outlet temperature sacrificing exactness in the simulation of the bottom node, as the bottom node, in reality, is surrounded by the mantle.

For the period with no flow through the shell but with draws the calculated temperature of most nodes is relatively close to the experimental data. The exceptions are the simulation results for the inner tank nodes 2, 3 and 5. The simulated temperature values are too low for node 2 and 3 and too high for node 5. The experimental tank has a higher degree of stratification

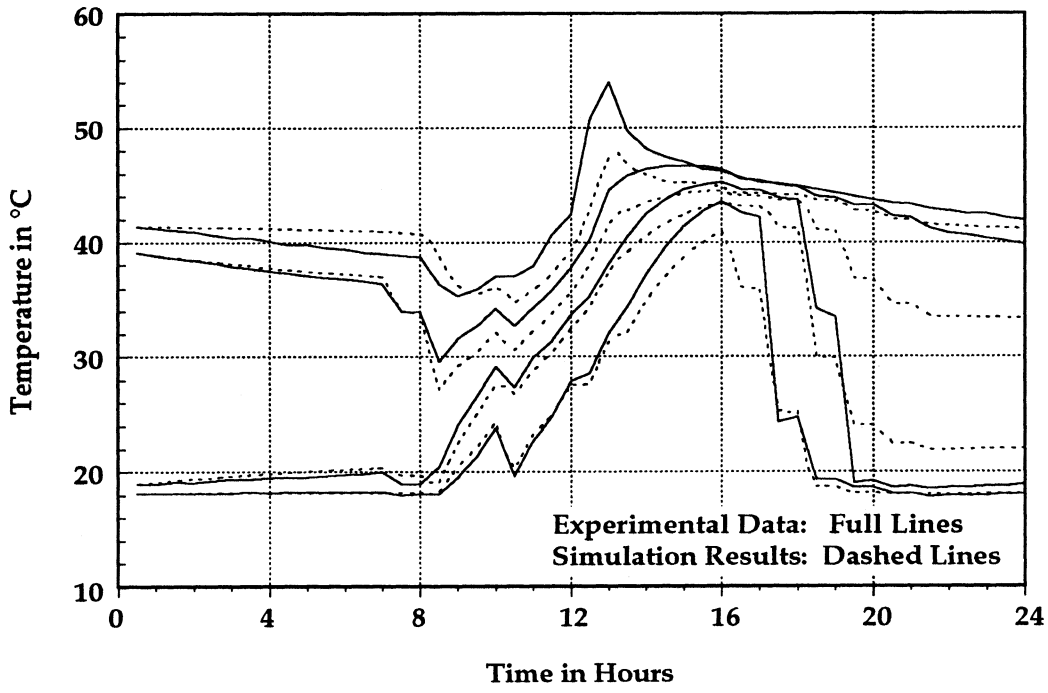

Figure 4.25a.: Temp. in Tank Nodes 1, 3, 5, 7 obtained with Model I (C_1=1.0)

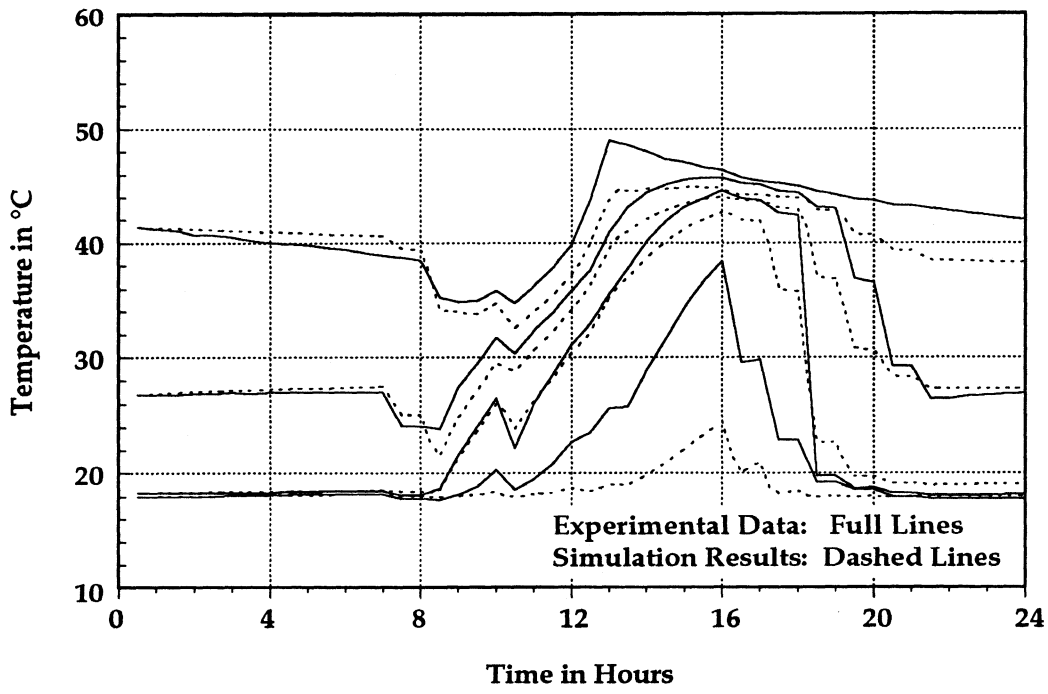

Figure 4.25b.: Temp. in Tank Nodes 2, 4, 6, 8 obtained with Model I (C_1=1.0)

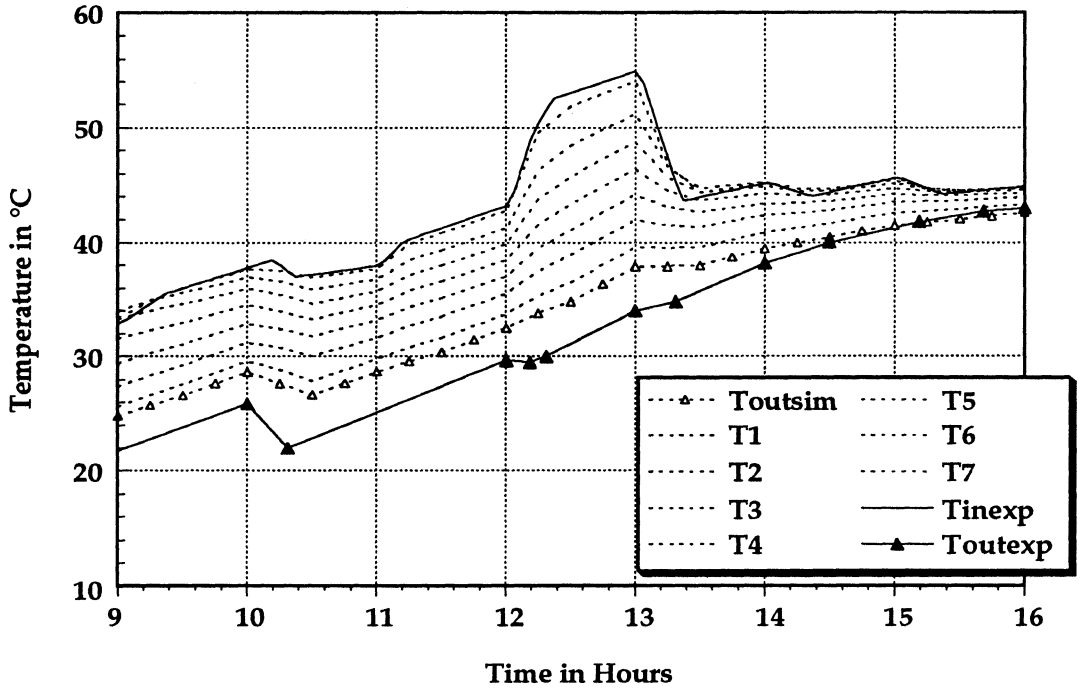

Figure 4.26.: Temperature in Mantle Nodes, obtained with Model I (C_1=1.0)

than the simulated tank. The temperatures in the outer tank nodes and at the outer tank outlet are plotted in Figure 4.26 together with the measured values of the outer tank inlet and outlet temperatures. These temperatures are plotted only between 9 am and 4 pm as model I does not calculate the temperature in the mantle during times without flow through the shell. The calculated temperature at the outlet of the outer tank is higher than observed in the experiment.

To obtain Figure 4.27a , 4.27b and 4.28 the heat transfer coefficient between outer and inner tank has been changed by using a correction factor of C_1 = 1.8 instead of C_1 = 1.0. The temperature curves obtained with this higher heat transfer correction factor show a much better agreement with the experimental results than for C_1 = 1.0. The simulations of the top and bottom

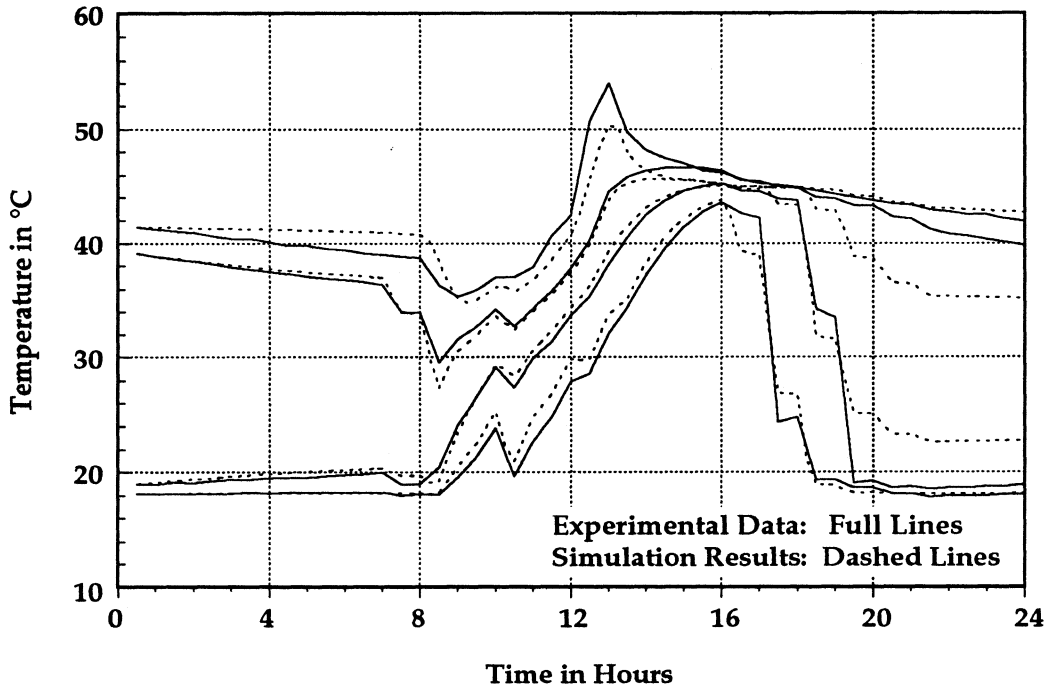

Figure 4.27a.: Temp. in Tank Nodes 1, 3, 5, 7 obtained with Model I (C_1=1.8)

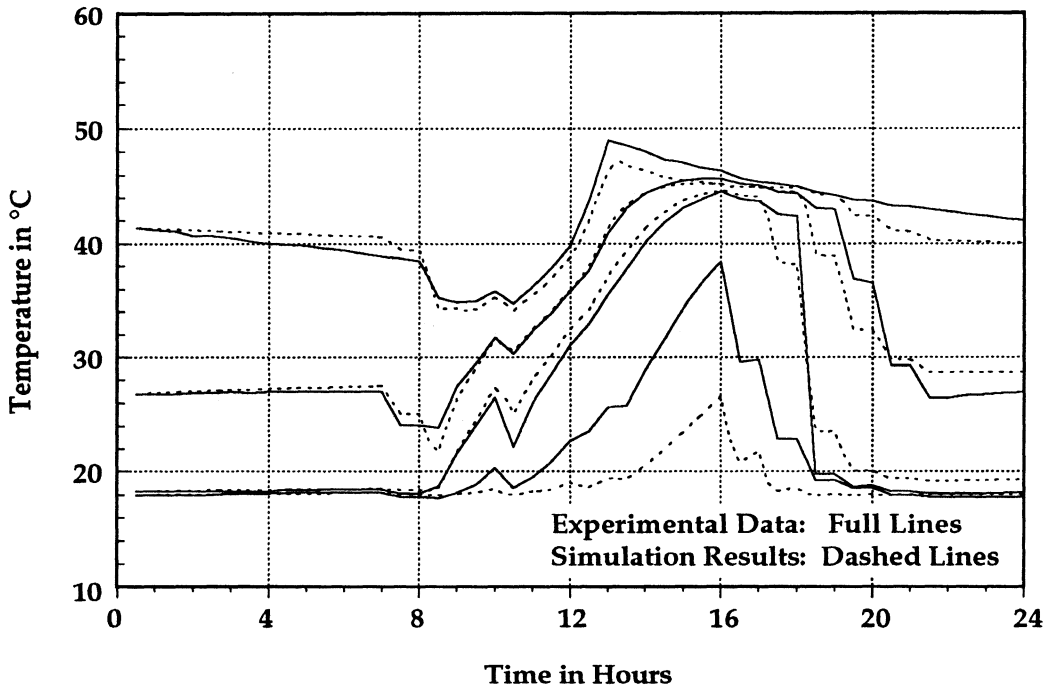

Figure 4.27b.: Temp. in Tank Nodes 2, 4, 6, 8 obtained with Model I (C_1=1.8)

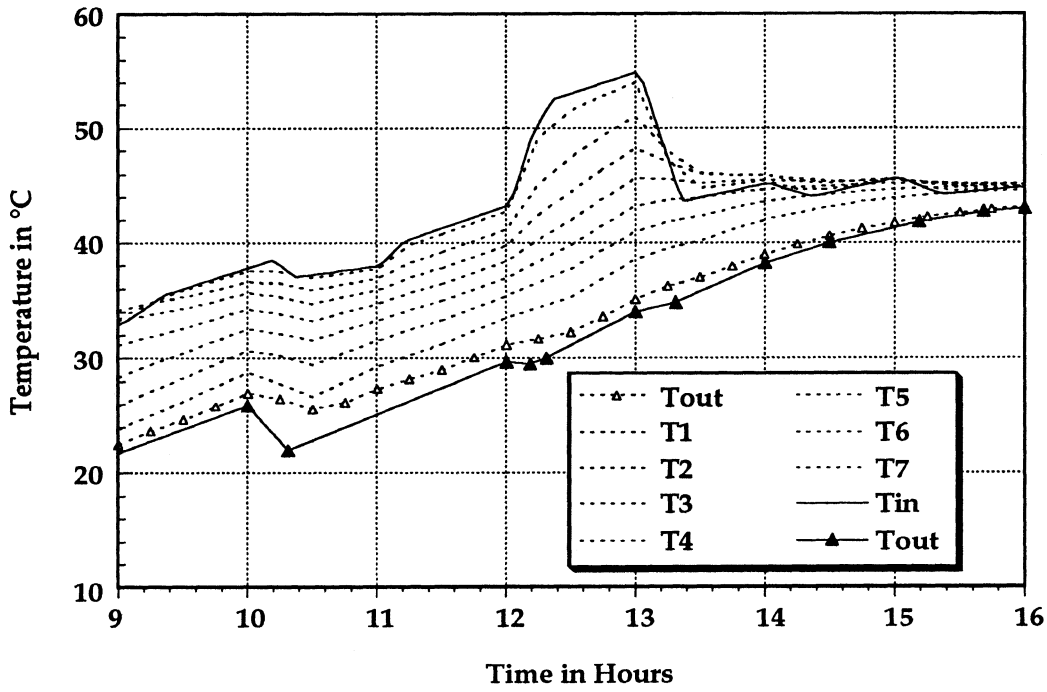

Figure 4.28.: Temperature in Mantle Nodes, obtained with Model I (C_1=1.8)

node behave much better and show a reduction of the maximum temperature deviation of about 30%. As a consequence of the higher heat transfer coefficient, more energy is transferred from the liquid in the shell to the tank. Therefore the simulated temperature of the shell outlet is colder and closer to the measured temperature.

4. 3. 3. Simulation Results with Model II

A simulation using model II has been performed with a heat transfer correction factor of C_1 = 1.8. The temperatures of the tank nodes are displayed in Figure 4.29a and 4.29b. The corresponding temperatures in the outer tank are shown in Figure 4.30. The temperatures are displayed for the whole time of the experiment as model II has the capability of determining the mantle

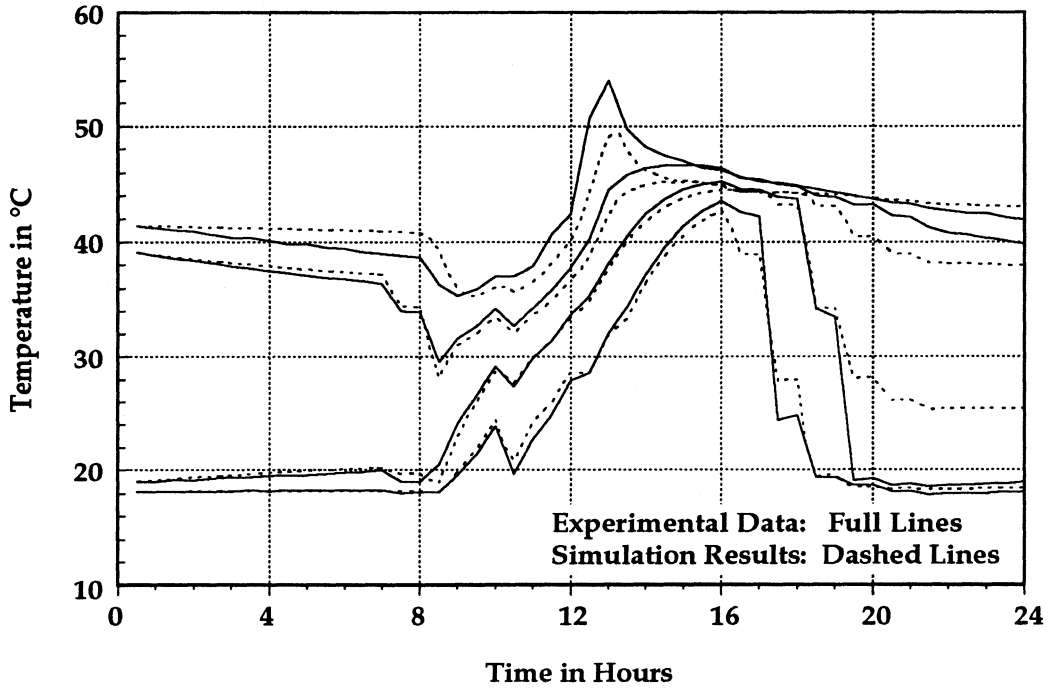

Figure 4.29a.: Temperatures in Tank Nodes 1, 3, 5, 7 obtained with Model II

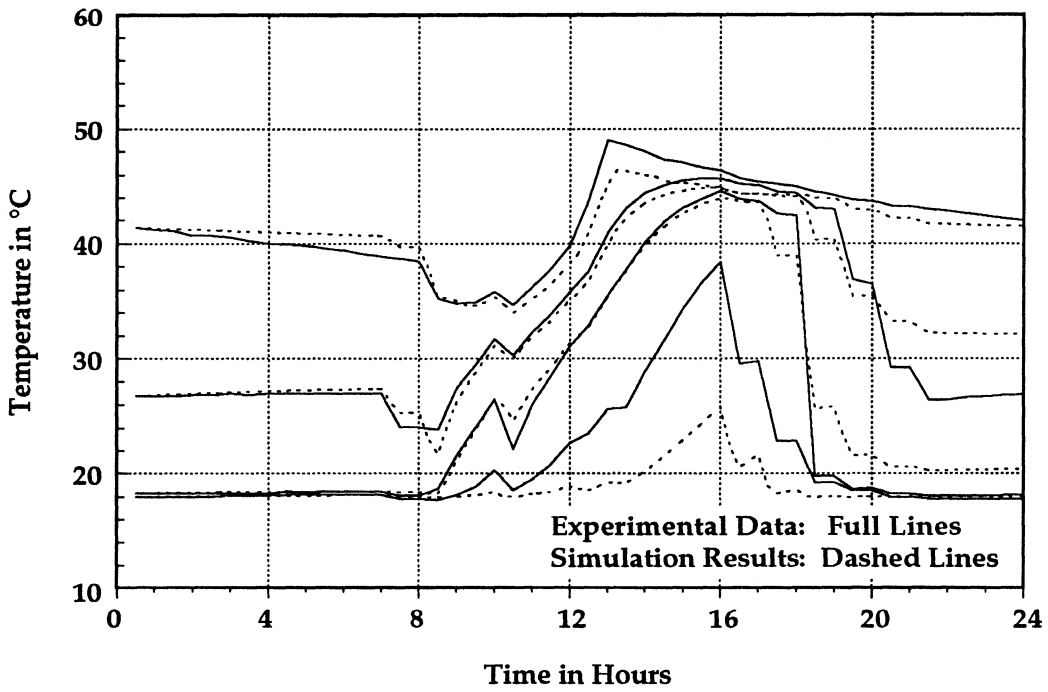

Figure 4.29b.: Temperatures in Tank Nodes 2, 4, 6, 8 obtained with Model II

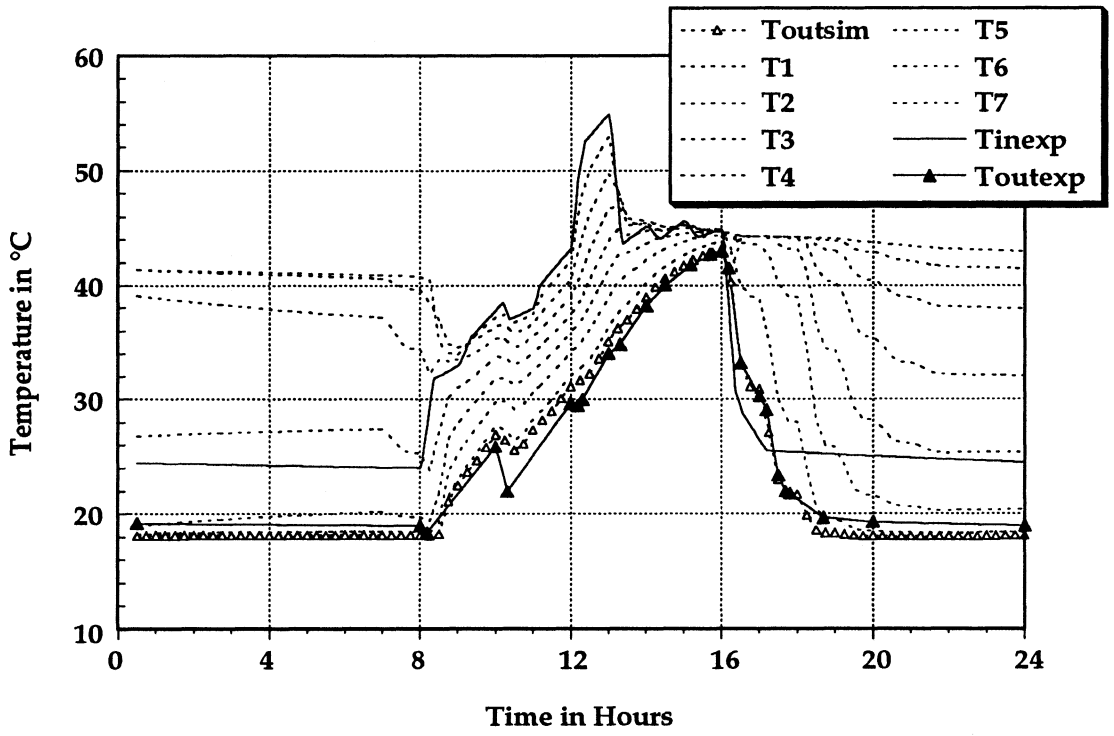

Figure 4.30.: Mantle Temperatures with Model II

temperatures without flow through the mantle. The simulation results are very similar to the results obtained with model I and a heat transfer correction factor of $C_1 = 1.8$. The reason why the simulation results here obtained with model I and model II are much more similar than in the experiments with low collector flow rates (section 4.2.) is that the influence of the energy stored in the outer tank is smaller for higher flow rates. In the experiment discussed in this section the liquid in the shell is exchanged 4.5 times per hour whereas the liquid in the mantle is exchanged once per hour or less in the experiments with low flow rates in section 4.2.

The difference between the two models is that with model II the tank temperatures react slightly slower to energy inputs and outputs. While the tank is being heated the temperatures calculated with model II are slightly

lower than for model I and during times of draws. During the time when there is no mass flow through the shell and energy is drawn from the tank, the tank nodes simulated with model II cool at a slower rate than in model I. The faster reaction of the tank simulated with model I is caused by the fact that model I does not account for energy storage in the mantle.

5. Investigation of Mantle Heat Exchanger Tanks

Computer simulations of energy systems are performed to optimize their energy yield. In this chapter, yearly simulations of a sample system are performed to investigate the impact of different parameters on the system's output. In the first part of this chapter the performance of the mantle heat exchanger subroutine is analyzed for different parameters. The energy outputs for the two different models are compared for different collector flow rates, different loads, and different heat transfer correction factors. In the second part the system with mantle heat exchanger is compared to a system with a regular tank and a separate heat exchanger.

5. 1 Base Case System

The base case system is a domestic hot water system with a solar collector and a hot water storage tank. The collector loop is separated from the storage unit by a heat exchanger. The system is located in Sacramento, California and has to meet a hot water load which is varied between 200 liters and 400 liters a day. The solar collector is of the flat plate type and has an area of 5 m^2. The

single glazed collector has a linear efficiency which is defined by $F_R(\tau\alpha)=0.7$ and $F_RU_L=4.17\ W/m^2K$. The incidence angle modifier constant is $b_o=0.1$. The liquid in the collector loop is water. The storage tank has a volume of 200 liters. For the simulations it is divided into 10 equal nodes (apart from the one node simulation of the regular tank). The load requires water at a temperature of 60°C and is supplied by either mixing the water from the tank with water from the mains if the water from the tank is too hot, or by heating it with an auxiliary heater if it is colder than 60°C. The 200 liters/day load profile used is displayed in Figure 5.1. The 400 liter/day and the 600 liter/day load are obtained by multiplying this load by 2 or 3, respectively. The performance of the solar system is compared in terms of solar fractions, the fraction of the total energy required which is supplied by the sun.

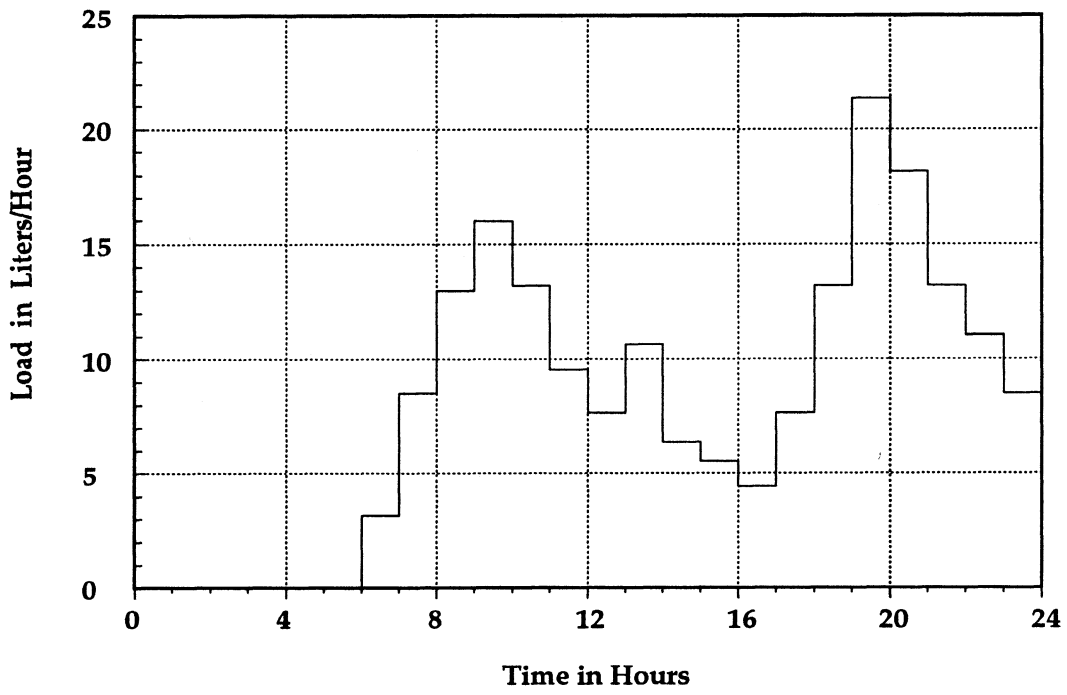

Figure 5.1.: Load Profile for a Hot Water Consumption of 200 liters/day

5. 3. Variation of Parameters

The simulation with model II was chosen as the standard situation for the parametrical analysis. 150 liters/hour was used as collector flow rate. The solar fractions for different heat transfer correction factors and for different hot water consumptions are displayed in Figure 5.2. The hot water loads were chosen to obtain solar fractions in different regions. For high solar fractions, different heat transfer coefficients have a relatively small impact on the system performance. Doubling the heat transfer coefficient results in a only 2.5 % higher solar fraction, halving it causes 5 % lower results. For intermediate and small solar fractions the differences are larger. Doubling the heat transfer coefficient there causes an increase in solar fraction of 8 %, to half it results in a by 12.5 % reduced solar fraction.

To obtain Figure 5.3 the same simulations were run again, but with an almost doubled collector flow rate of 270 liters/hour. The results for the different collector flow rates hardly vary. For solar fractions between 30% and 60% they are between 1% and 2% higher when the high flow rate is used instead of the low flow rate. For the high solar fractions of about 80% the situation is inverted, and the solar fractions increase with a decrease of the flow rate.

Model II, the model which does not include the heat storage in the mantle was simulate for a flow rate of 150 liters/hour. The results of the annual simulations are displayed in Figure 5.4. The solar fractions are between 2% and 16% lower for model I compared to the solar fractions obtained with model II. The reason for that behavior is, that neglecting the energy stored in the mantle is equivalent to using a smaller storage volume, in this case

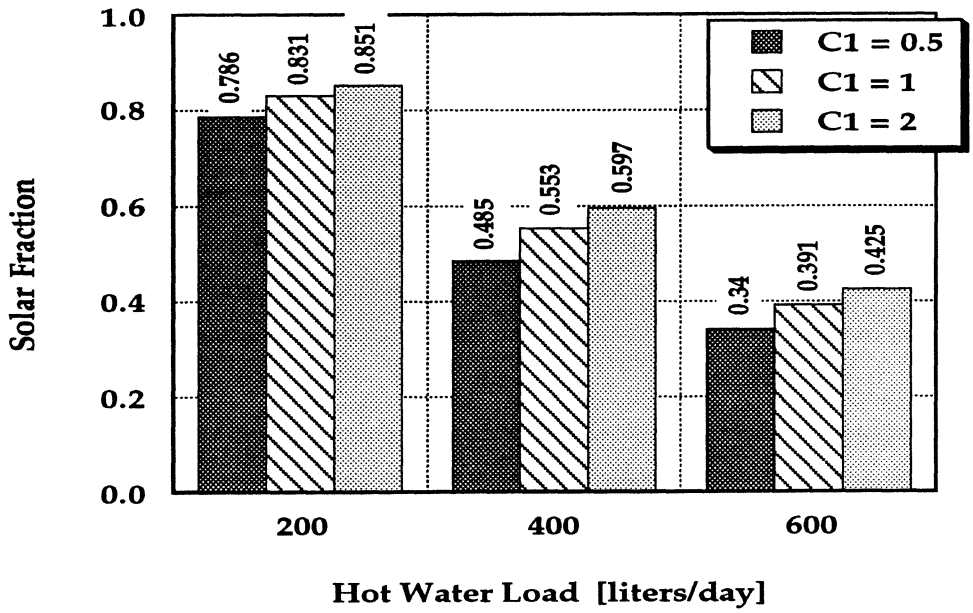

Figure 5.2.: Solar Fraction for Model II and a Collector Flow Rate of 150 l/hr for 3 different correction factors

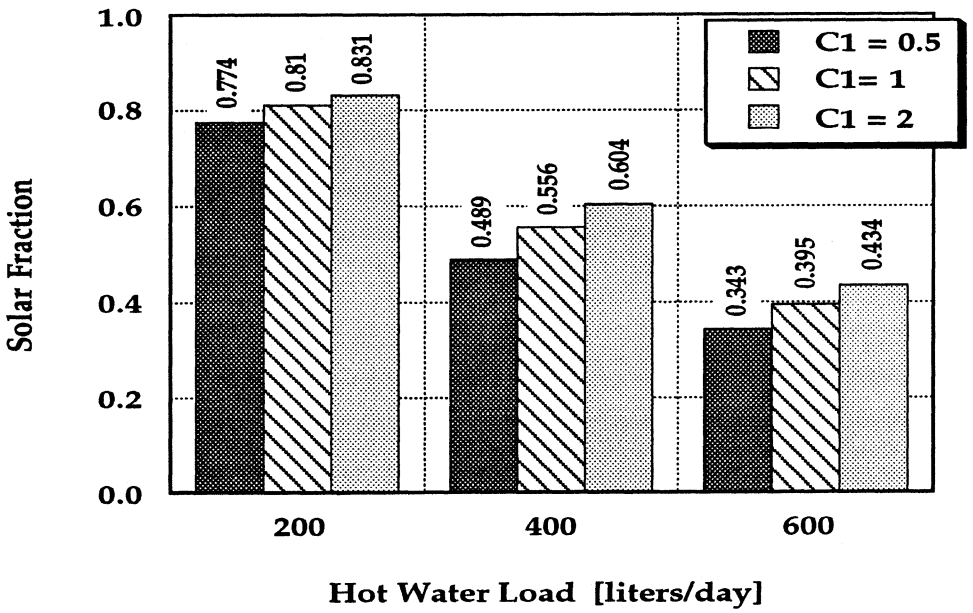

Figure 5.3.: Solar Fraction for Model II and a Collector Flow Rate of 270 l/hr for 3 different correction factors

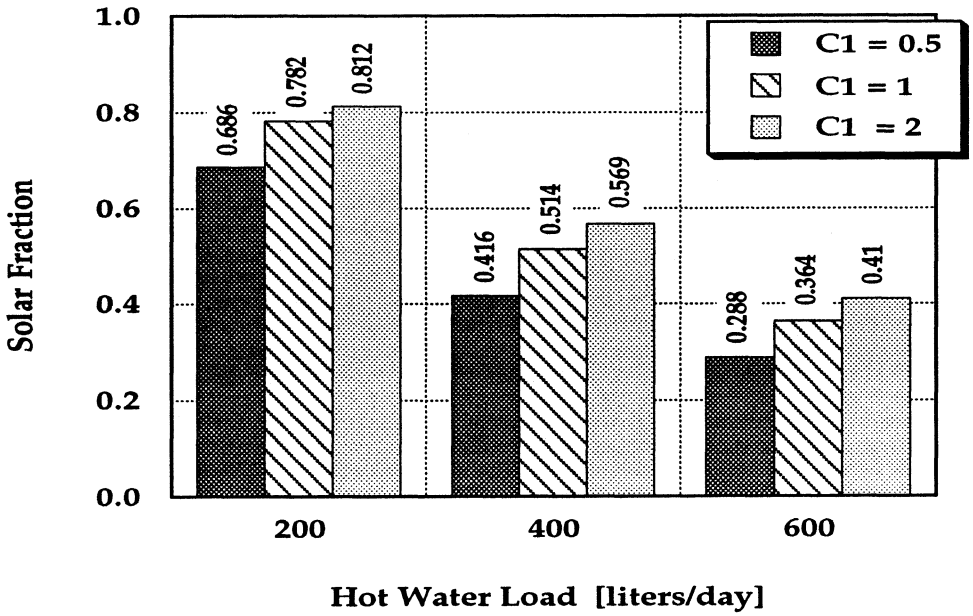

Figure 5.4.: Solar Fraction for Model I and a Collector Flow Rate of 150 l/hr for 3 different correction factors

reduced by approximately 15%. The energy outputs, predicted with model I are further away from the outputs predicted with model II for small heat transfer coefficients.

5. 3 . Mantle Heat Exchanger vs. System with Separate Heat Exchanger

In this section the performance of a tank with a mantle heat exchanger is compared to a regular tank with a separate heat exchanger. The heat exchanger effectiveness has been varied in the system having the separate tank. The values of the heat exchanger effectiveness used in the simulation

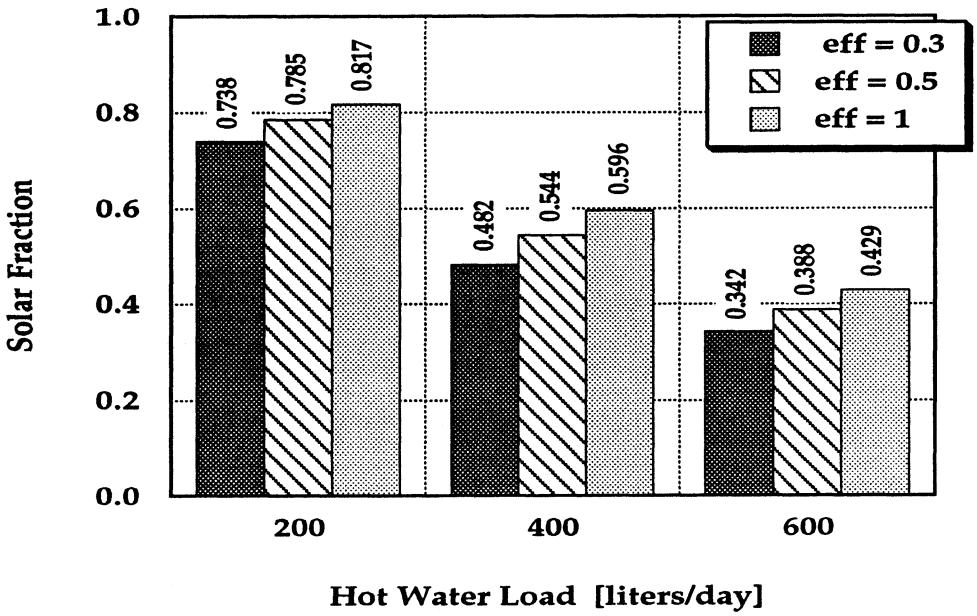

Figure 5.5.: Tank with Separate Heat Exchanger and 10 Nodes

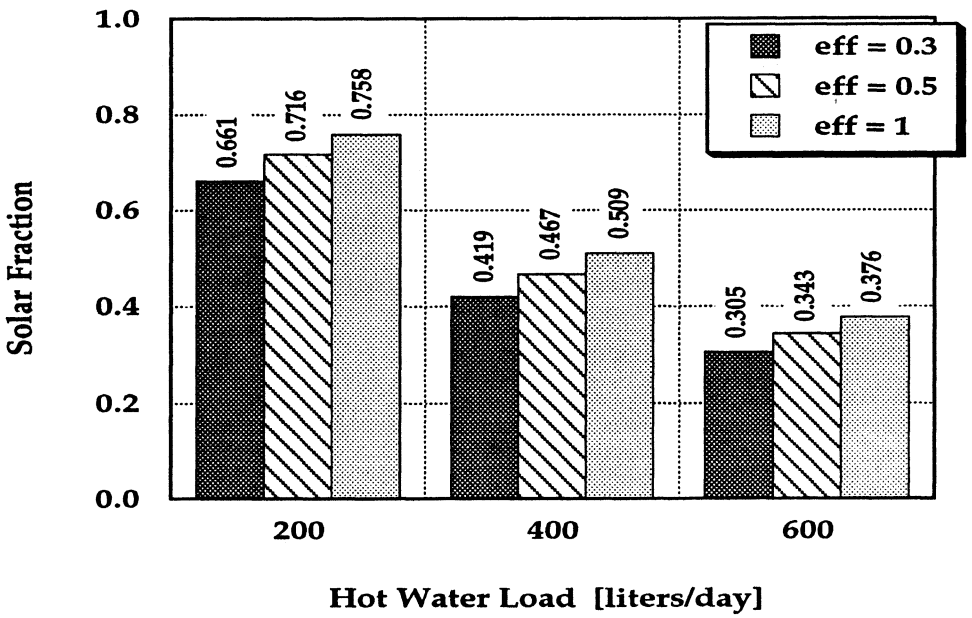

Figure 5.6.: Tank with Separate Heat Exchanger and 1 Node

were set to be 0.3 to represent the lower limit, 0.5 which represents a commonly used type of heat exchanger and 1.0 to get the upper performance limit.

The simulation results for a regular tank with the same node configuration as the mantle heat exchanger tank are displayed in Figure 5.5. If the results for this regular tank with external heat exchanger are to be compared to the results from the simulations using the mantle heat exchanger model II, it is appropriate to relate the regular tank with an effectiveness of the external heat exchanger eff = 1.0 to the results from model II with a heat transfer correction factor of $C_1 = 2$. The heat exchanger effectiveness of eff = 1.0 represents the upper performance limit of the regular tank system. A heat transfer correction factor of $C_1 = 2$ is in the region where model II works best. When these two configurations are compared, the mantle heat exchanger tank performs 3 % better for high solar fractions and almost equal for low and intermediate solar fractions.

A problem connected with this comparison is that the tank with mantle heat exchanger has additional storage capacity in the mantle. The total volume (including mantle) is therefore 230 liters. Yearly simulations for a regular tank with separate heat exchanger and a storage capacity of 230 liters have been performed. If the regular system with a 200 liter tank is compared to the system with the 230 liter tank, the system with the large tank has between 0.3 % (high solar fractions) and 1.5 % (intermediate and low solar fractions) higher solar fractions.

If a regular tank is divided into ten nodes an unrealistically high stratification in the tank to be calculated whereas the simulated high stratification in a tank with a mantle heat exchanger is not unreasonable as

experiments have shown [2]. If the thermal stratification is overpredicted the simulated value of the solar fraction is also too high. A simulation with ten nodes therefore yields the upper limit of the performance that can be expected. The lower limit for the performance of a tank can be obtained by simulating the tank as fully mixed with only one node. A simulation with only one node certainly underpredicts the thermal performance of the tank. Yearly simulations for a tank with one node have been done and the results are presented in Figure 5.6. The solar fractions are calculated to be between 10% and 24% lower than for the mantle heat exchanger model.

These results indicate that the thermal performance of a tank with mantle heat exchanger is better than the thermal performance of a tank with a separate heat exchanger as the upper performance limit of the tank with a separate heat exchanger just reaches the performance of a normal mantle heat exchanger tank.

6. Conclusion and Recommendations

A simulation model for a hot water storage tank with a built-in mantle heat exchanger has been developed. Two different approaches have been taken. One approach treats the flow through the mantle as being at steady state during the time step and therefore does not take into account the energy stored in the mantle. In the second modeling approach, the tank is divided into control volumes for which energy balances are applied. Model II is therefore capable of accounting for the energy stored in the mantle.

The heat transfer coefficient from the mantle liquid to the heat transfer wall has been obtained from an empirical correlation. To make the model II agree with experimental measurements the heat transfer coefficient obtained by the correlation has to be multiplied by a correction factor of 1.8 for model II. Model I works best for a correction factor of 1.0.

The predicted performance for the heating experiment with a low flow rate is reasonable for model II while the error with model I is not acceptable. For the experiment with draws and for the cooling experiment both models predict a similar behavior like the real tank, but the calculated temperatures are relatively far off. For the tank-in-tank experiment both models perform very well. The only weak spot is the period were draws are extracted, but the

flow through the mantle is already shut off. It can be concluded that the predictions with model I are not sufficiently accurate. The accuracy of the simulations with model II are satisfactory with the exception of the experiment with a low mantle flow rate and draws. To be sure that model II predicts reliable results, it is therefore necessary to further investigate model II by running more simulations for different experiments.

The attempt to include free convection as a heat transfer mode shows that it the water in the tank cannot be assumed to be an infinite medium with the wall being at a constant temperature. A model including free convection based on these assumptions greatly overpredicts the decay of stratification in the cooling experiment (section 4. 2. 3). However in the cooling experiment with only conduction as a heat transfer coefficient the stratification decays too slow, which indicates that a small amount of free convection actually occurs.

As shown by yearly simulations of a mantle heat exchanger tank and a tank with separate heat exchanger for similar conditions, the mantle heat exchanger has a slightly superior thermal performance which is most likely due to the stratification in this tank.

No satisfactory relations could be found which describe the heat transfer that occurs in an enclosure like a tank. Further investigations are necessary to obtain a relation for the Nusselt number for the heat transfer from the mantle liquid to the wall between mantle and tank, and for the heat transfer from the wall to the liquid in the tank. However, additional experiments are needed as there is not enough experimental data available today.

Future improvement of the mantle heat exchanger model should involve a separate mode for tank-in-tank systems in order to include the larger heat transfer areas on the tank top and bottom.

Appendix A: TRNSYS Component Configuration

PARAMETERS NO.		DESCRIPTION
1	Mode:	- 3 tank with mantle heat exchanger
2	V	- tank volume
3	c_p	- specific heat of fluid in tank
4	ρ	- density of fluid in tank
5	$U_{t\text{-}env}$	- loss coefficient from tank to environment
6	H or H_1	- if > 0 height of node 1 if < 0 then all nodes are the same size and the total tank height is H
if Parameter 6 > 0 :		
5 + i	H_i	- height of ith node
•		•
5 + n	H_n	- height of nth node (n < 16)
Parameter for Mantle		
last - 9	h_{man}	- distance to top of mantle from bottom of tank
last - 8	e_{man}	- distance to bottom of mantle from bottom of tank

last - 7	$U_{m\text{-}env}$	- loss coefficient from mantle to environment
last - 6	C_1	- heat transfer correction factor on mantle side of heat exchanger surface
last - 5	p	- propylene glycol percentage in anti freeze liquid in %
last - 4	$c_{p,af}$	- specific heat of anti freeze in collector loop
last - 3	t_w	thickness of heat transfer surface
last - 2	D_{man}	- diameter of mantle
last - 1	k_{st}	- conductivity of steel walls (if k_{st}=0 the conductivity of water is automatically set to zero, too)
last	h	heat transfer coefficient from wall to tank node

INPUT NO.		DESCRIPTION
1	T_H	- temperature of fluid from heat source
2	$\dot{m}_H$	- mass flow rate from heat source
3	T_L	- temperature of replacement fluid
4	$\dot{m}_L$	- mass flow rate to load
5	T_{env}	- ambient temperature

OUTPUT NO.		DESCRIPTION
1	T_N	- temperature to heat source
2	$\dot{m}_H$	- mass flow rate to heat source
3	T_L	- temperature of replacement fluid
4	$\dot{m}_L$	- mass flow rate to load
5	Q_{env}	- rate of energy loss to the environment
6	Q_s	- rate at which energy is removed to supply load
7	ΔE	- internal energy change of the tank
9	Q_{in}	- rate of energy input to tank from hot fluid stream
10	$\overline{T}$	- average storage temperature
11	T_2	- tank temperature of second node
•		•
9+i	T_i	- tank temperature of i^{th} node
•		•
9+n	T_n	- tank temperature of n^{th} node
9+n+i	$T_{m,i}$	- mantle temperature at height of i^{th} tank node (if the mantle surrounds node i)
•		•
9+2n	$T_{m,n}$	- mantle temperature at height of n^{th} tank node (if the mantle surrounds node n)

DERIVATIVE NO.		DESCRIPTION
1	T_1	- initial temperature of top tank node
•		•
i	T_i	- initial temperature of i^{th} tank node
•		•
n	T_n	- initial temperature of n^{th} tank node

Initial Temperatures for the Mantle only for Model II:

n+i	$T_{m,i}$	- initial mantle temperature at height of i^{th} tank node (if no mantle at node i: $T_{m,i}=0$)
•		•
2n	$T_{m,n}$	- initial mantle temperature at height of n^{th} tank node (if no mantle at node n: $T_{m,n}=0$)

Appendix B: Property Relations for Aqueous Propylene-Glycol

The curve fits for the properties of aqueous propylene glycol were obtained by Tim McDowell from property tables in [8]. The properties depend on the liquid temperature T in °K and the propylene-glycol percentage p in %.

Heat Capacity of Anti-Freeze Liquid

$C_{p,\,af} = B + C*T$ in kJ/kg-C

with $B = 3.865 - 0.0237*p - 0.0001128*p^2$

$C = 0.001024 + 5.663e\text{-}5*p$

Density of Anti-Freeze Liquid

$\rho_{af} = B + C*T + D*T^2$ in kg/m^3

with $B = 875.5 + 2.151*p$

$C = 1.119 - 0.00076*p - 4.924e\text{-}5*p^2$

$D = -0.00238 - 9.138e\text{-}6*p + 1.087e\text{-}7*p^2$

Thermal Conductivity of Anti-Freeze Liquid

$k_{af} = B + C*T + D*T^2$ in W/m-C

with $B = -0.786 + 0.01556*p - 4.893e\text{-}5*p^2$

$C = 0.007687 - 0.0001156*p + 3.66e\text{-}7*p^2$

$D = -9.998e\text{-}6 + 1.456e\text{-}7*p - 4.588e\text{-}10*p^2$

Viscosity of Anti-Freeze Liquid

$\mu_{af} = \exp(B+C*p)$ in Pa s

with $B = 71.639 - 0.6698*T + 0.001915*T^2 - 1.8587e\text{-}6*T^3$

$C = 0.2702 - 0.00123*T + 1.5045e\text{-}6*T^2$

Appendix C: TRNSYS-Decks

Experiment 1: Heat Up Test

This TRNSYS-Deck is for model 2 with energy storage in the mantle. To use it for model I a bigger time step can be applied and the second half of the DERIVATIVES in UNIT 4, the module for the tank, have to be eliminated.

```
* * * * * * * * * * * * * * * * * * * * * * * * * * * * * * * * * * * * * * *
*                                                                             *
*          Simulation of Experiment 1 (Heat Up Test)                          *
*          Test.dck1e for energy storage in mantle                            *
*           14 control volumes with various sizes                             *
*                                                                             *
* * * * * * * * * * * * * * * * * * * * * * * * * * * * * * * * * * * * * * *

SIMULATION 0.0  26.0  0.015625

TOLERANCES 0.001 0.001

WIDTH 72

EQUATIONS 7
   ufac = 1.8
   htc = 2000.
   *htc is htc at inside tank wall
   Qin=[4,9]
   Qtank=[4,6]
   Qenv=[4,5]
   Qtot=Qin-Qtank-Qenv
   Delau=[4,7]
```

```
UNIT 4 TYPE 4 storage tank with mantle heat exchanger
PARAMETERS 29
  3.0  0.197 4.186 1000. 3.204
  *mode  vol   cp   rho   utank
  0.092 0.05 0.15 0.05 0.15 0.05 0.13 0.05 0.16 0.05 0.14 0.05 0.05 0.04
  *h1   h2   h3   h4   h5   h6   h7   h8   h9   h10  h11  h12  h13  h14
  1.013  0.098  3.204  Ufac  0.  4.186  0.005  0.504 216. htc
  *hman  eman   uman   Ufac perc  cph    tht    dman kst  htc

INPUTS 5
  14,1   15,1   0,0  0,0   0,0
  30.0   22.2    15  0.0  20.4
  *Ts     mdoth   Tl mdotl Tenv

DERIVATIVES 28
  29.5 29.5 29.5 29.5 29.5 29.5 29.5
  29.5 29.3 29.2 29.0 28.7 28.2 27.7
  0.0  0.0 29.5 29.5 29.5 29.5 29.5
  29.5 29.3 29.2 29.0 28.7  0.0  0.0

UNIT 14 TYPE 14 mantle inlet temperature
PARAMETERS 16
  0. 30. 0.2 30. 0.5 47. 1. 49.2 2. 49.3 9. 49.3 11. 49.4 26. 49.4

UNIT 15 TYPE 14 mantle flow rate
PARAMETERS 12
  0. 22.2 .5 25.8 1. 28.2 3. 28.8 6. 31.2 26. 31.2
```

```
UNIT 25 TYPE 25 printer
PARAMETERS 4
  0.5  0.  26.  10
INPUTS 8
  4,11 4,13 4,15 4,17 4,19 4,21 4,23  4,1
  t1   t2   t3   t4   t5   t6   t7   Tmout

UNIT 27 TYPE 25 printer for mantle temperatures
PARAMETERS 4
  0.25  0.  26.  11
INPUTS 8
  4,25  4,27  4,29  4,31 4,33  4,35 4,37   4,1
  tm1   tm2   tm3   tm4  tm5   tm6  tm7  Tmout

UNIT 26 TYPE 25 printer for energy
PARAMETERS 4
  1.  0.  26.  12
INPUTS 5
  Qin Qtank Qenv Qtot Delau
  Qin Qtank Qenv Qtot Delau
END.
```

Experiment 2: Test with Draws

This TRNSYS-Deck is for model 2 with energy storage in the mantle. To use it for model one a bigger time step can be applied and the second half of the DERIVATIVES in UNIT 4, the modul for the tank, have to be eliminated.

```
* * * * * * * * * * * * * * * * * * * * * * * * * * * * * * * * * * * * *
*                                                                       *
*          Simulation of Experiment 2 (Test with Draws)                 *
*          Test.dck2e for energy storage in mantle                      *
*           14 control volumes with various sizes                       *
*                                                                       *
* * * * * * * * * * * * * * * * * * * * * * * * * * * * * * * * * * * * *

SIMULATION 0.0  11.0  0.0078125

TOLERANCES 0.001 0.0001

WIDTH 72

EQUATIONS 9
   utman =1.8
   htc = 2000
   Qin=[4,9]
   Qtank=[4,6]
   Qenv=[4,5]
   Qtot=Qin-Qtank-Qenv
   Delau=[4,7]
   Tmanin=[14,1]
   mload=[15,1]

UNIT 16 TYPE 14 mheat source(time)
PARAMETERS 20
0.  23.4 1.  22.2 1.5  22.2 1.6  23.4 3.57 24.0
3.87 24  3.88 23.4 5.72 23.4 5.88 22.2 10.  21.6

UNIT 15 TYPE 14 mload(time)
PARAMETERS 20
   0. 0. 1.   0.  1.   396.8 1.125 396.8  1.125 0.
   3.5 0. 3.5 401.6 3.625 401.6 3.625 0.   11.   0.
```

```
UNIT 14 TYPE 14 Tmanin(time)
PARAMETERS 48
  0.  29.5 1.0  29.7 1.6  29.7 1.62 34.6 1.78 59.4
  1.95 67.0 2.12 69.0 2.28 69.7 2.95 69.9 3.28 70.1
  5.72 70.1 5.88 69.1 6.05 56.9 6.22 45.  6.38 37.5
  6.55 32.7 6.72 30.9 6.88 30.3 7.05 30.0 7.72 29.9
  8.05 29.8 9.05 29.7 10.05 29.7 11.0 29.5

UNIT 4 TYPE 4 tank with mantle heat exchanger
PARAMETERS 29
3  .0  0.197 4.186 1000. 3.204 0.092 0.05 0.15 0.05
  *mode vol   cp  rho utank  h1   h2   h3   h4
  0.15 0.05 0.13 0.05 0.16 0.05 0.14 0.05 0.05 0.04
  *h5   h6   h7   h8   h9   h10  h11  h12  h13  h14
  1.013  0.098  3.204  Utman  0.  4.186  0.005  0.504 216 htc
  *hman   eman   uman  Utman  perc  cph    tht    dman kst htc
INPUTS 5
  Tmanin  16,1  0,0  mload  0,0
  29.5   23.4  14.2   0.0  21.5
  * Ts   mdoth   Tl   mload  Tenv
DERIVATIVES 28
  19.1 19.1 18.4 17.8 17.3 16.8 16.8
  16.7 16.6 16.5 16.6 16.7 16.6 16.5
  0.0  0.0 18.4 17.8 17.3 16.8 16.8
  16.7 16.6 16.5 16.6 16.7  0.0  0.0

UNIT 25 TYPE 25 printer
PARAMETERS 4
  0.125  0.  26.  10
INPUTS 8
  4,11 4,13 4,15 4,17 4,19 4,21 4,23  4,1
  t1   t2   t3   t4   t5   t6   t7   Tmout
```

```
UNIT 27 TYPE 25 printer for mantle temperatures
PARAMETERS 4
  0.25 0. 26. 11
INPUTS 8
  4,25 4,27 4,29 4,31 4,33 4,35 4,37  4,1
  tm1  tm2  tm3  tm4  tm5  tm6  tm7 Tmout

UNIT 26 TYPE 25 printer for energy
PARAMETERS 4
  1. 0. 26. 12
INPUTS 5
  Qin Qtank Qenv Qtot Delau
  Qin Qtank Qenv Qtot Delau

END.
```

Experiment 3: Cool Down Test

This TRNSYS-Deck is for model 2 with energy storage in the mantle. To use it for model one a bigger time step can be applied and the second half of the DERIVATIVES in UNIT 4, the modul for the tank, have to be eliminated.

```
* * * * * * * * * * * * * * * * * * * * * * * * * * * * * * * * * * * *
*                                                                     *
*          Simulation of Experiment 3 (Cool Down Test)                *
*          Test.dck3e for energy storage in mantle                    *
*           14 control volumes with various sizes                     *
*                                                                     *
* * * * * * * * * * * * * * * * * * * * * * * * * * * * * * * * * * * *

SIMULATION 0.0  25.0  0.0625
```

```
TOLERANCES 0.001 0.001

WIDTH 72

EQUATIONS 7
   utman = 1.8
   htc = 2000
   Qin=[4,9]
   Qtank=[4,6]
   Qenv=[4,5]
   Qtot=Qin-Qtank-Qenv
   Delau=[4,7]

UNIT 4 TYPE 4 tank with mantle heat exchanger
PARAMETERS 29
   3.0  0.197 4.186 1000. 3.204 0.092 0.05 0.15 0.05
   *mode vol   cp   rho utank  h1   h2   h3   h4
   0.15 0.05 0.13 0.05 0.16 0.05 0.14 0.05 0.05 0.04
   *h5   h6   h7   h8   h9   h10  h11  h12  h13  h14
   1.013  0.098  3.204  Utman  0.  4.186  0.005  0.504 216 htc
   *hman  eman  uman Utman perc cph   tht   dman kst htc
INPUTS 5
   Tmanin  16,1  0,0  mload  0,0
   29.5   23.4  14.2   0.0  21.5
   * Ts   mdoth  Tl   mload  Tenv
DERIVATIVES 28
   48.0 48.0 47.9 47.8 46.0 44.3 33.6
   22.9 21.2 19.4 19.3 19.3 19.2 19.1
   48.0 48.0 47.9 47.8 46.0 44.3 33.6
   22.9 21.2 19.4 19.3 19.3 19.2 19.1

UNIT 25 TYPE 25 printer
PARAMETERS 4
   0.125  0.  26.  10
```

```
INPUTS 8
  4,11 4,13 4,15 4,17 4,19 4,21 4,23  4,1
  t1  t2  t3  t4  t5  t6  t7  Tmout

UNIT 27 TYPE 25 printer for mantle temperatures
PARAMETERS 4
  0.25 0. 26. 11
INPUTS 8
  4,25 4,27 4,29 4,31 4,33 4,35 4,37  4,1
  tm1  tm2  tm3  tm4  tm5  tm6  tm7  Tmout

UNIT 26 TYPE 25 printer for energy
PARAMETERS 4
  1. 0. 26. 12
INPUTS 5
  Qin Qtank Qenv Qtot Delau
  Qin Qtank Qenv Qtot Delau

END.
```

Appendix D: FORTRAN Source Code of Model II

```
      SUBROUTINE    TYPE4(TIME,XIN,OUT,T,DTDT,PAR,INFO)
C     THIS ROUTINE SIMULATES A STRATIFIED STORAGE TANK CONSISTING OF NEQ
C     FULLY MIXED SECTIONS, THE VALUE OF NEQ BEING CHOSEN BY THE USER.
C     REFERENCE 'EXPERIMENTAL AND SIMULATED PERFORMANCE OF A CLOSED
C     LOOP SOLAR WATER HEATING SYSTEM', BY P.I.COOPER, S.A.KLEIN,
C     AND C.W.S.DIXON PRESENTED AT THE ISES MEETING IN AUGUST,1975
C     THIS SUBROUTINE WAS CHANGED TO MODEL A TANK WITH A MANTLE HEAT
C     EXCHANGER. THE MANTLE IS DIVIDED UP IN CONTROL VOLUMES, ON WHICH
C     ENERGYBALANCES ARE APPLIED.
      INTEGER FINAL,DIRECT,AVG,OLD,MANP,AUXP,INV, NMANIN, NMANOUT,
     +        FLAG
      REAL MSCP, MCPN
      REAL HMAN,UMAN,KTMAN,RHOH,CPH,THT,DMAN,AMAN,ALOSS,UTMAN,
     +     ACTHIGH,EXCHIGH,CONST,FLWSS,QENV,TSPEC,TIME,DELAU,
     +     UTMANX,EMAN,XUT,KAOXH2O(15),KAOXST(15),HTCX,DELX,KAF,
     +     KH2O,KST,KAOX(15),REY,PR,DH,X1,X2,HTC(15),HTC1(15),MY,
     +     DELAUMAN,TMANAV,TMANAV2,AAMAN,BBMAN,ACROSSMAN,TMANI,
     +     TMANF,T2,T1,TL,PERC,CPDF,DENSITY,THCOND,VISC
      DIMENSION T(30),DTDT(30),XIN(10),OUT(40),PAR(40),INFO(10)
      DIMENSION U(16),V(16),QB(16),H(15)
      COMMON/SIM/ TIME0,TFINAL,DELT
      COMMON/STORE/ NSTORE,IAV,S(5000)
      DATA NSTK/5/,QB/16*0.0/,PI/3.1415193/,LOCT/0/
      EXTERNAL CPDF,DENSITY,THCOND,VISC
C
      IF (INFO(7).GE.0) GO TO 10
C     FIRST CALL OF SIMULATION
C SPECIFY SIZE OF OUTPUT ARRAY
      INFO(6) = 40
      NI = 5
```

```
      IF (INFO(3) .EQ. 6) NI = 6
      MANP = 10
C       IF (PAR(1).EQ.3) MANP = 8
      NEQ=INFO(5)/2
      IF(PAR(6).GT.0.) GO TO 2
      NP=6 + MANP
      GO TO 3
2     NP=5+NEQ+MANP
3     IF (NEQ.LT.1 .OR. NEQ.GT.15) CALL TYPECK(5,INFO,0,0,0)
      INFO(10) = 2*(NEQ*4+4)
      NP=INFO(4)
      CALL TYPECK(1,INFO,NI,NP,(NEQ*2))
C     FIND AVERAGE TEMPERATURE AND SET INITIAL TEMPERATURES IN TANK
      IS = INFO(10) + NEQ - 1
      IAVG = INFO(10) + NEQ*2 - 1
      IOLD = INFO(10) + NEQ*3 - 1
      TI = 0.
      HIGH = 0.
      DO 5 J = 1,NEQ
        IS = IS + 1
        IAVG = IAVG + 1
        IOLD = IOLD + 1
        S(IS) = T(J)
        S(IAVG) = T(J)
        S(IOLD) = T(J)
        S(IS-NEQ)=T(J)
        HN=ABS(PAR(6))/FLOAT(NEQ)
        IF(PAR(6).LT.0.) GO TO 4
        HN=PAR(5+J)
4       HIGH = HIGH + HN
        TI = TI + T(J)*HN
5     CONTINUE
      TI = TI/HIGH
      IS=INFO(10)+NEQ*4-1
```

```
          S(IS+1)=TI
C
C FIND NODE NUMBER OF MANTLE TOP AND BOTTOM (NMANIN,NMANOUT)
          IND=1
           IF(PAR(6).GT.0.) IND=NEQ
           HMAN= PAR(5+IND+1)
           EMAN= PAR(5+IND+2)
          FLAG=0
           ACTHIGH=HIGH
           DO 6 J=1,NEQ
              HN=ABS(PAR(6))/FLOAT(NEQ)
              IF(PAR(6).LT.0.) GO TO 7
              HN=PAR(5+J)
7             ACTHIGH = ACTHIGH - HN
               IF ((ACTHIGH.LT.HMAN).AND.(FLAG.LT.1.)) THEN
                        FLAG=2
                        NMANIN=J
                     ENDIF
               IF ((ACTHIGH.LE.EMAN).AND.(FLAG.LT.3.)) THEN
                        FLAG=4
                        NMANOUT=J
                     ENDIF
6         CONTINUE

C READ IN MANTLE INITIAL TEMPERATURES
          IS = INFO(10)+ NEQ*4+4 + NEQ - 1
          IAVG = INFO(10)+ NEQ*4+4 + NEQ*2 - 1
          IOLD = INFO(10)+ NEQ*4+4 + NEQ*3 - 1
C           DO 8 J = NMANIN,NMANOUT
          DO 8 J = 1,NEQ
            IS = IS + 1
            IAVG = IAVG + 1
            IOLD = IOLD + 1
            S(IS) = T(J+NEQ)
```

```
            S(IAVG) = T(J+NEQ)
            S(IOLD) = T(J+NEQ)
            S(IS-NEQ)=T(J+NEQ)
8       CONTINUE
        IUNIT=0
C
C END OF PART FOR 1ST SUBROUTINE CALL
C
C
C    SET LOCAL VARIABLES TO PARAMETER VALUES.
C     PARAMETERS ARE READ IN ONLY THE FIRST TIME, OR AT EVERY CALL IF THERE
C     IS MORE THAN ONE TYPE4 SPECIFIED IN THE DECK
10      IF (INFO(1).EQ.IUNIT) GO TO 30
        IUNIT=INFO(1)
        NEQ = INFO(5)/2
        XNEQ = FLOAT(NEQ)
        MODE=INT(PAR(1)+0.1)
        VOL = PAR(2)
        CPF=PAR(3)
        RHOF=PAR(4)
        ULOSS=PAR(5)
        IND=1
        IF(PAR(6).GT.0.) IND=NEQ
C
C ADDITIONAL PARAMETERS FOR MANTLE HEAT EXCHANGER MODEL
        IF (MANP .EQ. 10) THEN
      HMAN= PAR(5+IND +1)
       EMAN= PAR(5+IND +2)
      UMAN= PAR(5+IND +3)
      UTMAN=PAR(5+IND +4)
      PERC= PAR(5+IND +5)
      CPH=    PAR(5+IND +6)
      THT=    PAR(5+IND +7)
      DMAN= PAR(5+IND +8)
```

```
                KST=    PAR(5+IND +9)
                HTCX= PAR(5+IND +10)
            ACROSSMAN=PI/4.*DMAN**2 - VOL/HIGH
            DH= DMAN - 2*(THT+ (VOL/PI/HIGH)**0.5)
          ENDIF
          INIT = INFO(10) - 1
          FINAL = INIT + NEQ
          AVG = FINAL + NEQ
          OLD = AVG + NEQ
          IS=OLD+NEQ
          UAE=ULOSS*VOL/HIGH
          PER=(4.*PI*VOL/HIGH)**0.5
30        CONTINUE
C
C     SET INPUTS (EVERY CALL OF SUBROUTINE)
          TIN=XIN(1)
          FLWSS=XIN(2)
          TL=XIN(3)
          FLWLL=XIN(4)
          TENV=XIN(5)
          FLWS=FLWSS*CPH
          FLWL=FLWLL*CPF
C
C     CORRECT FOR TEMP. INVERSIONS ONLY ONCE PER TIMESTEP
1000      IF (INFO(7).GT.0) GO TO 1060
          INV=0
          TMIX=S(FINAL+NEQ)
          HMIX=H(NEQ)
          FLAG=0
C FLAG = NUMBER OF NODES IN MIX - 1
          DO 1005 JJ=NEQ-1,1,-1
            IF(S(FINAL+JJ).LT.TMIX) THEN
              FLAG =FLAG+1
                    TMIX=(TMIX*HMIX+S(FINAL+JJ)*H(JJ))/(HMIX+H(JJ))
```

```
                HMIX=HMIX+H(JJ)
                 IF ((S(FINAL+JJ-1).GE.TMIX).OR.(JJ.EQ.1)) THEN
                  DO 1007 KK=JJ,(JJ+FLAG)
                              S(FINAL+KK)=TMIX
1007               CONTINUE
                FLAG=0
                 TMIX=S(FINAL+JJ)
                 HMIX=H(JJ)
                 ENDIF
              ELSE
                 HMIX=H(JJ)
                 TMIX=S(FINAL+JJ)
              ENDIF
1005    CONTINUE
C
C     CHECK FOR INVERSIONS DUE TO MIXING, REPEAT INVERSION ALGORITHM
C     IF THERE ARE STILL INVERSIONS
         FLAG=0
          DO 1008 JJ=NEQ-1,1,-1
             IF(S(FINAL+JJ).LT.S(FINAL+JJ+1)) FLAG =1
1008     CONTINUE
          IF (FLAG.EQ.1) GOTO 1000
          MSCP=VOL*DENSITY(PERC,40)*CPF
C
         DO 1050 K = 1,NEQ
            KI = INIT + K
            KF = FINAL + K
C RESET T INITIAL FOR NEW TIME STEP WITH T FINAL FROM OLD TIME STEP
              S(KI+NEQ*4+4)=S(KF+NEQ*4+4)
1050         S(KI) = S(KF)
1060    CONTINUE
C
C     CALCULATION OF TEMPERATURES IN ALL TANK AND MANTLE NODES
          ACTHIGH=HIGH
```

```
      QENV=0.
      DELAU=0.
      DELAUMAN=0.
      DO 1900 N=1,NEQ
      NODE =N
C     ENTERING FLOWSTREAMS TO TANK
      T1=S(AVG+NODE)
      IF (NODE .LT.NEQ) THEN
           T2 = S(AVG+NODE+1)
        ELSE
      T2=TL
      ENDIF
C
C     ENTERING FLOWSTREAMS TO MANTLE
        IF ((N.GE.NMANIN).AND.(N.LE.NMANOUT)) THEN
          TMANAV=S(4+4*NEQ + AVG + NODE)
          IF (NODE .EQ. NMANIN) THEN
              TMANAV2 = TIN
           ELSE
          TMANAV2 = S(4+4*NEQ + AVG + NODE - 1)
         ENDIF
       ELSE
          TMANAV=0.
       ENDIF
C
C     AREA FOR HEAT EXCHANGE WITH MANTLE AND/OR ENVIRONMENT
      AMAN=0.
      ALOSS=0.
      EXCHIGH=0.
       IF (N.LT.NMANIN) THEN
            ALOSS=PER*H(NODE)
           EXCHIGH=0.
      ELSE
          IF ((N.GT.NMANIN).AND.(N.LT.NMANOUT)) THEN
```

```
                    AMAN=PER*H(NODE)
                    EXCHIGH=H(NODE)
               ELSE
C     IF BEGINNING OR END OF MANTLE CUTS A NODE
                  IF (N.EQ.NMANIN) THEN
                        EXCHIGH= HMAN - ACTHIGH + H(NODE)
                       ENDIF
                       IF (N.EQ.NMANOUT) THEN

EXCHIGH=-(EMAN-ACTHIGH)
                  ENDIF
                    ALOSS=PER*(H(NODE)-EXCHIGH)
                   AMAN=PER*EXCHIGH
        ENDIF
          ENDIF
C
C     HEAT TRANSFER COEFFICIENT OF TOP AND BOTTOM CAN BE CHANGED
C     BY INCLUDING THE FACTORS
            IF (NODE.EQ.1) ALOSS=ALOSS+ VOL/HIGH
C       +    *1.79/0.89
            IF (NEQ.EQ.NODE)ALOSS=ALOSS+VOL/HIGH
C       +    *2.97/0.89
C
C CALCULATION OF MANTLE FLUID TEMPERATURE REGARDING LOSSES TO ENV.
              IF (EXCHIGH .GT. 0.) THEN
                 KAF=THCOND(PERC,TMANAV)*3.6
                 MY=VISC(PERC,TMANAV)*3600
                 PR=MY*CPDF(PERC,TMANAV)*1000/KAF*3.6/3600
                 IF (INFO(7).LT.0.) THEN
                             WRITE (17,*)'DH,MY,FLWSS,(DMAN**2-(DMAN-DH)**2)'
                             WRITE (17,*)DH,MY,FLWSS,(DMAN**2-(DMAN-DH)**2)
               ENDIF
                  REY=DH/MY*FLWSS/(PI/4.*(DMAN**2-(DMAN-DH)**2))
                 X1=HMAN-ACTHIGH
```

```
                X2=HMAN- (ACTHIGH-H(N))
                    IF (X1.LE.0.) X1=0.2/0.93*X2
C     LOCAL HEAT TRANSFER COEFFICIENT AT INSIDE OF TANK
                HTC(N)=UTMAN*KAF/DH*(
     +            (4.9+0.0606*(REY*PR/X2*DH)**(1.2)/
     +                (1.+0.0909*(REY*PR/X2*DH)**(0.7)*PR**0.17))*X2 -
     +            (4.9+0.0606*(REY*PR/X1*DH)**(1.2)/
     +                (1.+0.0909*(REY*PR/X1*DH)**(0.7)*PR**0.17))*X1)/(X2-X1)
                    UTMANX=1./(1./HTCX + 1./HTC(N))
C
        ENDIF
C
C----CALC.--OF---CONDUCTION--PARAMETERS--------------------------
        IF (INFO(7).EQ.-1) THEN
        IF (KST.EQ.0) THEN
                    KAOX(NX)=0.
       ELSE
        KH2O=0.63*3.6
        DO 1070 NX=1,(NEQ-1)
                IF (HTCX.GT.0) HTC(NX)=HTCX
          DELX=(H(NX)+H(NX+1))/2.
          KAOXH2O(NX)=VOL/HIGH*KH2O/DELX
          KAOXST(NX)=1./( (2*DELX/HTC(NX)/H(NX)/H(NX+1)/PER )+
     +
     (DELX/THT/PER/KST))
          KAOX(NX)=KAOXH2O(NX)+KAOXST(NX)
1070   CONTINUE
        KAOX(0)=0.
        KAOX(NEQ)=0.
       ENDIF
C
        MCPN=MSCP*H(NODE)/HIGH
C
C SOLVE DIFFERENTIAL EQUATION FOR TANK NODE TEMPERATURE
```

```
          KI = INIT + NODE
          KF = FINAL + NODE
          KAVG = AVG + NODE
           AA = -(FLWL + UTMANX*AMAN + ULOSS*ALOSS +
        +                                KAOX(N) + KAOX(N-1))/MCPN
          BB = +(FLWL*T2 + UTMANX*AMAN*TMANAV +
        +          ULOSS*ALOSS*TENV+
        +           KAOX(N)*S(KAVG+1) + KAOX(N-1)*S(KAVG-1))/MCPN
          TI = S(KI)
           CALL DIFFEQ(TIME,AA,BB,TI,TF,TAVG)
          S(KF) = TF
          S(KAVG) = TAVG
C
C SOLVE DIFFERENTIAL EQUATION FOR MANTLE NODE TEMPERATURE
           IF (EXCHIGH.GT.0.)THEN
             RHOH=DENSITY(PERC,TMANAV)
             AAMAN = - (FLWS + UMAN*DMAN*PI*EXCHIGH
        +                + UTMANX*PER*EXCHIGH)/
        +                 (RHOH*ACROSSMAN*CPH*EXCHIGH)
              BBMAN = (FLWS*TMANAV2 + UMAN*DMAN*PI*EXCHIGH*TENV
        +                + UTMANX*PER*EXCHIGH*TAVG)/
        +                 (RHOH*ACROSSMAN*CPH*EXCHIGH)
            TMANI = S(NEQ*4+4+KI)
             CALL DIFFEQ(TIME,AAMAN,BBMAN,TMANI,TMANF,TMANAV)
            S(NEQ*4+4+KF) = TMANF
            S(NEQ*4+4+KAVG) = TMANAV
C
C INTERNAL ENERGY CHANGE IN THE MANTLE
             DELAUMAN=DELAUMAN+RHOH*ACROSSMAN*CPH*EXCHIGH*
        +              (TMANF-TMANI)/(DELT)
           ENDIF
C
C ENERGY LOSS FROM TANK
            QENV=QENV + ALOSS*ULOSS*(TAVG-TENV)+
```

```
     +                AMAN/PER*PI*DMAN*UMAN*(TMANAV-TENV)
C
C INTERNAL ENERGY CHANGE
          DELAU=DELAU+MSCP*H(NODE)/HIGH*(TF-TI)/(DELT)
C
          ACTHIGH=ACTHIGH-H(NODE)
1900   CONTINUE
300    TF = 0.
          DO 310 K = 1,NEQ
          KI = K + INIT
          KF = K + FINAL
          KAVG = K + AVG
          KOLD = K + OLD
          S(KOLD) = S(KAVG)
          TF = TF + S(KF)*H(K)
          UA = ULOSS*PER*H(K)
          IF(K.EQ.1 .OR. K.EQ.NEQ) UA = UA + UAE
          UAFI=0.
          DTDT(K) = (S(KF) - S(KI))/DELT
310    CONTINUE
          TF = TF/HIGH
320    QTANK = FLWL*(S(AVG+1) - TL)
          QIN=FLWSS*CPH*(TIN-S(AVG + NEQ*4+4 + NMANOUT))
          QTOT=QIN-QTANK-QENV-DELAUMAN
C
C   SET OUTPUTS
          OUT(1)=S(AVG+NEQ)
          IF (MODE .EQ. 3) OUT(1)=S(AVG + NEQ*4+4 + NMANOUT)
          OUT(2)=FLWSS
          OUT(3)=S(AVG+1)
          OUT(4)=FLWLL
          OUT(5)=QENV
          OUT(6)=QTANK
          OUT(7)=DELAU
```

```
      OUT(8)=QBTOT
      OUT(9)=QIN
      OUT(10)=TF
      N=MIN0(12,NEQ-1)
      IF(N.LT.2) RETURN
      DO 350 I=2,NEQ
      OUT(9+I)=S(AVG+I)
350   OUT(9+I+NEQ)=S(AVG + NEQ*4+4 + I)
      OUT(9+NEQ+1)=S(AVG + NEQ*4+4 + 1)
      RETURN
      END

C     FUNCTION FOR PROPYLENE-GLYCOL PROPERTIES

      FUNCTION    CPDF(PERCENT,T1)
      REAL T,T1,PERCENT,B,C,CPDF
      T=T1+273.15
      B = 3.865 - 0.0237*PERCENT - 0.0001128*PERCENT**2
      C = 0.001024 + 5.663E-5*PERCENT
      CPDF = B + C*T
C     {KJ/KG-C}
      RETURN
      END

      FUNCTION    DENSITY(PERCENT,T1)
      REAL T,T1,PERCENT,B,C,D,DENSITY
      T=T1+273.15
      B = 875.5 + 2.151*PERCENT
      C = 1.119 - 0.00076*PERCENT - 4.924E-5*PERCENT**2
      D = -0.00238- 9.138E-6*PERCENT + 1.087E-7*PERCENT**2
      DENSITY = B + C*T + D*T**2
C {KG/M^3}
      RETURN
      END
```

```
      FUNCTION    THCOND(PERCENT,T1)
      REAL T,T1,PERCENT,B,C,D,THCOND
     T=T1+273.15
      B = -0.786 + 0.01556*PERCENT - 4.893E-5*PERCENT**2
      C = 0.007687 - 0.0001156*PERCENT + 3.66E-7*PERCENT**2
      D = -9.998E-6 + 1.456E-7*PERCENT - 4.588E-10*PERCENT**2
      THCOND = B + C*T + D*T**2
C     {W/M-C}
      RETURN
      END

      FUNCTION    VISC(PERCENT,T1)
      REAL T,T1,PERCENT,B,C,VISC
     T=T1+273.15
      B = 71.639 - 0.6698*T + 0.001915*T**2 - 1.8587E-6*T**3
      C = 0.2702 - 0.00123*T + 1.5045E-6*T**2
      VISC = EXP(B+C*PERCENT)
C     {PA S}
      RETURN
      END
```

References

[1] Furbo, S. Berg, P., Calculation of the Thermal Performance of Small Hot Water Solar Heating Systems using Low Flow Operation, Thermal Insulation Laboratory, Technical University of Denmark, January 1992

[2] Fanney, A.H., Klein, S. A., "Performance of Solar Domestic Hot Water Systems at the National Bureau of Standards - Measurements and Predictions", Journal of Solar Energy Engineering, Vol.105, August 1983

[3] Incopera, F. P., DeWitt, D. P., Introduction to Heat Transfer, Second Edition, John Wiley & Sons, Inc., 1990

[4] TRNSYS, Version 13.1, Solar Energy Laboratory, University of Wisconsin, Madison, September 1990

[5] J. A. Duffie, W. A. Beckman, Solar Engineering of Thermal Processes, Second Edition, John Wiley & Sons, Inc., 1991

[6] WATSUN-manual, Watsun Simulation Laboratory, University of Waterloo, Ontario, Canada

[7] Mercer, W. E., Pearce, W. M., and Hitckcock, J. E., "Laminar Forced Convection in the Entrance Region Between Parallel Flat Plates", Trans.ASME, J. Heat Transfer, 89,251 (1967),

[8] Dowfrost, Engineering and Operation Guide for Dowfrost and Dowfrost HD Inhibited Propylene Glycol-based Heat Transfer Fluids, Form No. 180-1286-1190 AMS, Nov 1990